Universidade do Minho
Escola de Engenharia

Mariana Conde Carvalho Gonçalves Carneiro

Test-strips for monitoring cancer biomarkers in point-of-care

April 2024

Test-strips for monitoring cancer biomarkers in point-of-care
Mariana Conde Carvalho Gonçalves Carneiro
UMinho | 2024

Universidade do Minho
Escola de Engenharia

Mariana Conde Carvalho Gonçalves Carneiro

Test-strips for monitoring cancer biomarkers in point-of-care

Doctoral Thesis
Doctoral Program in Chemical and Biological Engineering

Work developed under supervision of
Professor Maria Goreti Ferreira Sales
and
Professor Lígia Raquel Marona Rodrigues

April 2024

DIREITOS DE AUTOR E CONDIÇÕES DE UTILIZAÇÃO DO TRABALHO POR TERCEIROS

Acknowledgments

I want to acknowledge to my supervisors Prof. Goreti Sales and Prof. Lígia Rodrigues for their support, encouragement, scientific knowledge, and guidance throughout this work. For their insightful comments and suggestions that made me grow as a scientist.

I would like to give my warmest thanks to my co-supervisor, Felismina Moreira for her guidance and advice that carried me through all stage of laboratory work and writing my thesis. For her continuous support and belief in me.

I would also like to give special thanks to all my colleagues at Biomark Sensor Research group, for helping me, for sharing with me their scientific knowledge and for the good times together. For those who become friends for life, I would like to thank for continuous encouragement and friendship.

I am deeply grateful to my parents, Nazaré and Alberto, for their continuous support and understanding along these years and for letting me through all the difficulties.

I would not could not have undertaken this journey without the endlessly enthusiasm of my boyfriend, Patrick Pais, that supported me and give me strength to not give up, comforting me at the end of each hard day.

To my baby daughter, Beatriz, for being so lovely and providing me decent night's sleep, keeping me sane in this final process of writing the thesis.

Finally, I want to acknowledge Portuguese Foundation for Science and Technology (FCT) for funding this work through the PhD grant reference SFRH/BD/131959/2017.

STATEMENT OF INTEGRITY

I hereby declare having conducted this academic work with integrity. I confirm that I have not used plagiarism or any form of undue use of information or falsification of results along the process leading to its elaboration.

I further declare that I have fully acknowledged the Code of Ethical Conduct of the University of Minho.

Resumo

Tiras de teste para monitorizar biomarcadores do cancro em *point-of-care*

O cancro da mama é a forma de cancro mais prevalente, em mulheres, em todo o mundo, com crescente incidência e mortalidade. Estudos indicam que a sua deteção precoce pode potenciar o efeito da terapia e reduzir a mortalidade. No entanto, as atuais técnicas de diagnóstico apresentam desvantagens, uma vez que requerem equipamentos específicos e profissionais formados para execução da técnica e análise de resultados, sendo bastante dispendiosas e demoradas. Além disso, nos países de baixo rendimento os cuidados de saúde são de difícil acesso e, mesmo em países mais desenvolvidos, as técnicas de diagnóstico não são acessíveis para grupos socioeconómicos desfavorecidos, levando a atrasos na deteção e menores taxas de sobrevivência. Para ultrapassar este problema mundial, é urgente definir um método de deteção de baixo custo, rápido e com elevada sensibilidade e seletividade. Investigadores de todo o mundo têm desenvolvido sensores para deteção de biomarcadores do cancro, devido às suas vantagens, como o custo-benefício, portabilidade, e capacidade *multiplex*. O papel é uma opção de baixo custo como substrato para a construção de sensores, permitindo o desenvolvimento de um dispositivo de diagnóstico ideal, oferecendo uma resposta qualitativa e quantitativa para o utilizador final, seja o próprio paciente ou um profissional de saúde. Um resultado positivo pode encaminhar o paciente a realizar testes mais específicos para confirmação e identificação do estado da doença. Em combinação com substratos de papel, a deteção ótica é sensível, precisa e rápida.

Esta tese focou-se no desenvolvimento de sensores colorimétricos em papel para biomarcadores do cancro. Foi desenvolvido um sensor colorimétrico enzimático para a glicose, como prova de conceito da combinação da deteção colorimétrica num suporte de papel. De seguida, foi produzido um imunossensor para o antigénio cancerígeno 15-3, em papel, e finalmente foi utilizado um polímero de impressão molecular para substituir o anticorpo previamente utilizado.

Estes sensores permitiram detetar os alvos dentro dos valores de interesse clínico e demonstraram bom desempenho analítico em soluções tampão e amostras de soro, com uma seletividade aceitável contra interferentes. O conceito destes sensores é passível de ser aplicado a outros biomarcadores do cancro e usado em dispositivos portáteis e de baixo custo especialmente benéficos em países mais desfavorecidos.

Palavras-chave: cancro da mama, colorimetria, immunosensor, polímeros de impressão molecular, sensores em papel.

Abstract

Test-strips for monitoring cancer biomarkers in point-of-care

Breast cancer is the most common cancer in women worldwide, with increasing incidence and mortality rates. Studies suggest that early cancer diagnosis can improve the effectiveness of therapy and thus reduce mortality rates. However, current diagnostic techniques for detecting breast cancer, have shortcomings. They require sophisticated equipment and trained professionals to perform the technique and analyse the results, which is expensive and time-consuming. Despite this, low- and middle-income countries do not have easy access to healthcare facilities, and even in developed countries, some diagnostic techniques are not affordable for vulnerable populations, resulting in delayed diagnosis and lower survival rates. To solve this problem globally, low-cost, rapid, and highly sensitive and selective methods for early diagnosis are urgently needed.

In recent years, researchers worldwide have made efforts to develop sensors for the detection of cancer biomarkers, as they offer several advantages over existing diagnostic methods, such as cost-effectiveness, portability, and multiplexing capability. Paper is a cost-effective option for use as a substrate for sensor construction. Paper-based sensors fulfil the requirements for an ideal screening device as they can provide a qualitative or quantitative response and the end user can be either the patient themselves or a trained or untrained healthcare professional. If the result of the test is positive, the patient can see a doctor who will perform a full screening protocol to determine the stage of the disease. In conjunction with paper-based substrates, the optical detection techniques are sensitive, accurate, rapid, and non-invasive.

The aim of this work was to develop colorimetric paper-based sensors for cancer biomarkers. For this purpose, an enzymatic colorimetric sensor for glucose was developed, which served as proof of concept for the conjugation of colorimetric detection onto a paper substrate. Subsequently, an immunosensor was assembled onto the paper substrate for cancer antigen 15-3 detection and finally a synthetic recognition element, a molecularly imprinted polymer, was used to replace the antibody in the previous device.

The developed sensors work in the clinical range of the selected targets and showed good performance in both buffer solutions and serum samples, as well as acceptable selectivity towards interfering species that might be present in more complex samples. In addition, the concept of the developed sensors can be extended to other cancer biomarkers and used as point-of-care devices in resource-poor settings.

Keywords: breast cancer, colorimetry, immunosensor, molecular imprinting polymers, paper-based sensors.

Index

Abbreviations and Symbols

	3-APBA	3-aminophenylboronic acid
	4CN	4-chloro-1-naphthol
	μPAD	microfluidic paper analytical device
A	ABTS	2,2'-azino-bis 3-ethylbenzthiazoline-6-sulfonic acid
	AFM	atomic force microscopy
	AgNP	silver nanoparticle
	AGU	anydroglucose unit
	ALP	alkaline phosphatase
	APS	ammonium persulfate
	APTES	3-aminopropyltrimethoxysilane
	ATM	ataxia telangiectasia-mutated
	AuNP	gold nanoparticle
B	BC	breast cancer
	B-ELISA	biomimetic enzyme-linked immunosorbent assay
	BRCA1	breast cancer gene 1
	BRCA2	breast cancer gene 2
	BSA	bovine serum albumin
C	CA125	cancer antigen 125
	CA15-3	cancer antigen 15-3
	CA15-9	cancer antigen 15-9
	CA19-9	cancer antigen 19-9
	CA27.29	cancer antigen 27.29
	CEA	carcinoembryonic antigen
	CHEK2	checkpoint kinase 2
	CL	chemiluminescence
	cLFA	competitive lateral flow assay
	CM	colorimetry
	CNP	carbon nanoparticle
	CtDNA	circulatory tumor deoxyribonucleid acid
	CV	cyclic voltammetry
	CYP1A1	cytochrome P450 family 1 subfamily A member 1
D	DAB	3,3′ -diaminobenzidine
	DAC	dialdehyde cellulose
	DCIS	ductal carcinoma in situ
	DIBA	dot-immunobinding assay
	DNA	deoxyribonucleic acid
	DPV	differential pulse voltammetry
	DVB	divinylbenzene
E	ECL	electrochemiluminescence

	EDC	1-ethyl-3-(3-imethylaminopropyl) carbodiimide
	EGDMA	ethylene glycol dimethacrylate
	EGF	epidermal growth factor
	EGFR	epidermal growth factor receptor
	EIS	electrochemical impedance spectroscopy
	ELISA	enzyme-linked immunosorbent assay
	EMA	epithelial membrane antigen
	ER	estrogen receptor
	ERα	estrogen alpha receptor
F	Fab	fragment antigen binding
	FBS	foetal bovine serum
	Fc	fragment crystallizable
	FDA	food and drug administration
	FET	field-effect biosensor
	FGFR2	fibroblast growth factor receptor 2
	FIA	fluorescence immunoassay
	FTIR	Fourier-transform infrared spectroscopy
G	GA	glutaraldehyde
	GO	graphene oxide
	GOx	glucose oxidase
H	HER2	human epidermal growth factor receptor 2
	HIV	human immunodeficiency virus
	HRP	horseradish peroxidase
	HSB	hue, saturation and brightness
I	IBC	inflammatory breast cancer
	IDC	invasive ductal carcinoma
	Ig	immunoglobulin
	ILC	invasive lobular carcinoma
L	LCIS	lobular carcinoma in situ
	LED	light-emitting diode strip
	LFA	lateral flow assay
	LFIA	lateral flow immunoassay
	LOD	limit of detection
	LSPR	localized surface plasmon resonance
	LSV	linear sweep voltammetry
M	MAP3K1	mitogen-activated protein kinase kinase kinase
	MBAA	N'-methylene bis-acrylamide
	MIP	molecular imprinting polymer
	miRNA	micro ribonucleic acid
	MIT	molecular imprinting technology
	MNP	magnetic nanoparticle
	MRI	magnetic resonance imaging

	mRNA	messenger ribonucleic acid
	MS	mass spectrometry
	MUC	mucin
	MUC1-N	mucin 1-N terminal subunit
	MUC1-C	mucin 1-C terminal subunit
	MWCNT	multi-walled carbon nanotube
N	NC	nanocellulose
	NHS	N-hydroxysuccinimide
	NIP	non-imprinted polymer
	NP	nanoparticle
O	OPD	orto-phenylenediamine
P	PAD	paper analytical device
	PAI-1	plasminogen activator inhibitor 1
	PB	phosphate buffer
	PBS	phosphate buffered saline
	PCR	polymerase chain reaction
	PEG	polyethylene glycol
	P-ELISA	paper-based enzyme-linked immunosorbent assay
	PEM	polymorphic epithelial mucin
	PoC	point-of-care
	PSA	prostate specific antigen
	PTEN	phosphatase and tensin homolog gene
Q	QD	quantum dot
R	RE	recognition element
	RGB	red, green and blue
	RIA	radioimmunoassay
	RNA	ribonucleic acid
S	SEM	scanning electronic microscopy
	SERS	surface-enhanced Raman scattering
	sLFA	sandwich lateral flow assay
	SNP	single nucleotide polymorphism
	SPR	surface plasmon resonance
	STK11	serin/threonine kinase 11 gene
	SWV	square wave voltammetry
T	TEMED	*N,N,N′,N′*-Tetramethyl-ethylene diamine
	TEMPO	2,2,6,6-Tetramethyl piperidine-1-oxyl radical
	TEPS	triethoxyphenylsilane
	TGA	thermogravimetric analysis
	TGFB1	transforming growth factor ß 1
	TMB	3,3′,5,5′-tetramethylbenzidine
	TNBC	triple negative breast cancer

	TP53	tumor protein 53
	TRIM	trimethylopropane trimethacrylate
U	uPA	urokinase plasminogen activator
	UV	ultraviolet
	UV/Vis	ultraviolet-visible
V	VEGF	vascular endothelial growth factor
W	WHO	world health organization

List of Figures

List of Tables

“Nothing in life is to be feared, it is only to be understood.

Now is the time to understand more, so that we may fear less.”

Marie Curie

Chapter 1

Introduction

In this chapter, the context and motivation of the developed work is given. The research aims are listed, and the structure and framework of the thesis are described, Finally, the outcomes of the thesis are enounced, including published papers and related presentations.

1. Introduction

1.1. Motivation

Cancer is a major cause of mortality and morbidity worldwide (1). Breast, lung, colorectum, prostate, skin and stomach were the most common cancer types all over the world in 2020 and 60.467 new cases of cancer occurred in Portugal (2).

Conventional methodologies for cancer diagnosis require significant time, human and economic resources, as they involve complex procedures and need to be performed at hospitals, by trained technicians, not being available in a point-of-care (PoC) format (3). These drawbacks often result in late diagnosis, occurring at an advanced stage of the disease. Thus, it is urgent to find ways for an early and proper cancer diagnosis, as well as for a suitable treatment. Actually, between 30% and 50% of cancer deaths could be prevented by an early diagnosis, accordingly to World Health Organization (WHO) (4). Searching for specific biomarkers that can be related with a certain cancer type and the development of methodologies for its fast and low-cost detection are two topics that are currently under the attention of researchers. PoC devices are suitable for screening protocols as they enable testing patients in a convenient way, providing useful and timely information to further carry out more accurate diagnosis (5). Early cancer diagnosis led to an increase in survival rates, an enhancement of quality of patient's life and thus an improvement of disease overall outcome (6). These devices should be low-cost, small, and portable, and easy to use. Biosensors fulfil the requirements of a PoC device and can be a powerful tool for cancer monitoring.

Up to date some biosensors for cancer biomarkers have been developed (7-9). Several types of recognition elements (REs) are available for cancer biosensor's design, including antigens or antibodies (10, 11), enzymes (12), nucleic acids (13, 14) or aptamers (15, 16) . Most of the published works for cancer monitoring use antibodies as REs (11, 17-21). Despite the well-established role of antibodies as REs and their undoubtedly selectivity for their targets (22), antibodies present some disadvantages, as its production is expensive and present low stability (23). For that reason, researchers are searching for new REs as molecular imprinting polymers (MIPs) or aptamers (1, 24). MIPs are artificial receptors, capable of mimicking the biological recognition. They are highly specific for their templates due to the formation of specific cavities and interaction of their binding sites with the desired template and can be produced over a countless number of targets. They can be applied as REs in biosensors coupled with several transduction systems thus providing sensitive devices.

Besides that, they offer stability, robustness and resistance to external conditions and its production process is reproducible and cost-effective, which offer advantages over antibodies (25).

Despite the interest of new REs, a proper transduction system is also a concern. Electrochemistry is the most often transduction system applied to cancer biosensors, especially immunosensors, which require an energy source thus compromising the portability of the device. Optical transduction provides a visible response and eradicate the need of specific equipment to read the results, while allowing the sensor to be portable (22). Among optical transducers, colorimetric ones enable biomarker's detection and quantification through color changes that could be observed by naked eye, both in solution or solid supports as paper (26). Paper is a suitable and versatile substrate due to its chemical and physical properties and the interest in paper analytical devices (PADs) has grown exponentially in the last decade, especially when conjugated with portable readers as smartphones, thus meeting the criteria for PoC devices (27-29).

Hence, the motivation of this plan is to develop novel biosensors for properly but simple detection of cancer biomarkers that can be used as PoC devices for cancer screening. Cancer antigen 15-3 (CA15-3) was selected as breast cancer (BC) biomarker and the goal is to use alternative REs to the well-established antibodies, and a transduction system compatible with a portable device, as optical transduction. Paper was used as support material for the development of the biosensors. Firstly, as a proof-of-concept, an enzymatic colorimetric sensor was developed for glucose, then an immunosensor was assembled onto the paper substrate for CA15-3 detection and finally a RE from synthetic nature, a MIP, was used to replace the antibody in the previous device.

The specific objectives defined for this purpose include:

(1) selection of suitable substrate for sensor assembly;

(2) production of synthetic REs (plastic antibodies or aptamers);

(3) development of a biosensor using the selected REs;

(4) and signal transduction to generate analytical data.

1.2. Structure of this thesis

This thesis reports the development of colorimetric paper-based sensors for biomolecules, and it is organized in 5 chapters:

Chapter I: Gives the context and motivation of the work developed. It lists the research aims and describes its structure and framework, as well as the publication outcomes and related presentations.

Chapter II: Provides a state of the art about cancer, focusing on cancer diagnosis based on biomarkers detection. BC is highlighted, once BC biomarkers were selected as targets for the sensors reported in this thesis. Finally, biosensors as an innovative approach for cancer biomarkers detection are described.

The following chapters from III to V report the development and characterisation of paper-based colorimetric biosensors for cancer biomarkers with different REs.

Chapter III: Presents the development of a sensor in which a well-known RE, an enzyme, was applied to detect a general biomarker, glucose, in a colorimetric paper-based enzymatic sensor.

Chapter IV: Describes the use of another well-known RE, an antibody, to detect a specific cancer biomarker, CA15-3, in a colorimetric paper-based immunosensor.

Chapter V: Focuses on the development of an artificial RE, a MIP, to assembly a biomimetic paper-based colorimetric biosensor for CA15-3.

Finally, chapter VI gathers the general conclusions of this thesis and its future perspectives.

1.3. List of publications

1.3.1. Papers published in international scientific journals (included in the thesis)

- Neubauerova, K., **Carneiro, M. C. C. G.**, Rodrigues, L. R., Moreira, F. T. C., & Sales, M. G. F. (2020). Nanocellulose- based biosensor for colorimetric detection of glucose. Sensing and Bio-Sensing Research, 29, 100368. doi:10.1016/j.sbsr.2020.100368;
- **C.C.G. Carneiro, M.**, Rodrigues, L. R., Moreira, F. T. C., & Goreti F. Sales, M. (2022). Paper-based ELISA for fast CA15–3 detection in point-of-care. Microchemical Journal, 181, 107756. doi:10.1016/j.microc.2022.107756;
- **C.C.G. Carneiro, M.**, Rodrigues, L. R., Moreira, F., & Goreti F. Sales, M.. Paper-based biommimetic test-strip for CA15-3 with colored readout. Microchemical Journal. 2024;196:109640.

1.3.2. Papers published in international scientific journals (not included in the thesis)

- **Carneiro, M.**, Rodrigues, LR., Moreira, F. T. C., & Sales, M. G. F. (2022). Colorimetric Paper-Based Sensors against Cancer Biomarkers. Sensors, 22(3221).

doi:10.3390/s22093221;

- Sousa, D. A., **Carneiro, M.**, Ferreira, D., Moreira, F. T. C., Sales, M. G. F., & Rodrigues, L. R. (2022). Recent Advances in the Selection of Cancer-Specific Aptamers for the Development of Biosensors. Curr. Med. Chem. 29 (1875-533X (Electronic)), 5850-5880. doi:10.2174/0929867329666220224155037.

1.3.3. Presentations at scientific conferences

- **Carneiro, M. C. C. G.**, Rodrigues, L. R., Moreira, F., & Sales, M. G. F. (26-29 july, 2021). Poster P5.054: Paper-based ELISA for rapid protein detection. Presented at the 31st anniversary world congress on biosensors, Live and On-demand.
- **Carneiro, M.**, Rodrigues, L. R., Moreira, F., & Sales, M. G. F. (2021). Poster: Test-strips for monitoring cancer biomarkers in point-of-care. Presented at the Encontro Ciência '21.

Chapter 2

State of the art

This chapter covers the literature review that contextualizes the work. It includes an overview on cancer, including the carcinogenesis process, incidence, risk factors, current diagnostic methods, and therapeutic approaches, focusing on BC. It also introduces biosensors and its components, describing the REs and related transduction methodologies, but highlighting those with greater relevance to the present research work. The use of paper as a versatile substrate for sensor development is debated and the importance of PoC devices for cancer is also discussed.

2. State of the art

2.1. Cancer overview

Cancer is a multistage process of malignant transformation in which normal cells undergo uncontrolled proliferation and grow into an abnormal cell mass, called tumor (3, 30-32). Unlike normal cells, cells from primary tumor further grow acquiring new vascularization and metastatic capacity, spreading to other parts of the body (3, 30). Thus, metastasis can be defined as the process through which malignant tumors spread all over the body, using lymphatic system or bloodstream (33).

This malignant transformation can be translated by some metabolic, hormonal, and immunological changes. Manifestations in earlier stages of tumor development as changes in premalignant tissues should be monitored, especially in people with an increasing risk of cancer, due to genetic factors (32). On the other hand, benign tumor remains at their origin location without spreading, neither to subjacent nor distant parts of the body. This kind of tumor grows slowly, has well defined borders and unlike malignant tumors, does not grow back after surgical removal (34).

The hallmarks of cancer (Figure 2-1), the major mechanisms leading to cancer progression, include maintenance of proliferative signalling, evasion of growth suppressors, evasion of destruction by the immune system, facilitation of replicative immortality, activation of invasion and metastasis, initiation of angiogenesis, resistance to cell death and deregulating cellular genetics (32).

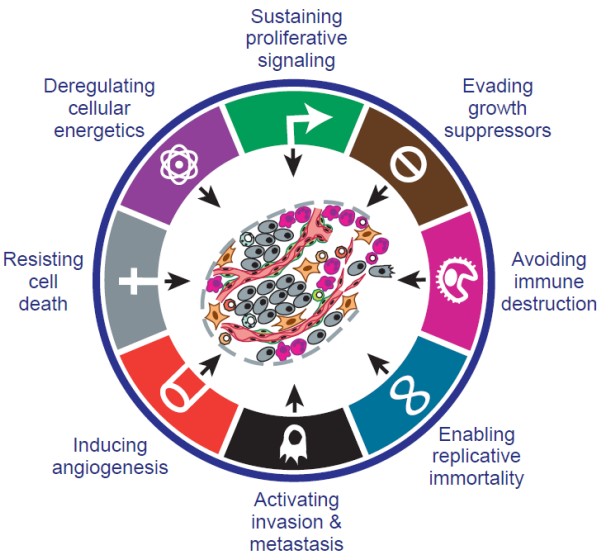

Figure 2-1. The hallmarks of cancer. Taken from (32).

Cancer is the second major cause of deaths worldwide, after cardiovascular diseases (26). According to WHO, cancer was responsible for about 10 million deaths in 2020, which corresponds

to every 1 in 6 deaths (4). It is expected around 30.2 million new cases by 2040, a 56% rise in comparison to 2020 (35).

Breast (2.26 million cases), lung (2.21 million cases), colorectum (1.93 million cases), prostate (1.41 million cases), skin (1.20 million cases) and stomach (1.09 million cases) were the most common cancer types in 2020 all over the world (Figure 2-2) (36).

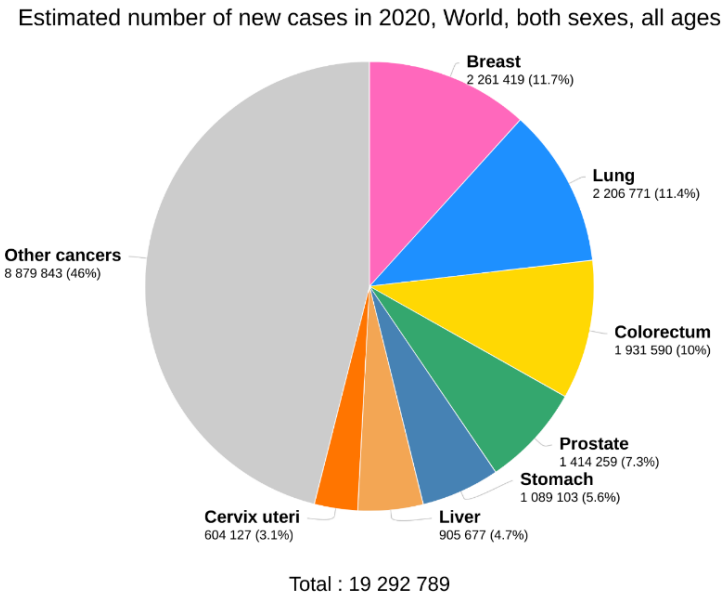

Figure 2-2. Estimated number of new cases of cancer in 2020. Taken from (36).

Cancer incidence varies between different countries, which depends on its lifestyles and local risk factors, namely behavioural factors and environmental factors (32). Developing countries account with higher mortality and morbidity in consequence of cancer due to poverty, deficiency of awareness about the disease and lack of health facilities (26).

In Portugal, 60.467 new cases of cancer occurred in 2020. Considering both sex, colorectum cancer is the most prevalent, with 10.501 new cases, followed by BC that counts with 7.041 new cases, in 2020 (Figure 2-3) (36).

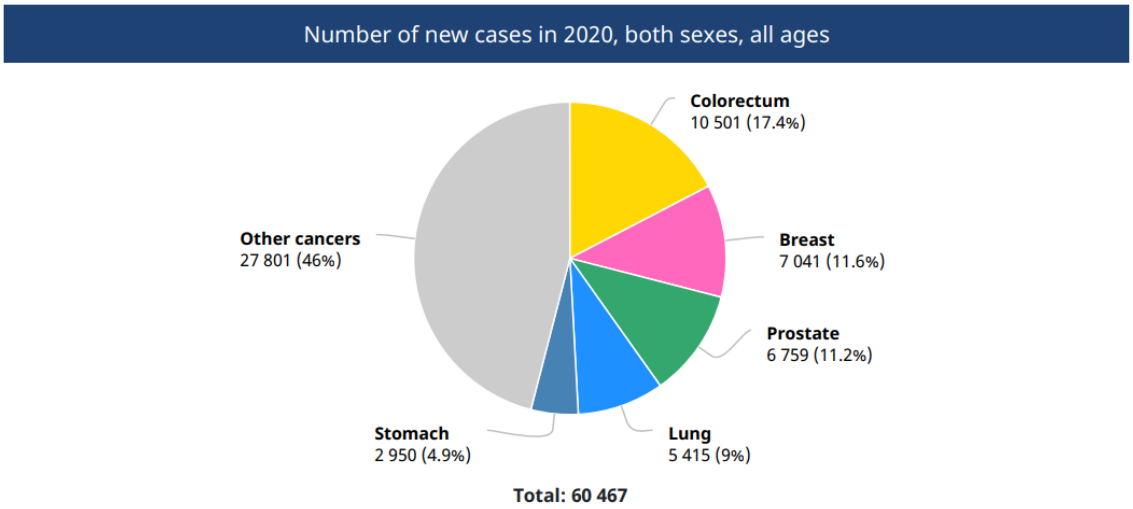

Figure 2-3. Estimated number of new cases of cancer, in Portugal, in 2020. Taken from (36).

Cancer is a multifactorial disease (6) with origin in mutations or environmental factors (3). The cumulative exposure to risk factors and the increasing in life expectancy is leading to a growing in the incidence of different types of cancer (37).

The majority of cancer cases are caused by exposure to carcinogen agents (e.g. hazardous chemicals, radiation, infectious agents) which will induce mutations on organisms (32). On the other hand, sporadic cancers occur without an evident exposure to risk factors or genetic susceptibility. Cancer can also be caused by interaction between carcinogenic agents and weak genetic susceptibility. However, the evaluation of causal evidence in that case is usually ambiguous (32).

Behavioural factors such as alcohol or tobacco consumption, unbalanced diet (low consumption of fruit, vegetables and fibre and high consumption of sugar-sweet beverages, refined carbohydrates, red and processed meat and consumption of carcinogenic substances in the diet), metabolic factors (e.g. obesity, high levels of cholesterol, high blood pressure), hormonal and reproductive factors, lack of exercise, ultraviolet (UV) and ionizing radiation, as well as water, soil or air pollution are examples of risk factors for cancer development (32). Some chronic inflammatory diseases caused by infectious agents such as human papillomavirus (HPV), hepatitis B and C virus, Epstein-Barr virus or Helicobacter pylori can also be a risk factor for cancer (32). Changes in gene structure or function by highly penetrant inherited mutations can predispose for cancer development, which are responsible for 5 to 10% of all cancers (32).

The burden of cancer can be minimized through preventive behaviours, implementation of screening programs and therapeutic strategies (32, 38). Prevention of cancer can be achieved by reducing or eradicating exposure to carcinogen agents, as well as encourage a lifestyle that lowers cancer risk.

Tobacco control and vaccination programs are the major successful strategies for cancer prevention. Screening tests to detect lesions at early stages and identification of individuals and family's hereditary cancer and thus increased risk for cancer development are also effective preventive approaches. When available, preventive therapy can also be applied, namely the use of particular drugs as the use of selective estrogen receptor (ER) modulators (e.g. tamoxifen and raloxifene) for BC prevention and low-dose aspirin for colorectal, stomach, and esophageal cancer (32).

Cancer treatment protocols are meant to eradicate cancer or, at least, prolong patient's life and improve their quality of life (4). The choice of the cancer treatment depends on the type of cancer and how advanced it is. For some people, only one type of treatment is used, but a combination of approaches may also be required. The most common therapeutic scheme is surgery in combination with chemotherapy and/or radiotherapy. Other types of therapy include hormone therapy, immunotherapy, targeted therapy, stem cell transplants, hyperthermia and photodynamic therapy (2, 39).

2.2. Cancer diagnosis

Low survival rates associated to cancer are generally due to late diagnosis and poor prognosis, as many cancers only are diagnosed after metastasis being detected (9, 30, 40). Cancer patients early diagnosed can have higher survival rates and up to 50% of cancer deaths could be prevented by an early diagnosis, accordingly to WHO (4). For that reason, asymptomatic individuals should be submitted to regular screening and symptomatic patients should be properly evaluated for an early diagnosis (at preclinical stage) to offer timely and accurate treatment and reduce mortality rates (9, 30, 32, 40).

Proper cancer screening methodologies, as mammography, applied to a large population even before the symptoms can provide early detection of cancer when it is easier to treat. In European Union countries there are evident differences in the practices adopted for cancer screening. These include the type of procedures used for screening, as well as the age ranges that are targeted for screening and the time interval between screening tests (32). However, among the available conventional methodologies for cancer screening, no single one has enough accuracy to detect cancer at early stages and could be expensive and time-consuming for patients and healthcare systems (7, 9, 22, 26). The solution would be to combine different screening tests to assure an adequate diagnosis and subsequently a proper and attempted treatment (32).

When a person is suspected to have cancer, either by a screening test result or due to experienced symptoms, diagnostic methodologies should be carried out. Cancer diagnosis can be performed either through conventional techniques (as image methodologies like magnetic resonance imaging (MRI), endoscopy, computing tomography, X-rays, ultrasound imaging, mass spectroscopy and biopsy) or by cancer biomarkers detection (usually performed by immunoassays as enzyme-linked immunosorbent assay (ELISA), radioimmunoassay (RIA) or fluorescence immunoassay (FIA), or by electrophoresis, polymerase chain reaction (PCR) and mass spectrometry (MS)). Among these, immunoassays and PCR are the gold standard in clinical diagnosis for biomarker detection as they are highly sensitive and specific (3, 6, 8, 9, 17, 40). However, these clinical tests can be invasive, expensive, and time-consuming for patients and healthcare systems as they imply complex and high-cost protocols with multiple analytical steps as wash steps and incubations, large consumption of reagents and samples, sophisticated equipment and are not available in some regions with lack of economic resources or trained personnel, compromising the accurate diagnosis and further effective treatment. For these reasons, these procedures are impractical in developing countries and places with low resources (1, 3, 5-7, 9, 24, 25, 40-43).

Therefore, researchers keep looking for alternative and sensitive methodologies for cancer screening and diagnosis, focusing on functional images and biomarkers detection (32).

2.2.1. Cancer biomarkers detection

Biomarkers are molecules responsible for several functions in our organism, including storage and transmission of genetic information, catalytic activity, regulation of biological activities or transport, and should be capable to differentiate normal and disease stages. The ideal biomarker should be specific for the disease of interest; do not exist in healthy people; and lead to the identification of the disease before the clinical diagnostic (44-46).

Cancer biomarkers represent a very large group of molecules as genes, nucleic acid sequences (deoxyribonucleic acid (DNA), ribonucleic acid (RNA) and microRNA (miRNA)), proteins/enzymes/hormones, lipids, small molecules as secondary metabolites, extracellular vesicles or circulating tumor cells and changes can occur in terms of structure, expression, function or abundance (26). Several molecules have been identified and characterised as cancer biomarkers, being currently in clinical use (44-46).

These molecules could be present in tissues as tumor tissues or in body fluids such as blood, urine or oral fluids (1, 3, 6, 17, 41). Biomarkers that could be detected and measured in patients'

(bio)fluids must have a special attention by researchers once they can be easily collected by minimally invasive procedures, being an advantage over conventional methodologies (24, 44-46) as they enable cancer detection through less invasive processes (17, 32). They have high clinical significance once its study enables to understand more about the risk and progression of the disease and to establish a diagnosis and prognosis (and subsequently, timely and adequate treatments), as well as detect disease recurrence. They can also be useful on the assessment of patients' response to therapy, for monitoring and prediction about drug resistance, as well as development of new treatments (3, 5-7, 9, 17, 37, 40-42, 47, 48).

Despite the undoubted advantages of measuring biomarkers for cancer detection, most of the discovered biomarkers suffer from lack of sensitivity or selectivity and the use of a new biomarker in clinical diagnosis is a complex process, involving time and money consuming, once it requires analytical and clinical validation and subsequent evidence of the biomarker's clinical value (22).

The detection of biomarkers could also be confusing, as some of these molecules are released in low concentrations, which is very common in cancer, especially in the early stages of the disease (32, 41, 43). Moreover, some of them are associated with only one type of cancer, whereas other ones are related to several types of cancer. For these reasons, the detection of a biomarker in complex samples could be difficult and the detection of a single cancer biomarker may not be indicative of the disease, so a panel of biomarkers are often required for an accurate diagnosis (3, 6, 41, 43). Also, considering the organ involved, cancer could be classified in many sub-groups and a specific biomarker can show different levels in different type of cancer (6). For these reasons, actual detection of cancer biomarkers is only performed as a complement to conventional methodology (22).

2.3. Breast cancer overview

BC is the most common type of cancer, accounting for 12.5% of new cancer cases worldwide (49). It is also the major cause of death in women, registering 684.996 deaths in 2020 (38). The majority of BC types are detected in low- and middle-income countries, especially at later stages due to poor health accesses (32). At present, about 80% of BC cases have more than 50 years old and their survival depends on the stage of the cancer at the moment of detection, as well as its molecular subtype (38).

BC displays high heterogenicity regarding tumor morphology, molecular features and clinical response (32). BC subtypes can be described accordingly to different models of classification. Concerning the

origin of the tumor and its cellular behaviour, BC can be classified into invasive or non-invasive. A BC case classified as non-invasive, means that it does not spread to the adjacent breast tissue while invasive BC, as the name suggest, spread into the surrounding breast tissue. The most common type of non-invasive BC is ductal carcinoma in situ (DCIS) and corresponds to 16% of all BCs. Lobular carcinoma in situ (LCIS) is other type of non-invasive BC and it is considered a benign BC condition and does not spread outside the lobules. Invasive ductal carcinoma (IDC) represents 80% of the cases, being the most common type of invasive BC while invasive lobular carcinoma (ILC) is the second most common type of BC, with 10% of the cases. Inflammatory BC (IBC) is a less common type of invasive BC, accounting only 1-3% of the cases. Paget's disease of the nipple starts around the nipple and can spread to the areola and other areas of the breast. It counts with less than 5% of BC cases (22, 49). The most common and widely accepted classification is based on a five subtype classification model that takes into consideration the expression of hormone receptors and result in five subtypes (luminal A, luminal B, luminal B-like, human epidermal growth factor receptor 2 (HER2) positive, non-luminal, and triple negative BC (TNBC) whose receptor expression, incidence and prognosis is summarized in Table 2-1 (22).

Table 2-1. Receptors expression, incidence, and prognosis of different types of BC.

Types of BC		Incidence	Receptors expression			Prognosis
			PR	Estrogen alpha receptor (ERα)	HER2	
Luminal	Luminal A	70%	+	+	-	Good
	Luminal B		+	+	-	Medium
	Luminal B-like		+	+	+	Poor
Non-luminal	HER2 positive	10-15%	-	-	+	Poor
Basal	TNBC	20%	-	-	-	Poor

BC ethology is a result of a complex interaction between several modifiable and non-modifiable factors that contribute to the development of the disease. Non-modifiable factors include sex, age, genetic mutations, family history, race/ethnicity and reproductive factors, while modifiable factors are related with physical activity, body mass index, dietary and some behaviours as alcohol consumption and tobacco use, as well as environmental factors (22, 32, 38).

Female sex is the major factor related with increased risk of BC, due to several reproductive and hormonal factors (38) as lower parity, earlier ages at menarche, later ages of menopause and later ages at first birth (22, 32, 33). In men, BC is a rare disease that counts with less than 1% of cases and is usually detected at advanced stages of the disease (38). Cancer has a higher occurrence in older individuals, due to accumulation of several cellular changes as well as exposition to potential carcinogenic agents (38). Personal history of BC and other non-cancerous alterations in breasts is a significant risk factor for BC. It is known that about 13 to 19% of BC patients have a first-degree relative with cancer (38). Several genetic mutations are highly related with an augmented risk of BC, especially the ones responsible for high penetration, occurring in breast cancer gene 1 (BRCA1) and breast cancer gene 2 (BRCA2), but also in tumor protein p53 (TP53), cadherin-1 (CDH1), phosphatase and tensin homolog gene (PTEN), and serin/threonine kinase 11 gene (STK11). These mutations are principally transmitted by autosomal dominant inheritance, but some sporadic mutations have been reported (38). Inequalities regarding race and ethnicity are observed and BC incidence is higher among white non-hispanic women, while higher rates of mortality and lower survival rates are observed among black women (38).

Some reports indicate that some drugs (e.g. hormonal therapy, antibiotics and antidepressants) intake are related with higher risk of BC, as well as sedentary behaviour, high alcohol consumption (38), tobacco use, consumption of processed food , saturated fats, food rich in sodium or sugar. Some chemicals (e.g. polycyclic aromatic hydrocarbons, organic solvents, and insecticides) can induce epigenetic modifications and thus induce pro-carcinogen events (38).

Tumor size, tumor histologic grade and hormone receptors are traditional prognostic factors in BC, being axillary lymph node statues the most important one (50, 51). However, these can only be obtained from tissue samples, which is an invasive method. Some circulating tumor markers found in serum have been investigated in several studies as potential prognostic parameters for patient outcome and response to therapy. Examples include CA15-3 and carcinoembryonic antigen (CEA), which can be easily quantified in serum by a rapid and non-invasive test. High levels of these molecules have been associated in several reports with poorer prognosis and disease-free survival in patients with BC. Patients with normal CA15-3 and CEA levels had better disease-free survival than patients with elevated CA15-3 and/or CEA levels. The association between elevated CA15-3 and CEA levels and such major parameters as tumor size, as well as node metastases and an advanced stage of the disease was also verified (50, 52). This topic will be fully discussed in section 2.3.1. Breast cancer diagnosis.

Breast cancerous tissues can be surgical removed by partial mastectomy or complete mastectomy (38). Systemic treatment of BC involves preoperative or postoperative chemotherapy in which the selection of the proper drug is of main importance as different molecular BC subtypes have different response to therapy. Local treatment for BC comprises radiotherapy, usually performed after surgery and/or chemotherapy, being especially useful in the case of metastatic BC (38).

2.3.1. Breast cancer diagnosis

Alongside cervical and colorectal cancer, BC is one of the cancers for which the European Council recommends screening. Screening tests for BC are essentially based on mammography for women aged 50-69 years, with a recommended screening interval of 2 years and breast examination (both clinical and self-examination) (32).

Mammography is currently the golden standard methodology for BC screening, but it has some limitations as high rates of false positive results (22).

Moreover, mammography is less effective in younger women and dense breasts and less sensitive to small tumors. Contrast-enhanced mammography can be performed, which is more accurate than mammography and ultrasound in dense breasts. However, this technique is not widely available due to its high cost and the inconvenience of high radiation exposure. MRI could detect small lesions that are not noticed by mammography but has lack of selectivity and is too expensive.

In addition to the screening techniques mentioned, biopsies can also be performed to distinguish cancerous tissue from normal tissue. However, this is an invasive technique that is also expensive and requiring expert analysis (53).

Despite the above mentioned techniques, BC can be detected by measuring BC biomarkers levels. BC biomarkers currently used in clinical diagnosis include PR and ER, HER2, BRCA1 and BRCA2, Ki-67, CA15-3 and cancer antigen 27.29 (CA27.29), CEA, urokinase plasminogen activator (uPA) and plasminogen activator inhibitor 1 (PAI-1) (22). BC biomarkers can be classified, based on omics, into genomic (DNA molecules), transcriptomic (RNA molecules), proteomic (protein molecules) and metabolomic (small metabolites) biomarkers (26).

A person's genome profile can indicate the risk of developing cancer. Alterations in genes (e.g. deletions, amplifications or mutations in certain genes such as tumor suppressor genes, proto-oncogenes or cell cycle regulators) increase a person's predisposition to developing cancer. A single nucleotide polymorphism (SNP) is a variation in a single nucleotide at a specific position in a particular gene. When present in genes such as cytochrome P450 family 1 subfamily A member 1

(CYP1A1), RAD1, BRCA1, BRCA2, PTEN, TP53, checkpoint kinase 2 (CHEK2), ataxia telangiectasia mutation (ATM), PALB2, BRIP1, fibroblast growth factor receptor 2 (FGFR2), mitogen-activated protein kinase kinase (MAP3K1) and transforming growth factor ß 1 (TGFB1), it can lead to BC. BRCA1 and BRCA2 are the most commonly used genomic BC biomarkers and genomic screening for these genes is often performed to predict BC. Promising results have been obtained with the detection of these genes by biosensor-based techniques, especially electrochemical and optical.

Circulatory tumor DNA (ctDNA) and cell-free DNA also gained a significant attention as BC biomarkers in recently years (26). Transcriptomic biomarkers, as messenger RNA (mRNA) and miRNA also provide important information about cancer development. Different specific BC-associated miRNAs, as miRNA-21 (13) and miRNA-155 (14) were successfully detected by electrochemical and optical biosensors, respectively. Although nucleic acid biomarkers can provide important information related to the tumor growth, they do not enable early diagnosis due to low concentrations (53).

Since proteomic biomarkers are relatively abundant compared to RNAs and DNAs and play an important role in clinical diagnosis, they are the most frequently investigated molecules in BC. Numerous protein biomarkers are involved in the development of BC, such as CA15-3, cancer antigen 15-9 (CA15-9), cancer antigen 125 (CA125), CA27.29, cancer antigen 19-9 (CA19-9), CEA, epidermal growth factor (EGF), vascular endothelial growth factor (VEGF), TP53, cathepsin D, cyclin E, epidermal growth factor receptors (EGFR) and HER (26). Metabolomic biomarkers are low molecular weight molecules present in several biofluids whose concentrations can change during cancer development. Hence, metabolites can be potential cancer biomarkers used both in diagnosis and prognosis. In BC, lower levels of histidine and higher levels of lipids and glucose are common (26).

As mentioned above, proteins are important cancer biomarkers as their concentration significantly varies in the consequence of a cancer development (9, 54).

The human mucin (MUC) family comprises proteins with a high molecular weight, from MUC1 to MUC21. They can be secreted MUCs equipped with highly glycosylated tandem repeats that act as a physical barrier and limits exposure to external factors, thus protecting epithelial cells from stress and inflammation. MUCs can also be present in the form of transmembranes, which also contribute to this physical barrier and still have the task of transmitting survival and growth signals to the inside of the cell (55, 56). Deregulation of MUC production contributes to chronic inflammation response (55). Overexpression of transmembrane MUCs is related with several

carcinomas once it influences some processes that leads to oncogenesis (55). The surface of several types of carcinoma cells overexpress transmembrane MUCs and this expression is induced by inflammatory cytokines (57). MUC-1, is also known as polymorphic epithelial mucin (PEM), epithelial membrane antigen (EMA) and episialin (57).

MUC1-N terminal subunit (MUC1-N) is linked through stable hydrogen bounds with the MUC1-C terminal subunit (MUC1-C), forming a stable non-covalent complex that is expressed at the typical border of normal epithelial mammary cells (55, 58). MUC1-N terminus is extracellular and highly modified by O-linked glycans, acting as a cell barrier and restricting cell-cell and cell-extracellular matrix connections (55, 58). Under normal conditions, MUC1 expression is mostly restricted to the apical side of glandular epithelial cells, acting as a barrier to protect cells from injurious environments and pathogens invasion and provide resistance to stimuli (51, 57, 58). It also participate in adhesion during metastasis and contribute to cell surface lubrification, hydration and protection from degradative enzymes (58). However, MUC1 is overexpressed in several types of human carcinomas, including BC, as well as colon, lung, liver, pancreatic and ovarian cancer (58) as a consequence of genetic alterations and transcription dysregulation (56). MUC1 glycosylation suffers an alteration in human carcinomas as consequence of changes in glycotransferase expression of cancer cells (55, 58) and thus, MUC1 is usually less glycosylated in malignant than in normal tissue (Figure 2-4) (51, 58). In cancer cells, MUC1 can play either a pro or anti-inflammatory role, can limit the effectiveness of some drugs, can promotes invasion and migration of cancers and can inhibit cancer cell growth and apoptosis (58). In the presence of an epithelial stress response, MUC1-N is released from the cell surface and MUC1-C acts as a second line of defence, protecting the cell against loss of integrity. With loss of polarity in consequence of epithelial cell surface damage, MUC1-C domain is repositioned and expressed over the entire cell membrane (56, 57).

MUC1 can play an anti-inflammatory role by inhibiting the response of dendritic cells and thus the inflammatory process, or it can influence Toll-like receptors through immunomodulation. On the other hand, its pro-inflammatory role is related to its interaction with macrophages and dendritic cells by regulating the recruitment of inflammatory cells, which allows the tumor to escape the immune system and thus promote metastasis (58).
Overexpression of MUC1 can also limit the effectiveness of some therapies by reducing drugs intracellular uptake, promotes chemoresistance or radiotherapy resistance (58).
MUC1 is also involved in the regulation of some factors that promote cell invasion and metastasis,

as example, through the transforming growth factor (TGF) signalling pathway, by an increase in the production of exogenous platelet-derived growth factor (PDGF)-A or by inducing the expression of neutropilin-1 and its ligand VEGF thus promoting angiogenesis (58).

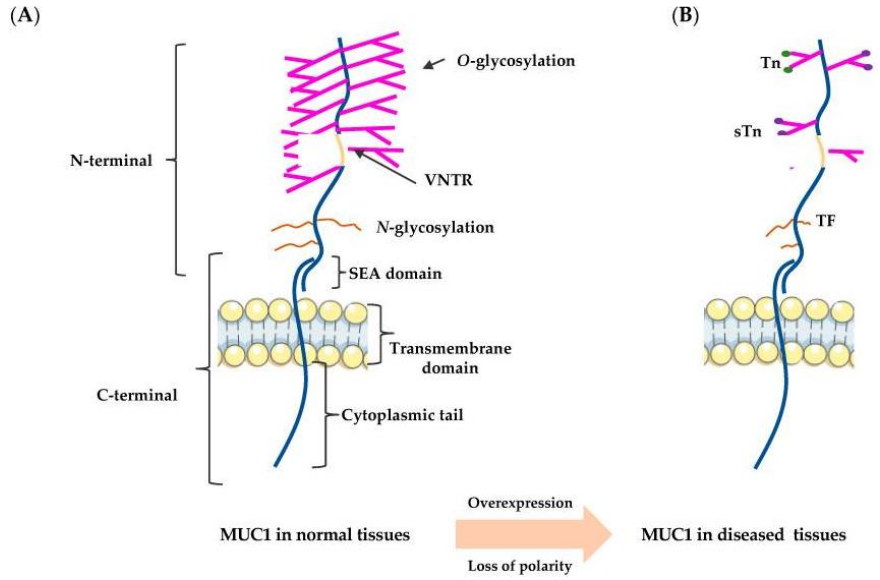

Figure 2-4. Structure of MUC1 in normal (A) and cancer cells (B). Adapted from (58).

Circulating MUC1 levels are determined by CA15-3 assay (55, 56), approved by US Food and Drug Administration (FDA) for monitoring BC patients during therapy and to detect disease recurrence at early stages (55).

CA15-3 is the soluble form of MUC-1 (59) with ≈400 kDa, secreted by BC cells (60). It is overexpressed in 90% of BC (37, 61) and is the most widely used biomarker in serum of patients with BC (59).

Despite CA15-3 has not enough sensitivity and selectivity for an early-stage BC diagnosis, it can be used for predicting prognosis and therapy monitoring of patients with metastatic disease (23, 52, 53, 59). The cut-off value for CA15-3 in clinical practice is 30 U mL $^{-1}$ and superior concentrations are associated with a poor prognosis in patients with invasive BC and can be an indicative factor to search for metastases (62). For this reason, the main clinical application of CA15-3 is BC patients monitoring following surgery, the detection of recurrences in a preclinical stage (63). CA15-3 prognostic value is independent of factors as patients age, tumor size and axillary node status. It is capable to predict outcome of the disease in both node-negative and node-positive patients as well as ER-negative and ER-positive. Finally, it was demonstrated that CA15-3 maintains it prognostic value independent of the type of therapy used (e.g. hormone

therapy, chemotherapy or radiotherapy) (64). Several studies have demonstrated the relation between CA15-3 levels and metastasis, poor prognosis and shorter overall survival (62-64). Shering et al. (63) performed a study (n=368), with a median follow-up time (3.28 years), during which the preoperative serum concentrations of CA15-3 were measured in BC patients. A cut-off value of 30.38 U mL -1 was used, and it was demonstrated that patients with high CA15-3 levels had a worse prognosis than those with concentrations below the cut-off value. The probability of disease-free survival at 5 years was calculated and was 44% in patients with higher CA15-3 levels compared to 65% in patients with lower CA15-3 levels. The probability of overall survival in these two groups was 67% and 83%, respectively. This study suggests that preoperative CA15-3 serum levels provide important information about patient outcome and may be a useful tool for selecting appropriate adjuvant therapy. In addition, this study found that CA15-3 levels were not dependent on age or ER status, but they were higher in patients with negative lymph node and larger tumors (63).

Later, the above reports were confirmed by Duffy et al. with a larger number of patients (n=600) and a longer follow-up (6.27 years). In patients with histologically confirmed BC, the CA15-3 concentration was measured at a preoperative stage. Follow-up of these patients suggests that those with high CA15-3 levels had a significantly shorter overall survival than those with lower levels of this protein. The results confirm previous findings on the prognostic value of CA15-3, as patients with high CA15-3 levels had poorer overall survival. However, in this study, CA15-3 showed prognostic value in the node-negative subset of patients, while this was not observed in the previous study. In addition, CA15-3 predicted outcome in ER-negative patients in this study, which was not observed in the previous study (64). In a study including 2036 patients, about 200 had CA15-3 concentrations above 30 U mL^{-1}. From these, metastases were found in 75 patients (62).

CA15-3 determination in clinical context is normally performed by ELISA or electrophoresis. However, the use of antibodies in ELISA restricts the stability and the storage conditions and increases the cost of the assay, and electrophoresis is not reliable for routine practice and PoC (23). Similar to what occurs with several serum biomarkers, the main limitation of CA15-3 is lack of sensitivity once its serum levels are slightly increased in patients with localized tumors or at early stages of the disease (59). Also, CA15-3 lacks from specificity, as most of the cancer biomarkers that are not organ specific, once its levels can be increased in ovarian, pancreatic, gastric and lung cancer (57, 59). Besides that, some benign conditions could also be

responsible for higher levels of CA15-3 (59). For that reason, CA15-3 should not be used alone for BC monitoring but in combination with other methodologies as physical examination, clinical history and imaging (59). Also, apparently, there are inconsistent results about the prognostic value of CA15-3 and CEA and a controversial opinion between researchers regarding which one has superior prognostic value in BC (37, 52). These inconsistency seems to be related with short follow-ups, small sample size, and variable cut-off values used in different studies (52). However, the simultaneous measurement of CA15-3 and CEA seems to be the most reasonable choice once it allows the early detection of metastasis in BC in up to 60-80% of patients (37). Besides the prognosis value of MUC1, it is also a promising target for vaccines development, as well as antibodies and drug inhibitors (55). Actually, inhibitors of MUC1-C terminal subunit have already been developed and it was proved that they block the oncogenic function of the protein, thus inducing death of BC cells, in *in vitro* assays (56). Also, several monoclonal antibodies have been produced against MUC1-N subunit (56).

Considering that CA15-3 is one of the biomarkers approved by FDA to monitor BC patients, due to its clinical significance in monitoring the BC patients therapy, as well as in the detection of the disease recurrence in early stages, we selected this biomarker as the target case study to develop our sensors.

2.4. Biosensors

Biosensors are analytical devices that combine an RE (e.g. enzymes, antigens or antibodies, metabolites, cells, nucleic acids, etc.), which is immobilised on a suitable substrate and has the function of detecting a specific target, and a transducer (e.g. optical, electrochemical, piezoelectric, photoelectrochemical, calorimetric, acoustic, etc.) responsible for converting the detection event into a measurable signal proportional to the analyte concentration and shown on a display, usually a computer or other digital device - Figure 2-5 and Figure 2-6 (65).

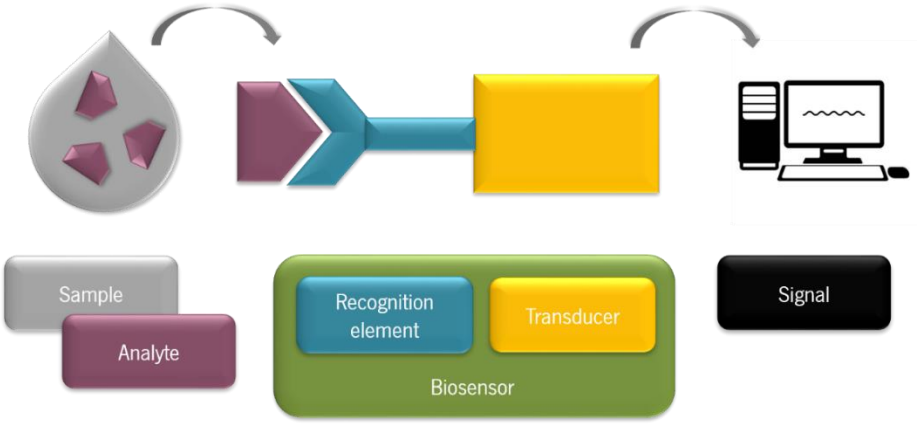

Figure 2-5. Schematic representation of a biosensor. Analytes present on the sample bind to RE of the biosensor, producing a change which is converted into a quantifiable signal by the transducer. Signal is shown by the display system.

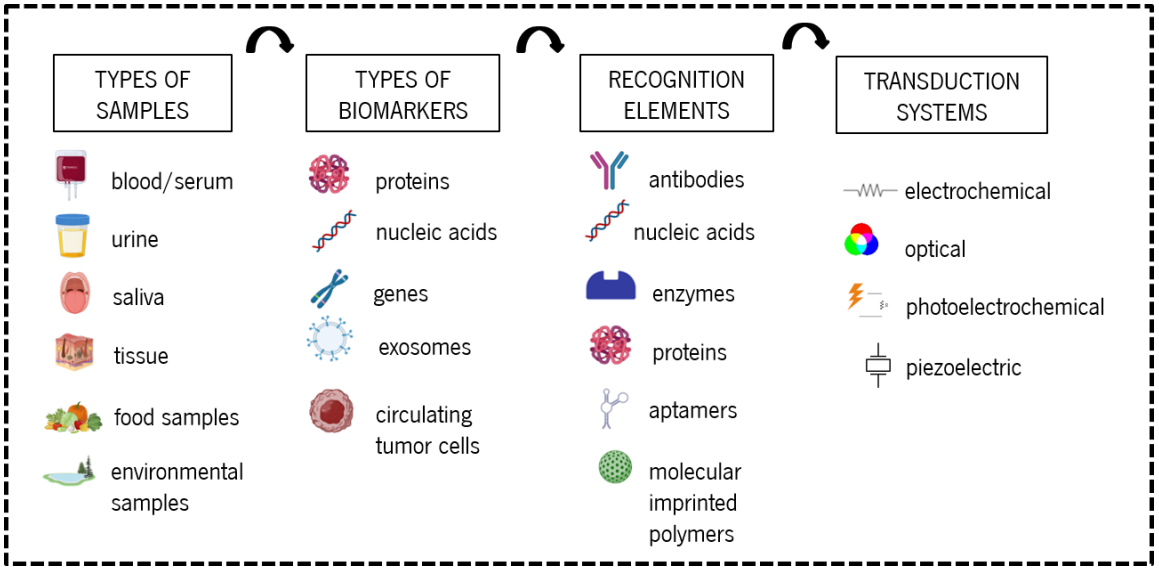

Figure 2-6. Example of types of samples and biomarkers that can be detected in biosensors. REs and transduction systems used in biosensors assembly.

A biosensor aims to detect a specific analyte in a wide range of concentrations without the interference of other substances. It can be achieved through the selection of an appropriate RE, immobilised by a suitable method, and an accurate transducer (66). Characteristic properties of a biosensor include selectivity, sensitivity, reproducibility, stability, and linearity. Selectivity is probably the most important parameter of the biosensor and depends on the ability of the RE to discriminate the target analyte, in a complex sample, from other interferent molecules, which depends essentially on the interaction between the RE and the target; sensitivity depends on the minimum amount of the analyte that the biosensor can detect. This value is usually known as limit of detection (LOD) and should be as low as possible to detect analytes at low concentrations. Reproducibility is the capacity of the sensor to

provide identical results when the experimental procedure is repeated. Stability is the extent of vulnerability of the sensor to ambient conditions that can cause a signal drift. Linearity is the accuracy of the obtained response and traduces the ability of the sensor to recognise small changes in concentration. It is related with the resolution of the sensor that is the smallest variation in the concentration of the analyte of interest necessary to originate a change in its response (22, 67, 68).

Biosensors can detect a single molecule, or they can be multiplex, detecting an array of molecules, with high selectivity even if they are at low concentrations (6, 7, 9). Additionally, they fulfil the requirements of PoC devices being easy-to-use and providing a rapid preliminary screening and with the possibility of being performed outside the laboratory (1, 3, 5, 7, 9, 25). For the above mentioned reasons, biosensors represent a reliable alternative to conventional techniques in biomarkers detection and several researchers have been focused on the development of biosensors for the detection of many diseases including cancer.

Biosensors can be developed based on a labelled or label-free format. The labelled format entails the use of a label (e.g. enzymes, fluorescent or colorimetric molecules, radioisotopes, electrochemically active probes, nanoparticles (NPs)), usually coupled with RE as antibodies or aptamers. This approach can be used when the recognition event is not capable of producing a measurable signal itself or to amplify the generated signal, thus increasing the sensitivity of the sensor. As a result, the signal indicates the number of analyte molecules bounded to the labels. Despite the advantages, labelled sensors involve the use of several reagents, increasing the complexity and the cost of the sensor and labelling can affect the binding sites of the molecule, thus hindering the affinity between the RE and the analyte (69-71). Label-free biosensors provide advantages in terms of simplicity and rapidity (70) as no label molecules are used, and the signal generation is based on physical features of the target as surface charge, atomic mass, size, index of refraction or electrical impedance (69). Most common label-free detection methods include MS, surface plasmon resonance (SPR) and localized surface plasmon resonance (LSPR) (71). Since no labels are used in label-free biosensors, their sensitivity can be enhanced through the use of nanomaterials as carbon NPs (CNPs), gold NPs (AuNPs) (69).

Biosensors are frequently classified according to the nature of REs, or the transducer used in the sensor assembly.

2.4.1. Recognition elements

REs comprises a key element in the design of a biosensor and should be carefully selected and used to selectively recognise the desired target. These molecules can have natural or artificial origin

and should have highly specific binding affinity towards the analyte (72). A wide variety of REs can be used in biosensors assembly, as antibodies, nucleic acids (e.g. DNA, miRNA, aptamers), enzymes and proteins, cells and tissues or MIPs (22) (Figure 2-6).

Cancer biosensors generally utilize antibodies or complementary nucleic acids as REs (9).

2.4.1.1. Enzymes

Enzymes are proteins with catalytic activity that catalyse chemical reactions of certain substrates, resulting in the production or consumption of a specific substance (22, 66, 73).

Due to its catalytic efficiency and high specificity, enzymes are frequently used as sensing elements in biosensors. These molecules can interact directly with the target thus generating a detectable product or they can react with the target causing an alteration in structure of the enzyme, including its activation or inhibition. They can be combined with different transduction systems to monitor the reaction as electrochemical, fluorescent, or colorimetric ones (22, 66). Most enzymatic sensors use electrochemical detection due its high sensitivity and ability in to exchange of electron and hydrogen occurring in catalytic reactions involving enzymes (66, 73). These devices are useful techniques both for quantitative and qualitative analysis of a wide variety of target molecules in different areas as clinical diagnosis, food quality monitoring and environmental control (73). Oxidase-family enzymes (glucose oxidase (GOx), cholesterol oxidase, lactate oxidase, choline oxidase and acetylcholinesterase) are frequently used (66, 73). The most well-known example of an enzymatic sensor is the glucose sensor, where GOx is used as RE. In that case, GOx catalyses the oxidation of glucose in the presence of oxygen, with generation of gluconolactone and H_2O_2 (70).

Despite its utility as RE, enzymes are functionally active molecules in a narrow bandwidth of pH, temperature, salt and metal concentrations and solvents, which can be a limitation in the use of enzymes as RES in biosensors, as it involves specific storage conditions and costs related with production and purification of enzymes (66, 70, 74). As enzymes are unstable and sensitive to several conditions, the development of an enzymatic sensor should be detailed planned and parameters that can affect enzyme activity and stability should be carefully optimised (73, 75). The preservation of bio-catalytic activity of enzymes should be considered during the biosensor assembly and immobilisation chemistries of the enzyme on sensor substrate should be studied to protect enzymes from denaturing and self-aggregation.

One of the major factors affecting enzymatic-sensor performance is enzyme immobilisation. Enzymes can be immobilised onto the substrate of the sensor, as paper for instance, by adsorption, covalent immobilisation, or polymeric entrapment. Each of these strategies have their pros and cons and enzymes can lose their activity during the immobilisation process as consequence of inappropriate orientation and weak accessibility of the redox system to the enzymes (73). For example, enzyme adsorption onto a substrate may provide fast and sensitive detection of the target but enzyme leaching during the different steps may be a concern. Covalent immobilisation of the enzyme can prevent this leaching. The integration of enzymes as RE into paper substrates, improves its catalytic efficiency, as well as stability which impact the sensor performance (73).

The weaknesses of using natural enzymes in biosensing can be overcome by using nanomaterials with enzyme-like properties, such as nanoenzymes, which are usually functionalised NPs that can mimic the catalytic activity of enzymes. Nanoenzymes can be produced on a large scale, with a simpler process and at a lower cost. They offer higher stability and robustness in harsh environments and are active in a wide pH and temperature range.

Nanomaterials with different compositions and structures have shown to have enzyme-like activity, including peroxidase-, oxidase-, catalase-, and super-oxide dismutase-like nanozymes. However, nanozymes can present some drawbacks as low specificity (70, 74).

2.4.1.2. Antibodies

Antibodies, also known as immunoglobulins (Ig), are large glycoproteins produced by the immune system of humans and higher animals, with the function of neutralizing pathogens or other foreign substances to the body (76-78). They are natural bioreceptors (72), being the most popular REs used in biosensors, due to the specificity of the antibody-antigen binding (22). The term “antibody” was first used by Paul Ehrlich, in 1891 (79), but these molecules were only used by the first time in immunosensors, in 1959, by Yalowan Berson (80). In immunosensors, the binding event is based on antigen-antibody interaction, which provides highly specific recognition capability to these sensors, enabling the identification and quantification of different analytes (3, 74, 81).

Regarding the production technique, antibodies can be classified as monoclonal or polyclonal. Monoclonal antibodies are laboratory-engineered proteins capable to recognise one specific epitope of an antigen (22). Firstly, an antigen is selected and used for immunization of to

immunize laboratory animals, that will produce antibodies as an immune response. These antibodies are then isolated from the animal and fused with myeloma cells. The result is hybridomas that retain the characteristics of both used cells and have de the ability to produce identical monoclonal antibodies in at on a large scale. Thus, the production of monoclonal antibodies therefore requires both in vivo and in vitro conditions. Polyclonal antibodies, by on the other side are produced in vivo through immunization of animals by repeated injections of the desired antigen of interest which elicits an immune response, and therefore antibodies production (82). They can detect multiple epitopes, having the capability of recognise an antigen from different orientations (22). Monoclonal antibodies require a higher initial investment and trained personal but once hybridomas are produced, they are an endless source of antibodies with low batch-to-batch variability which assures highly reproducible results (82). For this reason, they are usually preferred in the development of biosensors for cancer biomarkers (72, 82). By on the other hand, polyclonal antibodies are expensive for long-term production due to the use of animals and their maintenance over long periods of time. In addition, these animals are more susceptible to infections and may die because of the process. Despite the wide range of applications of polyclonal antibody production, they are not suitable for sensory applications due to their numerous binding sites and large variations in affinity and specificity between batches (82).

Antibodies consist of two fragment antigen binding (Fab) arms, which are responsible for binding to the foreign substances, and a third fragment, the crystallizable or constant fragment (Fc), which has the task of binding to the molecules intended for antigen elimination (78). An antibody has two heavy chains and two light chains, binding together by di-sulfide bonds, to form a Y-shape (77, 83). The heavy chains are composed by one variable region and three constant regions, enabling antibodies classification into five sub-classes (IgM, IgD, IgG, IgE and IgA). By the other side, the light chain is formed by one variable region and one constant region (77).

For immunosensors, the immobilisation and orientation of the recognition antibody, the amount of this antibody on the surface of the sensor and the configuration of the immunosensor should be considered as they can influence the performance of the sensor. These parameters depend on the antibody immobilisation technique used and the characteristics of the surface used (76). Immobilisation of antibodies should not affect their specificity and immunological activity (77) and can be achieved by non-covalent (physical adsorption), covalent (chemical) and polymer

grafting. Due to its simplicity and versatility, the majority of the protocols apply the physical approach, in which the biomolecule is adsorbed on the surface by physical forces as electrostatic modifications (76-78, 83-87). Physical adsorption of molecules on cellulose paper, the main substrate used in this thesis, can be achieved by (a) dipping the paper on a solution of interest, followed by a dry step, (b) layer-by-layer deposition in which different compounds are used to create cationic or hydrophobic or cationic zones on paper surface or (c) ink jet printing which is more expensive but provides more reliable patterns on paper surface (87). However, physical adsorption may not be suitable for the detection of low concentrations (84) and could lead to a weak binding strength, thus affecting the biosensor performance, essentially in terms of reproducibility and stability (86, 88-90).

On the other hand, the covalent coupling ensures an irreversible connection between the antibody and the sensor surface, thus guaranteeing long-term stability and improved reproducibility. It uses surface modification with chemical linkers to introduce reactive groups that allow antibodies to bind through amine, thiol or carboxyl coupling reactions. The carboxyl-amine cross-linking strategy is one of the best established strategies for covalent binding. In this method, a sensor surface functionalised with amine groups is connected to the carboxyl groups of the antibodies by carbodiimide-based chemistry using N-hydroxysuccinimide (NHS) and 1-ethyl-3-(3-methylaminopropyl) carbodiimide (EDC) as linkers (89). Another covalent approach employs the oxidation of hydroxy groups present on Fc region of antibodies through the use of sodium or potassium periodate, resulting in with aldehyde formation that will further react with aminated groups (83). Finally, polymer membranes and sol-gel films are also used, acting as a protective layer between the sensor surface and the antibodies, thus reducing unspecific binding or entrapping the recognition molecules and helping the orientation (3, 90). The correct orientation of the antibody could also be achieved by the use of aptamers or other probes that capture the Fc region of the antibody (76).

Although antibodies can be easily immobilised on solid supports through the above mentioned techniques, their affinity for antigen has a propensity to be impaired due to random orientation, denaturation, and steric hindrance. For that reason, several methods for the oriented immobilisation of antibodies have been developed. Studies in which oriented and random immobilisation of antibodies was qualitatively compared show that antibodies orientation can significantly improve the binding efficiency (83). Thus, a proper orientation should be assured to not compromise the exposure of the binding sites towards the analyte and to guarantee a

uniform distribution of the RE over the sensor surface, which translates in higher recognition rates and reproducibility (89). Fc and Fab regions are the most commonly used in the development of immunosensors for the immobilisation of antibodies exposed to antigen binding regions (83). Three major antibody immobilisation approaches are considered, including the total exposure of the Fab region, its non-exposure or its partial exposure (76). Regarding this, immobilised antibodies can assume four different orientations, namely side-on, in which one Fc and one Fab is attached to the surface; tail-on, in which only Fc bounds to the surface; head-on, in which the two Fabs are linked to the surface and, flat-on, in which all the fragments are linked to the surface Figure 2-7 (83).

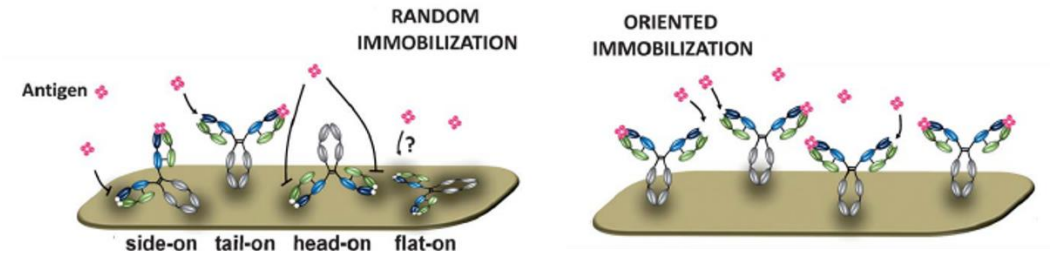

Figure 2-7. Schematic representation of random (side-one, tail-on, head-on and flat-on) and oriented immobilisation of antibodies. Adapted from (83).

Antibody-binding proteins as Protein A and Protein G can be used for oriented antibody immobilisation due to their ability to specifically bind to the Fc region of the antibody, while not interfere with the analyte binding. As Fc region do not bind to the antigen, using this Fc-binding proteins, assure that antibodies can be immobilised on the sensor surface while maintaining the Fab region available for antigen binding (90).

Several techniques can be used to analyse antibodies immobilised on a sensor surface, confirming its presence, and elucidating about its orientation, such as Fourier-transform infrared spectroscopy (FTIR) which enables the identification of specific chemical groups, fluorescence microscopy that allows to see the efficient binding of analytes in surfaces functionalised with antibodies, atomic force microscopy (AFM) that provides information about the degree of coverage of sensor surface, as well as thickness of the layer and shape of immobilised antibodies (83).

Immunoassays can be classified in two different categories. In homogeneous immunoassays, the biochemical reaction takes place in the solution phase, while in heterogeneous immunoassays the RE (an antibody or an antigen) is immobilised on the transducer surface,

where the binding interaction occurs (3). The detection can be direct where no labels are used and the changes resulting from the immunochemical reaction and formation of the complex are directly measured or it can be indirect, where a label is coupled to the antibody or antigen (3). An approach that widely uses antibodies as REs is ELISA. It was firstly described in 1971, by Peter Perlmann and Eva Engvall, for protein detection (91) and it is considered the gold standard method for detection of several molecules as proteins, antibodies, hormones, toxins and drugs (70) being applied not only in diagnosis but also in to food industry, toxicology or drug monitoring (76, 78). Several commercial ELISA kits are available for human immunodeficiency virus (HIV) detection, Influenza, Ebola, dengue, among others. ELISA procedures start with the adsorption of an antigen or antibody to a solid substrate (e.g. plastic microplates, cellulose paper). The test sample is then added followed by the reaction mixture. A wash step enables the removal of unbounded reactants. An enzyme-labelled antibody is added and finally the substrate enables color development whose intensity is usually proportional to the analyte concentration and can be visualized and quantified (78, 92). Furthermore, the ELISA readout can be performed by spectroscopy, colorimetry (CM), fluorescence, luminescence, or chemiluminescence (CL). Conventional ELISA is typically performed in 96 well plates of polystyrene, allowing several samples to be measured at each experiment. However, ELISA protocols take several hours due to several steps, such as long incubation times and washing or blocking steps. Also, high volumes of sample and reagents (20-200 µL) are consumed and specialized instruments are needed. These reasons limit its application in PoC devices and its use in low-resources areas (93). Apart from plastic materials (well plates) used in conventional ELISA, several immunoassays on paper-based substrates have been used, such as lateral flow immunochromatography on nitrocellulose membranes and dot-immunobinding assays (DIBA) in filter paper (94). As the work developed on this thesis was based on a paper-based ELISA (P-ELISA) approach, this topic will be discussed in more details at the section 2.4.3.1.4. Paper-based enzyme-linked immunosorbent assay.

Different signal transducers can be coupled to immunosensors, and thus they can be classified into optical, electrochemical, and piezoelectric immunosensors (3, 74, 81). Electrochemical immunoassays have high sensitivity and enable the development of low-cost devices with operational simplicity and potential automation and miniaturization. They are reliable for small and large molecules and enable the detection of trace amounts of biological molecules (3).

Different electrochemical methodologies have been employed on the development of electrochemical immunosensors, as amperometry, voltammetry, potentiometry, impedimetric, electrochemiluminescence (ECL), piezoelectricity and field-effect transistor. In these sensors, amplification strategies have been used, through the use of nanomaterials or enzymes for signal amplification (3). Colorimetric immunoassays may be based on changes on optical properties of nanomaterials, in consequence of three different phenomena: aggregation-based method, based on NPs aggregation induced by the presence of the analyte; morphology-based method, based on changes on its morphology; enzyme-mediated method, based on color changes of NPs produced by enzymatic reactions (3). Colorimetric immunoassays for cancer biomarkers detection have gain significant attention (17). In these sensors, detection probes are commonly used and labelled with enzymes, in ELISA. However, enzyme-based detection has some drawbacks, related with high costs and denaturation (3).

Despite the advantages of current immunoassays and their wide use in clinical diagnosis, they still face some important challenges that need further consideration. Continuous research in this area and its evolution is essential to broaden the applications of immunoassays, especially in the clinical field. Effective and stable integration of the RE into the transducer surface, adequate functionalisation of nanomaterials and biocompatibility of the nanoprobes with *in vivo* assays are some of the major challenges (3, 81).

2.4.1.3. Molecular imprinting polymers

MIPs are synthetic polymers that act as artificial receptors with high-affinity binding sites to a specific target analyte, due to the formation of complementary cavities on the polymer network. Molecular imprinting technology (MIT) is an emergent technique that enables the production of MIPs, capable of mimicking the biological recognition event. They are considered artificial receptors and can be used in alternative to natural receptors, allowing to overcome some of its limitations (95).

In 1955, Dickey (96) modified silica adsorbents with organic dies, based on the concept of molecular imprinting. However, the preparation of these materials reveals low reproducibility and only moderate selectivity for the target. Later in 1970 Wullf *et al.* (97) and Klotz (98) showed the impression of templates in organic polymers with formation of specific cavities. In 1993, Mosbach *et al.* (99) shows the utility of MIPs in replacing antibodies in biosensors through a radiolabelled ligand-binding assay (100).

MIPs have some unique properties that make their application suitable in different as separation, biosensing, catalysis and drug delivery (25, 101-103).

2.8.1.3.1. Production

MIPs production is a multi-step process (Figure 2-8) involving the combination of functional monomers and at some cases, cross-linking monomers and an initiator, in the presence of a target template (103-106).

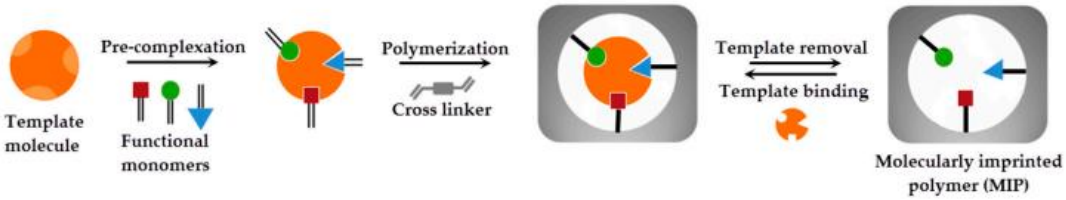

Figure 2-8. Steps of MIP production. Taken from (106).

The above mentioned components are dissolved in a porogenic solvent and covalent, non-covalent or semi-covalent chemistry leads to the formation of a complex between the functional monomers and the template (25, 101). When monomer and template are put together, functional groups of the monomer orient through their respective groups in the template molecule and cross-linker immobilises the orientation of functional groups (95). Then, free radical polymerization or electro polymerization enables the connection of molecules of functional monomer forming a 3D-network that could be induced by different external stimuli as heat, light, charge or even chemicals (25). For MIPs production, different imprinting approaches can be considered as bulk or surface imprinting (25, 101). Lastly, the template is removed from the imprinted material allowing the generation of template-specific binding cavities at the surface of the sensor. This removal step can be achieved via physical (heat) or chemical (acids/bases, detergents, enzymes) processes. Another type of protocols, such as washing surface with excess of ions or ultrasonic treatments are also reported in the literature (95). As orientation of functional groups remains after template removal, the formed cavities will have specific binding sites complementary in size, shape, and functionality to the target (104-107). A non-imprinted polymer (NIP) is prepared in parallel, in the same way as MIP but in absence of template (100).

The performance of a MIP can be affected by the combination of components in polymerization mixture and their amounts, such as type and concentration of monomer, cross-linker, initiator

and solvent, as well as experimental conditions as temperature or time of polymerization (108-110).

Templates used in molecular imprinting could be ions, atoms, molecules or cells (110). The selected template should have great chemical stability during polymerization reaction and must contain functional groups that establish complexes with functional monomers and do not inhibit polymerization reaction (110). In some cases, for example, when the template is a rare molecule or has a high toxicity or is not stable under imprinting conditions, structural analogues could be used instead of the template (95).

The number and variability of functional monomers that could be used in molecular imprinting is restricted, thus limiting selectivity and potential applications of MIPs (110). A functional monomer should be wisely chosen with respect to their functional groups to interact with template by covalent or non-covalent bindings, forming a stable complex and creating highly specific cavities (95, 102, 109). A strong interaction between functional monomer and template leads to the formation of a stable complex, thus improving the binding capacity of the MIP (109). Carboxylic acids (acrylic acid, methacrylic acid, vinylbenzoic acid), sulphonic acids (2-acrylamido-2-methylpropane sulphonic acid) and heteroaromatic bases (vinylpyridine, vinylimidazole) are commonly used as functional monomers (102, 109). Molar ratio between template and functional monomer also affects the binding affinity of the MIP and should be optimised, once lower molar ratios leads to less binding sites but higher molar ratios could induce non-specific binding (109). Combinatorial and computational methods have been used to predict the conformational and chemical complementarity between functional monomer and template and thus select the most suitable combination and their ratios and so improving MIP performance (111).

The cross-linker as the role to connect and fix the functional groups of the monomers around the template molecule forming a rigid 3D network polymer, thus contributing to the polymer morphology and the stability of imprinted binding sites after template removal (95, 102, 109).

The type and amount of cross-linker used in the polymerization affects the binding capacity of MIPs once low amounts of cross-linker doesn't allow to maintain the stability of the cavity configuration and could lead to non-specific binding and high amount of cross-linker could reduce number of recognition sites (109, 110). *N,N'*-methylene bis-acrylamide (MBAA), ethylene glycol dimethacrylate (EGDMA) (100), divinylbenzene (DVB), trimethylopropane trimethacrylate (TRIM) (102, 109) are some used cross-linkers.

When MIPs are prepared by free radical polymerization, initiators are used and reaction can be started in a thermal or photochemical way, being peroxy and azo compounds commonly used for that (110).

The porogenic solvent is responsible to bring together all the components of the MIP synthesis and produce pores in the polymer that enable access to imprinted binding sites (102, 110).

The solvent in which the MIP is prepared has a significant effect on the interaction between template and monomer. They should allow the dissolution of the other components but not interfere during the polymerization process. Organic solvents are usually selected for MIP production as they increase the hydrogen bonding and electrostatic interactions between monomer and template (112). The polarity of porogen influences interaction and strength of binding between template and functional monomers and in polymer morphology (109, 110). While less-polar solvents will stimulate the formation of monomer-template complex, enabling better imprinting factor, more polar solvents will hinder the formation of this complex, thus lowering the imprinting factor. However, the choice of a less polar solvent can compromise the solubility of the components thus leading to the precipitation of the produced MIP. The selection of a solvent with medium polarity will allow the dissolution of the components while not affecting so much the formation of the monomer-template complex (112). Organic solvents as toluene, chloroform, methanol, dichloromethane, tetrahydrofuran, *N,N*-dimethylformamide and acetonitrile are generally used (102, 110). When the template molecule or other component of the MIP is not compatible with organic solvents, for example when MIPs are designed to detect proteins, water or aqueous solutions as buffers can be used (113-117).

The imprinting of biological macromolecules as proteins, cells and viruses that remains a challenge in MIT once the polymer network can obstruct the mass transfer, thus causing slow leakage of template during removal step and slowing the rebinding kinetics (118). Macromolecules can even become entrapped in the network after polymerization, and cannot be extracted during removal step, thus hindering the rebinding (110, 119). Some strategies for imprinting of macromolecules have been suggested, such as surface imprinting, epitope-mediated or imprinting micro-contact imprinting (95, 109). Also, the presence of heterogeneous binding sites constitutes a problem in molecular imprinting, due to the formation of non-covalent bonds during polymerization step. Semi-covalent approach can be an alternative to surpass this question (109). In addition, when MIPs are synthetized in organic solvents, they show low binding capacity to the target in polar solvents such as aqueous media**.** To overcome this

situation, many methodologies have been developed, such as applying a two-step extraction method or using hydrophilic monomers for the development of water-compatible MIPs (109). Another challenging aspect related to the imprinting process is that changes in the protein conformation or protein denaturation can occur, which limit protein rebinding. Also, template removal could be successful, but the molecules used in removal procedure could be adsorbed in polymer, blocking binding sites and thus compromising template rebinding (25, 95, 101, 119).

2.8.1.3.2. Advantages and disadvantages of MIPs

MIPs have several advantages, such as high selectivity associated with the formation of cavities with affinity to the desired target and high sensitivity due to the transduction systems that can be applied. Stability, robustness and resistance to temperature and pressure are other advantages related to the synthetic nature of the materials. In addition, their manufacturing process is reproducible and cost-effective, with the possibility of mass production and compatibility with miniaturized devices, and the shelf life of the polymers is high. Nevertheless, MIP-based sensors can be designed to detect a variety of targets, including amino-acids, proteins, peptides, viruses, cells and chemicals as drugs or pollutants (25, 100, 102, 111).

Despite the several advantages of using MIPs and the simplicity of its production, the synthesis of a MIP for a specific template is time consuming and requires several tests until obtaining optimum conditions for several variables that affect the binding capacity of the final product (102). Also, as already mentioned, despite of the imprinting of small molecules (< 1500 Da) has been widely reported, macromolecular imprinting is still a challenge (103, 107, 118). In addition to that, in some cases, polymerization conditions are usually non-physiological, with harsh conditions that can trigger conformational changes in molecules such as proteins. Also, the existence of multiple heterogeneous binding sites in macromolecules could be the reason for nonspecific binding in the imprinting of this type of molecules. In addition, the choice of monomers for imprinting macromolecules may be limited if some monomers are only soluble in organic solvents which could compromise protein structure.

At least, not all the polymerization strategies are appropriate for all types of templates. For example, bulk imprinting is a standard imprinting method being successful for small molecules, but it is not suitable for macromolecules. Regarding that, many imprinting strategies have been developed to overcome these issues, as surface imprinting or epitope imprinting (107, 118).

2.4.2. Transducers

The transducer is the component of the biosensor responsible for converting the biochemical event that results from the interaction of the RE with the target molecule, into a measurable signal (Figure 2-5). Regarding the transducer technology, biosensors can be optical, electrochemical, piezoelectric (9). Electrochemical sensors are based on the conversion of the biological event into an electrochemical signal, while optical sensors detect the target based on modification of light absorption, fluorescence, luminescence, SPR, among other optical phenomena. On the other hand, piezoelectric sensors are mass-based transducers that identify mass changes to recognise and quantify the target (9, 120).

2.4.2.1. Electrochemical biosensors

Electrochemical biosensors enable the quantification of the target analyte through the detection of an electrochemical reaction (oxidation, reduction, or transfer of charges) on the electrode surface (61). These type of sensors are usually composed by a reference electrode, a counter electrode and a working electrode, the latter containing the RE (22). The intensity of the signal depends on the target concentration. Cyclic voltammetry (CV), square wave voltammetry (SWV), differential pulse voltammetry (DPV), linear sweep voltammetry (LSV), electrochemical impedance spectroscopy (EIS) and field-effect biosensor (FET) are the main electrochemical methods used in biosensors (61). Electrochemical biosensors provide fast responses, having high selectivity and sensitivity, and displaying a high potential for miniaturization and portability. As they provide fast response at ultra-low level of biomarker's concentration, electrochemical biosensors became a useful tool for BC biomarkers (26, 120).

Several electrochemical biosensors have been reported for BC biomarkers. The fabrication of these devices is technically simple, providing fast and cost-effective detection of cancer biomarkers, using low volumes of samples and with high sensitivity provided by electrochemical transduction systems. Also, these sensors can be integrated in small and portable PoC devices. However, electrochemistry requires the use of potentiostatic equipment for sensor construction and signal acquisition (10, 60, 121-123).

2.4.2.2. Optical biosensors

In optical biosensors, a RE is used in combination with an optical transducer system which provides a visible response, eliminating the need of an equipment to read the results and also

enabling the portability of the sensor (22). Optical sensors can provide direct label-free detection through quantification of luminescence or fluorescence or by color change/appearance/disappearance by the measurement of absorbance, transmittance, reflectance, phosphorescence or fluorescence emissions in different regions (UV, visible or near-infrared spectrum) (22, 41). Among these, CM is the most appropriate technique when simple and low-cost detection is intended. Also, it has potential for PoC devices and the results can be observed by naked eye (19, 124-126).

Optical-based sensors for cancer detection have been developed benefiting from the advantages of optical transducers and nanomaterials (3). For BC biomarkers detection, several biosensors have been reported, using different optical transduction methodologies, including fluorescence (15, 20), SPR (121), surface-enhanced Raman scattering (SERS) (127), ECL (123) and CM (128, 129). Optical biosensors usually offer good sensitivity and specificity for cancer biomarkers detection, enabling real-time responses. Also, the use of different tag molecules as fluorophores enables the detection of different molecules on the same device. However, some optical transduction methods require expensive equipment for signal acquisition. CM, that is the detection method used on for the sensors developed in this thesis overcome the need of this equipment, due to the possibility of naked eye detection.

2.4.2.2.1. Fluorescence

Among the optical properties used for monitoring a wide range of analytes, fluorescence is the most common, due to the selectivity of organic fluorophores and possibility of multiplexing (22). In fluorescence sensors, emission of fluorescence occurs due to the excitation of electrons at a certain wavelength and de-excitation at a superior wavelength. Fluorescent signal transduction highlights by their non-destructiveness, fast response, reproducibility and high signal intensity (130).

Compared to conventional molecular probes (e.g. fluorescent proteins and organic dyes), luminescent nanomaterials exhibit great physicochemical properties, such as long lifetime, high luminescence efficiency, narrow emission bands and high resistance to photobleaching. These properties depend on their size, shape and composition. Advances in nanotechnology enable the production of a wide range of fluorescent materials that can be used as diagnostic probes in various medical applications, such as noble metal nanoclusters, up-conversion nanomaterials, quantum dots (QDs), graphene oxides (GOs) or CNPs.

Fluorescent biosensors for cancer biomarkers as CA125 (131), CA15-3 (15), and BC-derived exosomes (132) have been reported.

2.4.2.2.2. Surface plasmon resonance

SPR is a sensitive optical technique that allows the real-time study of biomolecular interactions that occur close to the transducer surface, which is usually a thin-gold-film on a glass slide (3). On SPR-based sensors the binding interaction occurs between the RE immobilised on the transducer surface and its corresponding analyte, which causes changes in the refractive index, thus a shift in the resonance angle that can be detected and provide information about the concentration of the analyte that binds to the sensor, their affinity and association/dissociation kinetics (3, 26). Resonance is affected by the immobilisation of biomolecules onto the metallic layer, as well as the conformational changes of these molecules and interaction with other molecules (3).

SPR has been used as transduction method in biosensors to detect biomarkers, including the cancer ones, such as HER2 (133), CA125 (134) or miRNA-21 and miRNA-155 (135).

2.4.2.2.3. Surface-enhanced Raman scattering

Raman spectroscopy measures the inelastically scattered photons that result from vibrational frequencies when a molecule is excited with monochromatic light. It has been found that Raman scattering is strongly enhanced when a molecule is close enough to noble metal surfaces (e.g. silver or gold). This phenomenon of Raman scattering enhancement is known as SERS, increases the intensity of Raman scattering by up to 10-14 orders of magnitude and can be explained by chemical and electromagnetic components. It is considered a non-invasive and non-destructive technique (3).

Several cancer biomarkers, such as CEA (117), CA19-9 (136) and prostate specific antigen (PSA) (137), have been detected by SERS-based sensors.

2.4.2.2.4. Colorimetry

Colorimetric biosensors provide a highly sensitive response that can be applied to PoC devices as soon as the detection of biomarkers occurs through color changes that can be observed with the naked eye, both in solution and on solid supports (e.g. paper or plastic plates) (26). Several colorimetric formats have been developed to allow an easy interpretation of the results, as

distance-based, text-based, and time-based readouts. When coupled with a calibration curve, these assays can provide semi-quantitative instrument-free response (29).

Colorimetric assays detect the absence or the presence (and respective concentration) of the analyte of interest by evaluating absorbance or reflectance intensity changes due to chemical or biochemical reactions between the target and chromogenic substances used as probes (41, 138, 139). Absorbed or reflected light intensity generally results from optical properties changes due to SPR or structural shifts (41, 138).

Different types of nanomaterials and nanostructures have been used in colorimetric PADs with the function of carriers, target mediators or detection interfaces. The sensor surface could be modified with these materials to improve various parameters of the sensor such as sensitivity, LOD, detection range as well as selectivity towards interfering species (7, 43). In colorimetric assays, production or change of color could be induced by dyes, enzymes, or NPs (125, 139). Catalytic reactions or enzymatic conversion of chromogenic substrates is one of the most common approach used in colorimetric sensing, resulting from the reaction between an enzyme and their substrate thus forming an enzyme-substrate complex that produces color (125, 140). Oxidase enzymes catalyse the oxidation of chromogenic substrates thus producing H_2O_2 and other molecules and resulting in a color change (18).

Horseradish peroxidase (HRP) is an heme-containing oxidoreductase, found in the roots of horseradish (141) that catalyses the reaction of H_2O_2 with electron-donating substrates. Its small size (44 kDa), low-cost, high stability, capability to enhance signals, high catalytic substrate turnover rate, ease of conjugation with other molecules and solubility in aqueous media (141, 142) makes it broadly used in different applications, as research, industry and in sensing approaches, namely in ELISA, microarrays, Western blots and immunohistochemistry (143). Being a glycoprotein, HRP stability and high resistance to free-radical formation and temperature could be due to its large carbohydrate content; its ease of conjugation is related with a low number of lysine groups allowing a controllable conjugation process with other molecules; its high catalytic substrate turnover rate provides a quick colorimetric response when reacting with a chromogenic substrate. Also, this enzyme production is cheap and could be used in both colorimetric and chemiluminescent assays (141). Despite HRP, other enzymes as alkaline phosphatase (ALP) and β-galactosidase can be used in colorimetric assays (74, 78, 92). These enzymes catalyse the oxidation or reduction of chromogenic substrates, leading a color change whose intensity is proportional to target concentration. The result can be noticed

by naked eye for a qualitative response, or it can be analysed with a simple equipment as a smartphone or a spectrometer for a quantitative result (74). Substrates can be colorimetric, fluorescent or chemiluminescent, but the ones that provide color changes are preferred due to its simplicity and possibility to observe the results by naked eye (143). A wide variety of chromogenic substrates are available as o-phenylenediamine (OPD), 2,2'-azino-bis 3-ethylbenzthiazoline-6-sulfonic acid (ABTS), 3,3′-diaminobenzidine (DAB), pyrogallol, and 4-chloro-1-naphthol (4CN) (143, 144). However, most of these substrates are suspected to be mutagens or carcinogens (143). 3,3′,5,5′-tetramethylbenzidine (TMB) emerged as a safe alternative for the previously mentioned hazardous chromogenic substrates. TMB works as a hydrogen donor for the reduction of H_2O_2 by HRP, causing a color change (141).

When in reduced state, TMB originates a non-colored solution (diamine product), with a maximum absorption peak at 285 nm, which turns blue due to oxidation (142), with a characteristic absorption peak at 652 nm (74). The blue color intensity in consequence of TMB oxidization depended on the amount of HRP in the reaction (142). The presence of high amounts of H_2O_2 leads to a blue-green product and, at least, the complete conversion of the TMB (diamine form) into a two-electron-loss oxidation state that forms a yellow colored product (diimine form) and causes a peak shift from 652 to 405 nm (141). The above described reaction is illustrated in Figure 2-9. In ELISA methods using TMB, an acidic solution (hydrochloric acid or sulphuric acid) is usually added to stop the reaction and the formation of the yellow product. This low pH environment due to the addition of acid (from ≈5.5 to 1) switches off the HRP redox activity and this process resulted in an amplification of the absorbance signal (74, 141).

TMB is poorly soluble in aqueous buffers and has a low stability, so that the solutions must be freshly prepared before each experiment. However, TMB has advantages over other colorimetric substrates as it is neither mutagenic nor carcinogenic and has a higher sensitivity in HRP detection.

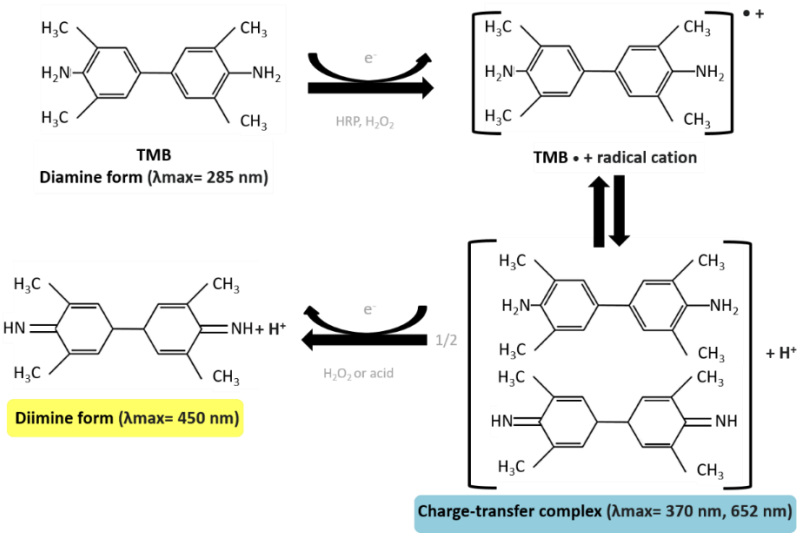

Figure 2-9. Catalytic oxidation of TMB by HRP.

Nevertheless, enzymes are natural molecules that sometimes offer little stability, sensitivity to environmental conditions and several drawbacks linked with their preparation and modification. To overcome these weaknesses, efforts have been made to mimetic peroxidase-like activity through the production catalytic nanomaterials (18). Metal nanoclusters, for example, have enzyme-like activity and could catalyse TMB in the presence of H_2O_2, leading to a blue product. This methodology has been used in the detection of cancerous cells (140). NPs are nanomaterials used as probes that are easy to synthetize with different shapes and from several materials and are easily functionalised. Metal NPs as AuNPs or silver NPs (AgNPs), magnetic NPs (MNPs), paramagnetic particles, cerium oxide NPs and CNPs as multi-walled carbon nanotubes (MWCNTs) and reduced GO lead to higher surface areas or allow the concentration of the target at the detection zone (18, 43, 145). NPs for labelling purposes should be chosen considering several parameters as their colloidal stability, efficacy of conjugation with REs and low non-specific binding capacity (146). Colloidal AuNPs are an interesting nanomaterial for colorimetric biosensing, being the most widely used label, with great potential to increase assay sensitivity.

In addition to enzyme-like nanomaterials, many other nanomaterials also exhibit optical properties due to their SPR effect, which can be influenced by parameters such as size, shape, composition, and distribution. Changes in these parameters lead to deviations in the maximum absorption wavelength and absorption intensity. Colorimetric sensors using NPs are usually based on color changes resulting from the interactions between analyte and NP and the subsequent aggregation or dispersion of the particles. The unique structural, optical (e.g. SPR

and LSPR) and catalytic properties of AuNPs make them an interesting material for use in sensing field (147, 148). These NPs can be easily synthetized through well-established and inexpensive protocols, from different materials, thus resulting in different compositions and originating different sizes and shapes. They exhibit high stability both in solution and in dried form and can also be easily modified, thus, emitting different wavelengths of resonance light scattering (18, 43, 128, 146). Antibodies, proteins, peptides or aptamers can be used to functionalise bare AuNPs in order to allow the specific target recognition, thus improving the performance of colorimetric detection (149). They are used to bind to secondary antibodies in immunoassays, booth in solution or solid supports, and their aggregation/disaggregation due to specific interaction with the analyte induces a change of color (125). The produced colorimetric response can be seen by naked eye or monitored by ultraviolet-visible (UV/Vis) spectroscopy. When the aggregation or enlargement of particles occur due to the presence of the target, distance between adjacent particles decreases and the SPR suffer a red shift of absorbance peak to higher wavelengths. This phenomenon leads to a color change from red to purple or blue and thus enabling the direct or indirect sensing the target analyte. A change of color from purple or blue to red is observed when dispersion of particles is induced (126, 147, 149, 150). If the sensitivity of the assay is not enough for naked eye detection, signal amplification approaches can be used (148). The above mentioned reasons make AuNPs a highly attractive material for chemical and biological biosensors and potentiate their use in colorimetric assays (149, 150), in alternative to enzymes or fluorescent, radioactive, chemiluminescent and bioluminescent labels (148, 150-152). They allow naked eye results, suitable for PoC devices because there is no need for advanced equipment or trained professionals (150).

2.4.3. Sensor's supports

All over the world, especially in developing countries, clinicians fight over high costs and limited resources for diagnostic systems. The use of inexpensive substrates, as paper, to develop sensor devices could be helpful.

2.4.3.1. Cellulose paper

Paper-based sensors are sensing devices fabricated on a paper substrate (72). Paper is mainly constituted by cellulose and is a widespread and highly versatile material, easy to fabricate,

storage and transport. It is often used for writing, drawing, printing, and wrapping (41). Its abundancy at low cost, makes it an interesting alternative to more expensive substrates as glass or polymer-based devices and a very fascinating material for the immobilisation of sensing materials and thus for the development of cost-effective devices (3, 5, 24, 153). Since paper has been used as substrate to measure pH in 1700s (154), PADs have been attracting attention as an interesting analytical tool for PoC detection in several areas, as fundamental parameters detection (e.g. temperature, humidity, pH), diagnosis and therapeutics (urine analysis, immunoassays, drug abuse), food and water quality control, environmental monitoring (e.g. pathogens, pesticides), and forensics (drugs, explosives) (155).

Cellulose $(C_6H_{10}O_5)_n$, which structure is represented in Figure 2-10 (153, 156, 157) is the a renewable polymer, obtained from trees, plants and some non-pathogenic bacteria (43). It is a linear homopolymer (shown in blue) consisting of repeating D-glucose units (shown in orange) covalently linked by β-(1,4)-glycosidic bonds between the hydroxyl group (-OH) in C4 and the carbon atom (43, 87, 158). Cellulose is the a renewable polymer, obtained from trees, plants and some non-pathogenic bacteria (43). Cellulose activation sites are the hydroxyl groups on 2, 3 or 5 positions (represented in red) on the pyranose ring (represented in green) (158).

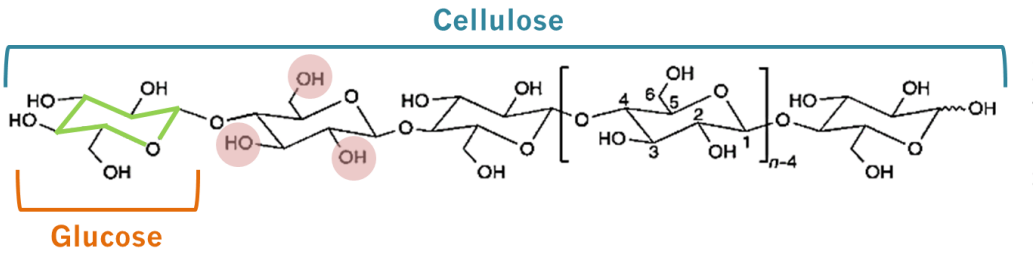

Figure 2-10. Molecular structure of cellulose. Adapted from (158).

Several chemical and physical properties of cellulose paper favour its applicability in bioanalytical applications. Their porosity and hydrophobicity as well as their characteristic surface chemistry influence their wet properties, which allow the penetration of liquids without pumping or external forces. Due to the large number of pores and the high surface area ratio, paper enables the immobilisation of reagents and subsequent drying, thereby storing these reagents for further use. Its anionic surface, rich in -OH groups, is very inert but can be easily modified with other functional groups so that several molecules can be immobilised. This modification can be done during the production of cellulose paper by mixing with organic

polymers or after production by soaking the paper. The cellulose surface can be oxidised to form aldehyde groups, which then react with amine groups on biological molecules such as enzymes or antibodies to form a Schiff base that enables stable covalent bonding. Paper is compatible with biological samples as proteins or antibodies and is biodegradable, allowing it facile disposable by incineration (24, 27, 41, 43, 66, 73, 87, 142, 153-156, 158-160). Optical properties of paper allow a white background, which is crucial for colorimetric assays, because it enable naked eye observation of colorimetric reactions without requiring additional instruments for signal detection (41).

A wide variety of paper materials is available, and several types of paper have been used in the development of PADs. The type of paper should be wisely chosen according to the fabrication method and application of the sensor (125). Whatman® paper No. 1 is the most commonly used, consisting of 98% of α-cellulose and having 180 μM of thickness and a pore size of 11 μM which provides a high wicking ability and medium flow rates (86, 153, 159). Other versions of this paper could be used as Whatman® paper No. 4 that has a larger pore size, providing higher retention rates. Filter paper is also frequently used in PADs (72), being characterised by an uniform thickness and wicking properties and thus leading to high adsorption and retention of reagents (125, 161). When filter paper is not suitable, nitrocellulose membranes can be used which is very common in lateral flow assays (LFAs) because their smooth surfaces with a 0.45 μM pore and several chemical functional groups, that enable covalent modification with biomolecules and provides high degree of retention (125, 161). Bioactive paper, whose surface is modified with biomolecules, nylon membranes and common paper (e.g. conventional printing paper or paper towel) are also used in the development of PADs (125, 159, 162). Lastly, bacterial cellulose could be used in PADs, due to its transparent property and special composition of nanofibers, being free of lignin and hemicellulose (159).

Paper is naturally hydrophilic, thus hydrophobic barriers are often required to restrict flow of samples and reagents to specific paths, preventing their mixing and contamination. These barriers can be produced by either chemical modifications or physical deposition. Photolithography, inkjet printing, wax printing, screen-printing, chemical vapor-phase deposition, plasma treatment, paper cutting, and laser treatment have been used to create these hydrophobic barriers, among other chemical and physical techniques (41, 72, 125, 129, 163, 164). Wax patterning has been the most used technology for paper patterning due to its

simplicity (164) and consist in using melted wax to print wax patterns on paper surface that create hydrophobic barriers that allow to control the flow of liquid samples and reagents (125). The interest in PADs has grown exponentially in the last decade and their conjugation with portable readers as smartphones make them meet the criteria for PoC devices (27, 153), represent an alternative to conventional methods for the detection of biomarkers, especially in places with limited resources, if they fulfil the WHO's ASSURED requirements (i.e. affordable, sensitive, specific, user-friendly, rapid and robust and available to the end user). Affordability is met by using inexpensive materials such as cellulose and plastic carriers. High sensitivity could be achieved by NPs of different materials as colorimetric probes, and they can be easily functionalised with REs to achieve good selectivity; sensitivity avoids false-negative results, while selectivity prevents false-positive results; PADs are also user-friendly and accessible to the end user as they are easy to use, do not require additional steps between sample collection and sample application and do not use invasive samples, so results are easy to understand and do not require trained personnel or sophisticated equipment; the porosity of the cellulose allows capillary forces to act, so a rapid result is achieved; .Also, PADs are robust devices due to their constituents; patients could self-test at home without the need to go to the hospital, due to the deliverability of these devices or they can be performed in a clinic or in a hospital in a rural setting (1, 24, 29, 41, 66, 155, 157, 159, 161). Different types of samples can be collected and used in PADs, as blood, urine, saliva, water, soil, food and drug samples (29). Poor sensitivity and the ineffectiveness to provide quantitative measurements are the main challenges of these types of devices but could be overcome by the development of new designs and application of new materials.

2.4.3.1.1. Types of paper analytical devices

Different designs of PADs (Figure 2-11), including spot tests, dip-sticks, LFAs, and microfluidic paper analytical devices (μPADs) (24, 75, 81, 129, 163), have been developed and used for detection of analytes in different areas as clinical diagnosis, environment monitoring and food quality (24, 125).

2.4.3.1.1.1 Spot tests

Spot tests are rapid and inexpensive devices (155) and were applied, for the first time, in the 1930s and 1940s, for metal ion detection using colorimetric ligands (165).

2.4.3.1.1.2 Dipsticks

Dipsticks are a very simple format of PAD, easy to produce and providing results easy to analyse. It is based on the impregnation of reagents in a paper strip, leading to a color change, in the presence of the analyte, directly observed by naked eye. However, it suffer from some drawbacks as low accuracy and long analysis time, only providing a qualitative response (124, 125) The first dipstick appeared at 1956 for glucose quantification in urine (166). Other examples of dipsticks are pH strips or urine test-strips that are used nowadays to simultaneously screen multiple disorders as diabetes and kidney disease (124, 157, 167).

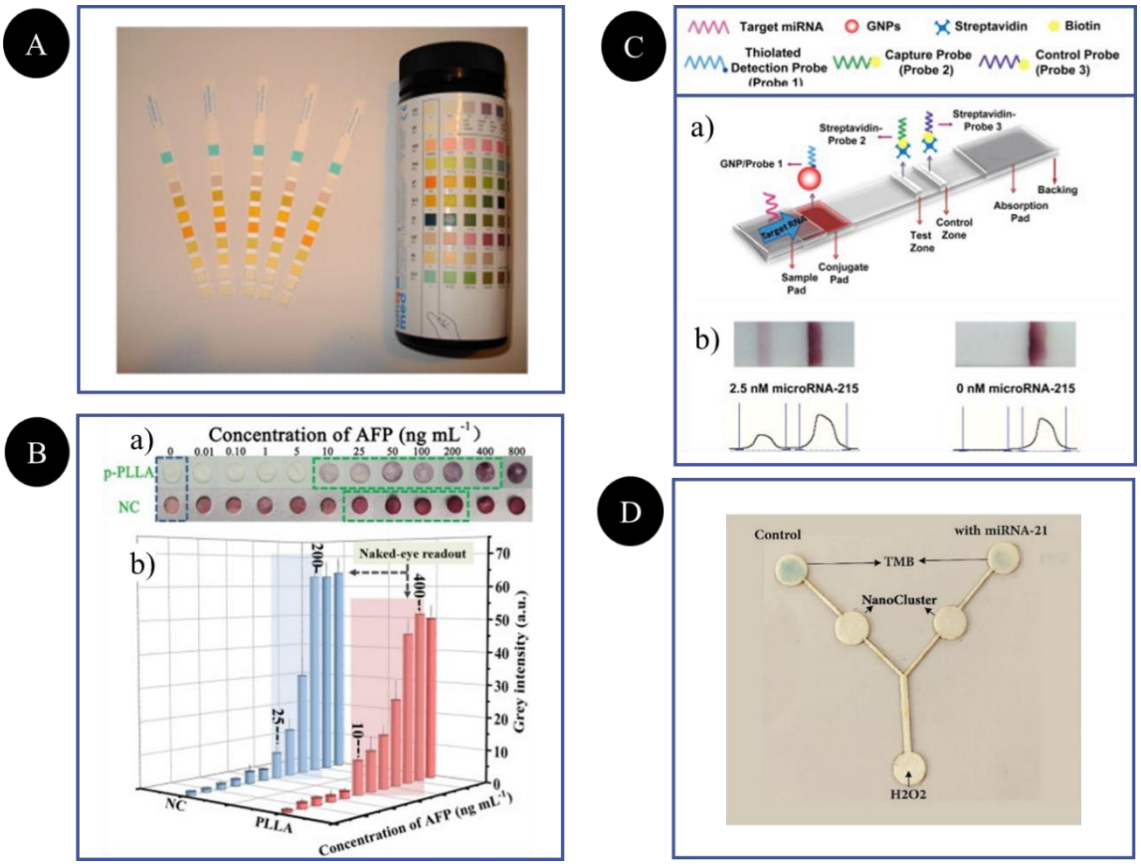

Figure 2-11. Examples of different formats of PADs. Photograph of dipsticks (A) for urine. Adapted from (168); Spot test (B): photographs (a) and bar charts (b) of grey values for alpha fetoprotein detection. Taken from (169); LFA (C): schematic representation (a) and photograph of a LFA for microRNA-125 detection. Adapted from (170); photograph of a μPAD (D) for microRNA-21 detection. Adapted from (171).

2.4.3.1.1.3 Lateral flow assays

First LFA was reported and patented in the 1956, by Plotz and Singer (172) and since then LFAs have been grown over the last decades with efforts to enhancing their performance (24). Pregnancy test is the most known example of LFA, being a very simple test that does not require

additional steps between sample (urine) collection and application in the test (29). LFAs are a powerful tool for several biomarkers' detection in clinical context as well as in food safety environmental monitoring (5, 167).

The principle of an LFA is that a liquid sample, containing or not the target, flows horizontally through the several pads of the device without the need of external forces and react with pre-immobilised reagents (146, 161). LFAs are generally formed by NC strips assembled on a plastic backing card, generally made of polyvinyl chloride and containing the different parts: sample pad, conjugate pad, flowing membrane or test pad and adsorbent pad (1, 16, 24, 75, 81, 161, 167). The sample and adsorbent pads are usually cellulose paper or glass fibers, whereas flowing membrane is commonly a NC membrane and conjugate pad is usually made by glass fibers (1, 75). The pads are assembled adjacently to allow a continuous lateral flow of the solutions and reagents when they are added on the sample pad (16). The sample is added to the sample pad that guarantees that the analyte reaches and bind to the capture reagents (146, 167). The sample further migrates along the conjugate pad which contains colored particles (e.g. metal NPs) responsible to capture the target once they are functionalised with REs (e.g. antibodies or aptamers) (16, 146). Then, the conjugate formed between the target and the RE, flows through the strip until it reach the test pad (146). The test pad is the platform for bio-analytical and recognition reactions once it is formed by NC strips that could be easily modified with different reagents to allow capture molecules immobilisation, thus forming the test and the control line (5, 16, 24). If the analyte is present, it will lead to a response at the test line, whereas the adequate flow through the strip could be assumed by the presence of color at the control line (146). Lastly, at the end of the strip, an adsorbent pad provides the continuous flow of sample based on capillary forces and, at the same time, it wicks the excess of reagents, preventing liquids reflux (16, 146, 167). The appearance or absence of colored lines at test line could be observed by naked eye or using an adequate reader (146).

Regarding the RE used, there are two principal groups of LFAs. Lateral flow immunoassays (LFIA) are the most common ones, in which the REs for the analyte of interest are labelled antibodies (146). On the other hand, aptamers could be used for target recognition, resulting in aptamer-based LFAs (167).

LFAs are usually associated to colorimetric or fluorescent transduction systems (146) and colloidal AuNPs are commonly used as colorimetric probes in LFAs once they have unique optical properties and are easy to functionalise for target recognition (24).

Two basic assay formats for LFA are considered: direct or sandwich LFA (sLFA), and competitive LFA (cLFA). sFLA is more suitable for high molecular weight compounds detection and includes two separated recognition steps that enhance the selectivity and sensitivity. In this assay, a primary antibody immobilised on the conjugate pad captures the analyte forming a complex that will be further captured by a transducer element immobilised at the test line, generally a colorimetric probe conjugated with a secondary antibody. The presence of the target at the test line led to the development of a positive signal that is proportional to the target concentrations. On the other hand, cLFA is more appropriate for small molecules detection, with single antigenic determinants. In this approach, the analyte competes and block the binding sites of the RE at the test line, preventing their interaction with the conjugates. Consequently, the concentration of the target is inversely proportional to the signal intensity (1, 3, 24).

LFAs have several advantages as it low-cost, user- friendly format, high shelf life, high sensitivity and selectivity, the requirement of small sample volumes, the possibility of multiplex detection and a wide range of applications (24, 43). Conversely, some drawbacks are implied and need to be overcome. Regarding membrane matrix and REs, novel materials have been explored in order to enhance their performance (24).

2.4.3.1.1.4 Microfluidic paper analytical devices

The first μPAD was created by a photolithography technique for colorimetric detection of glucose in urine from Whitesides laboratory in 2007 (173). μPADs are created by applying a pattern onto paper thus creating hydrophilic channels and defining different reaction zones, which enables multiplex detection. Also, these channels facilitate the direct flow of the sample, in opposite of which occurs in LFAs and spot tests (5, 143, 161). Two types of μPADs are considered, namely two-dimensional (2D) μPADs, formed by channels created by chemical or physical hydrophobic barriers, through several techniques as photolithography, wax printing, screen-printing, inkjet printing and plasma oxidation; three-dimensional (3D) μPADs constructed by folding several layers of patterned paper (5, 27, 28, 81, 161, 167). The fabrication technique should be chosen considering aspects as cost, substrate, time of fabrication and available equipment. Whatman® filter paper n° 1 is generally used in this type of devices due to uniform thickness and wicking properties. μPADs have the advantages of only require a very small amount of fluids (5 to 10 μL), could be miniaturized, could provide multiplex analysis by the creation of several channels, and simultaneously semi-quantitative and quantitative responses

and could provide low response times (28, 161). This type of PADs has been used in several applications as medical ones, environmental monitoring, food safety and forensic analysis (28, 81, 157).

2.4.3.1.2. Recognition elements and transduction systems used in paper analytical devices

The most common REs used in the development of PADs for cancer biomarker detection are antibodies and aptamers. Despite their broad application, researchers are continuously focused on develop new REs to improve the performance of these sensors, as MIPs.

When the target is a nucleic acid, oligonucleotides or aptamers are usually applied; for proteins, enzymes and cells detection, antibodies and aptamers are used (1). These receptors are immobilised on the paper surface and on nanomaterials, used as probes, and the immobilisation methodology should be wisely selected to enable the retention of molecules without comprising its bioactivity. In paper matrix, REs could be immobilised by either physical or chemical ways whereas the immobilisation of receptors as antibodies on tags, should occur by adsorption techniques, cross-linking (e.g. glutaraldehyde (GA), carbodiimide method) or covalent binding through cellulose binding domains (periodate oxidation, tosylation). Entrapment within a gel and microencapsulation can also be applied (159).

When using aptamers as REs, the attachment to NPs could occur using 5'-labelled sequences with thiol or amine groups, while for their immobilisation on the NC membrane, streptavidin-biotin interaction is commonly used (1, 159).

Ge et al. where the first group that demonstrated the potential and advantages of using MIPs as REs in PADs. They applied MIT into a μPAD, by electropolymerisation of a MIP in an AuNP-modified paper. The porous morphology of the paper substrate that provides high surface area in combination with the conductivity of the AuNP layer significantly increased the sensitivity of the sensor (174).

The methodology to prepare MIPs in PADs includes *in situ* polymerisation and post-introduction (Figure 2-12). *In situ* polymerisation strategy involves MIP synthesis directly on the surface of pre-modified paper fibers. Paper, which is rich in -OH groups, is usually treated with silane coupling agents to introduce other functional groups. This method is widely used due to its inherent simplicity. However, it requires the immersion of paper in solutions for a long time, which can affect the paper properties and introduce damages. In post-introduction method, the

MIP is directly synthetized in a solution phase through radical polymerisation or sol-gel polymerisation and then incorporated into PADs (175).

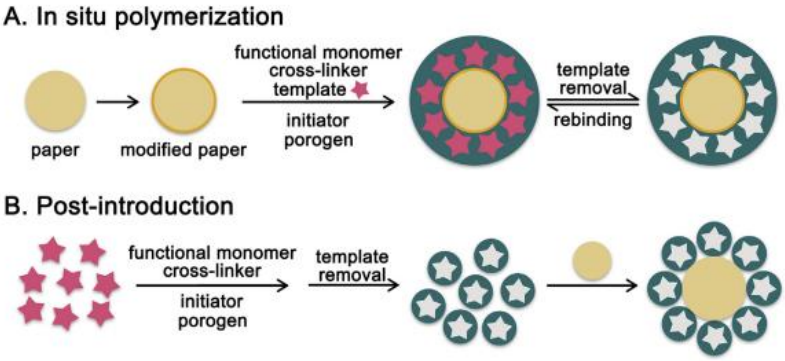

Figure 2-12. Schematic representation of MIP-PADs fabrication: (A) *in situ* polymerisation and (B) post-introduction. Taken from (105).

Optical transduction is the universal transduction system for PADs once it is the cheapest and simplest method (159).

Despite optical transduction, electrochemistry is also frequently used in PADs (72). Electrochemical is a suitable transduction system to be coupled with PADs due to the higher sensitivity, compared to optical detection (41). A three-electrode system is used, and the electrodes are deposited onto the paper surface by technologies as screen printing, physical deposition of metals, spraying or pencil-drawing of conductive inks (41, 168). As in other electrochemical devices, target analytes are analysed at the working electrode, while the redox reaction occurs at the reference electrode and the counter electrode is used to reduce the electrical current that flows to the reference electrode, thus maintaining a constant potential during the measurement (41).

Optical transduction as CM, fluorescence, CL, SPR, SERS and transmittance and electrochemical transduction such as electrochemistry, photoelectrochemistry, or ECL are usually coupled to MIP-based PADs to detect the analyte of interest. MIPs provide to optical sensors high selectivity to the target analyte and versatility as MIPs can be produced against a wide range of molecules (7, 41, 125, 153, 155, 159, 161, 167). Colorimetric PADs detect the analyte of interest when it interacts with a sensing element on the paper substrate, resulting in a color change. When colorimetric tests are performed on a solid substrate such as paper, detection is usually by reflectance, measuring the light reflected from the surface of the test (139). Colorimetric PADs have been applied for the diagnosis of different diseases as cancer

(128, 171), neurodegenerative (176, 177), infectious (178, 179), and chronic diseases (180, 181). As already mentioned, colorimetric sensing based on naked eye visual color changes is a very suitable approach for rapid tests and have several advantages over conventional methods once they allow a cost-effective, real-time, on-site and highly sensitive and specific detection of several molecules (162). However, these types of sensors usually suffer from lack of sensitivity, with interference of other molecules present on the sample. The combination of colorimetric detection with MIPs enables to overpass this drawback and allows these sensors to be used with complex samples (182). MIPs as RE coupled to colorimetric transduction enables a qualitative or semi-quantitative response by naked eye that can be performed in at home or in the field, without using any equipment (182).

In addition to selecting a suitable RE, a suitable transduction method should also be chosen to use paper-based sensors in analysers without compromising the simplicity, portability, and cost-effectiveness of the sensor.

2.4.3.1.3. Signal readout in paper analytical devices

Colorimetric detection is one of the most detection technique used in PADs once it offers the advantage of simple visual detection by naked eye, without the need of trained personal or sophisticated equipment as it provides an immediate qualitative ("yes" or "no") response or a semi-quantitative response by capturing the image with a camera and further transferred to a computer where image analysis will be performed by imaging software (153, 155, 162).

However, sometimes CM suffers from lack of selectivity and sensitivity originating heterogeneous signals that could be misunderstood by the users (41). Results can also be registered by readout devices that can be simple instruments as scanners, cameras, smartphones or more complex ones as spectrophotometers or fluorimeters (1, 24, 41, 124, 125, 139, 159, 161, 162). Smartphones are widely used for this purpose due to their advantageous properties as easy-of-use, high-resolution cameras and operative systems and wireless connectivity that enables real-time analysis (11, 138, 139). However, colorimetric detection with smartphones can have some drawbacks as the influence of light conditions, focal distance, and device orientation as well as camera characteristics as lens quality and aperture dimension (29, 73). For that reason, images should be carefully captured under controlled light conditions as in black or white boxes developed for this purpose, so it could not affect assay sensitivity and repeatability (24, 41, 139). In alternative to smartphones, office scanner could

also be used, being a device with high resolution and with the possibility of being portable and be used by unskilled personnel. Also, in this case, image is not affected by external light conditions (159). Still, spectrophotometers or fluorometers or more sophisticated equipment as microplate readers, photomultiplier tubes or even gel documentation systems could be used (159). Oppositely of colorimetric probes, fluorescent labels or paramagnetic particles cannot be read by naked eye thus requiring specific readers for quantitative measurements (146). Once captured, the images are transferred to a device such as a computer to be analysed using software such as Adobe Photoshop, Corel Photo Paint, ImageJ or DigitalColor Metre. This software is able to calculate parameters such as the red, green and blue (RGB) space or the hue, saturation and brightness (HSB) space. These values are used to calculate the target concentration (159).

Figure 2-13 illustrate several examples of samples that can be analysed in colorimetric PADs, as well as biomarkers that can be detected. Types of paper, REs and labels used on the assembly of PADs are also represented. Different types of signal readout coupled to PADs are mentioned.

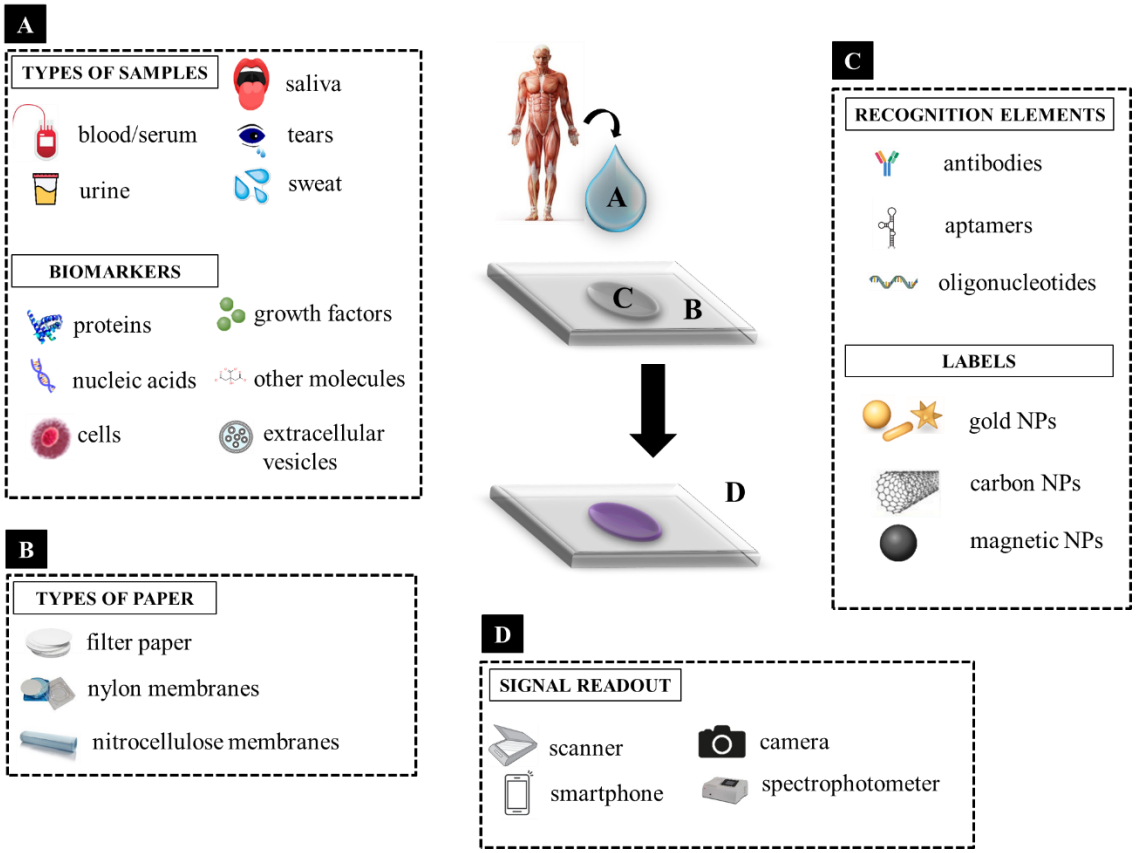

Figure 2-13. Examples of: (A) types of samples and biomarkers, (B) types of paper, (C) REs and labels, and (D) signal readouts used in colorimetric paper sensors. Taken from (183).

2.4.3.1.4. Paper-based enzyme-linked immunosorbent assay

As above mentioned, conventional ELISA is performed in plastic well plates, but it can be done in other type of supports, as cellulose paper. The first P-ELISA was performed by Cheng et al. (184) in 2010. They used filter paper as substrate for antibody-antigen recognition, through a simple and low-cost assay. High selectivity and sensitivity were achieved, about 10 times lower than the reached by conventional ELISA procedure in 96-well plates, for the same antigen-antibody pair (94).

The P-ELISA utilises the advantages of the high selectivity of the ELISA and the low cost of the paper substrate and thus offers a suitable diagnostic platform for the detection of biomarkers, which is particularly important in resource-poor areas. It is usually performed on 96-microzone paper plates, which are generally produced by structuring hydrophobic polymers in hydrophilic paper sheets. P-ELISAs have the advantage of high selectivity due to the antibody-antigen interaction and the ability to analyse complex samples without pretreatment procedures. This shortens the duration of the test as it can be performed in less than an hour, whereas conventional ELISAs can take several hours if they require an hour or more per step. The fast reaction is also due to the high surface-to-volume ratio of the paper. The reagents flow over a short distance and therefore require short incubation times. In addition, due to the small reaction area and high volume-to-surface ratios, only small amounts of samples and reagents are consumed (1-10 µL), which reduces the cost of the assay. Another advantage of P-ELISA is that results can be either qualitative or quantitative once observed with the naked eye or quantified using a desktop scanner instead of an expensive microplate reader. These advantages extend the application of ELISA to non-specialised laboratories and to developing countries. However, the sensitivity could be lower than conventional ELISA, which can be due to short antibody-antigen incubation times or non-specific interaction between antibodies and the cellulose paper. Other Another disadvantage of P-ELISA is that the test zones are subjected to environmental conditions as relative humidity and temperature, which could influence the rate of evaporation of water (84, 94, 159, 184-186).

2.4.3.1.4.1. Antibodies immobilisation

It was already mentioned the importance of antibodies immobilisation to the sensor surface and the related approaches for immobilisation (physical (non-covalent) or chemical (covalent). A study has shown that 40% of antibodies immobilised by physical adsorption onto cellulose paper

can desorb from cellulose fibres, thus affecting the sensor performance and not providing reproducible results (187). On the other hand, the chemical approach leads to stronger binding, thus enabling the development of effective PADs (78, 85, 86). Since cellulose paper surface have few functional groups for covalent immobilisation, it should be functionalised before biomolecules immobilisation (84). Biomolecules could be covalently attached to the substrate through the modification of the surface with agents such as GA, EDC, and NHS (78, 85). Cellulose chemical modification by oxidizing agents is also common leading to the formation of aldehyde (-CHO), ketone or carboxyl groups (188). Oxidation with periodate ($NaIO_4$) is used to graft biomolecules onto cellulose paper by cleaving the C2-C3 bond of the glucopyranoside ring, thereby converting the 1,2-dihydroxyl groups (glycol) of cellulose into aldehyde groups. Dialdehyde cellulose (DAC) is the resulting compound that is bound by antibodies through the formation of a reversible Schiff base between the aldehyde groups on the cellulose paper and the primary amine groups of the antibody (84, 85, 88, 188). Although it is a simple procedure, sodium periodate cannot be completely removed from cellulose fibers, thus causing oxidation of the immobilised antibodies (88). Chitosan could be used to modify the cellulose surface followed by GA that provide aldehyde groups for further biomolecules attachment (86). Another widely used technique is the silane coupling which enables grafting of amine functional groups that react with –OH groups on cellulose paper. 3-aminopropyltrimethoxysilane (APTES) is used to silane grafting (85).

2.4.3.1.4.2. Blocking step

Blocking agents should be added to the protocol, as without appropriate blocking, non-specific reactions may occur, resulting in a high background signal and low sensitivity. The use of a blocking buffer saturates the free binding sites on the paper surface and thus improves the signal-to-noise ratio. There are a variety of blocking buffers that should be optimised for each assay, taking into account the substrate, assay format and detection system. However, an ideal blocking agent must fulfil several requirements to reduce the background signal without compromising the selectivity of the assay. Firstly, it should inhibit the non-specific binding of other components to the surface of the assay. In addition, it should act as a stabiliser, not promote non-specific interactions between proteins and have no cross-reactivity with the other assay components. It must also have low enzyme activity so as not to interfere with the detection method and it should be reproducible between batches. The most common blockers are

detergents and proteins. Detergents used in ELISA assays are usually non-ionic (e.g. Tween-20, Triton-X) and are a cost-effective option for blocking despite the high concentrations used. However, as these are temporary blockers that can be removed by washing with water or buffer, they should not be used alone. Detergents should be added to the wash buffer to promote dissociation of weakly bound molecules and block the exposed binding sites. Protein blockers are permanent blockers. Bovine serum albumin (BSA), non-fat dry milk, ethanolamine, casein, normal whole serum and fish gelatine are common blocker proteins (76, 189). As detergents and proteins may not be suitable for all sensing surfaces, some polymers as polyethylene glycol (PEG) could be used for this purpose (76, 185).

2.4.3.1.4.3. Washing steps

Between the incubation steps in the ELISA protocol, the sensor surface should be carefully washed to remove the unbound molecules (78).

In conventional ELISA, the washing step is performed by filling the wells with the wash buffer using a pipette or squeeze bottle. The wells are then emptied by inverting the plate and the washing step is repeated, usually three times. After the last washing step, the plate is carefully dried with blotting paper (190). In paper-based ELISA, the paper surface can be washed by adding the washing buffer from the top and pressing the bottom of the paper against a blotting paper (84, 85, 184, 185). Several factors need to be considered, as the composition of the washing buffer, its volume, and the number of washing cycles. Regarding the composition of the washing solution, washing only with buffer as phosphate buffered saline (PBS) (27, 94, 186), or adding surfactants or salts to the buffer as PBST (PBS containing 0.05% of Tween-20) (84) or Tris buffer (50 mM) with NaCl (0.15 M) and 0.05% surfactant (85) have been used. Tween 20 (concentration up to 0.2%) is usually added to the washing buffer. Increasing the salt concentration (with NaCl up to 150 mM) can also help reducing the nonspecific interactions (190).

A low volume of wash solution or a low number of cycles might not remove the unbound molecules and thus lead to a high background, while a high volume or a high number of cycles might reduce the specific signal.

2.4.3.1.4.4. Antibodies concentration

The dilution factors of the sample and the capture and detection antibodies should be optimised. If the concentrations are not sufficient, the signal will be weak and interfere with the detection of the target molecule. However, if the dilution factor is too high, it may saturate the reaction of the assay.

2.4.3.1.4.5. Labelling (signal amplification)

Fluorescence and CL are the most common methods used in immunosensors to increase sensitivity. Fluorescence is the most used method as it is highly sensitive and non-destructive. NPs could also be used in the development of immunosensors. AuNPs and AgNPs are the most commonly used metal NPs in this type of sensor, but inorganic NPs, platinum NPs and europium NPs have also been used. A larger particle size enables the immobilisation of more antibodies and thus increases sensitivity. However, this approach could lead to unspecific binding (76).

2.4.3.1.4.6. Enzyme-linked immunoassay formats

There are many variations of ELISA protocol, including direct and indirect ELISA and sandwich and competitive ELISA (Figure 2-14) (78, 185). The choice of a proper ELISA configuration depends on several parameters as the purpose of the assay, the analyte size, the epitopes available and the availability of purified antigen (190). These formats are described for conventional ELISA performed in well plates, but the same formats can be adapted to P-ELISA. The direct ELISA is better suited for the detection of small analytes. First, the sample containing the analyte of interest is incubated on a solid support for a certain period. Washing steps between the different phases of the protocol remove excess or unbound biomolecules, leaving the antigen-antibody complex on the surface of the well (78, 185). Blocking agents helps minimizing the non-specific binding of other molecules. (185). Then, an enzyme-labelled antibody, specific to the analyte of interest, is added. The enzyme catalyses substrate conversion into a colorimetric product which absorbance could be measured at a certain wavelength. Finally, a stop buffer could be added to end the reaction (185). Direct ELISA is faster and simpler than other ELISA protocols and requires less buffers and reagents. On the other hand, it has some limitations related with the use of complex samples where several biomolecules could bind to the solid phase, thus lowering the selectivity of the assay. Besides

that, the sensitivity of the assay could not be enough to detect analytes in low concentrations (78, 190). The indirect ELISA is very similar to the direct ELISA, as it starts with the immobilisation of the antigen on the solid phase. Subsequently, a primary antibody is then added, followed by a secondary antibody coupled to an enzyme, that binds the Fc region of the primary antibody, thus leading to color development. The use of two antibodies in this methodology increases the selectivity of the assay. However, as well as like the direct ELISA, this methodology may have insufficient selectivity when complex samples are used (78). Sandwich ELISA is the most common used immunoassay format leading to the development of a wide number of commercial kits aimed for the quantification of clinical biomarkers (185). In sandwich ELISA, two different monoclonal antibodies are used, recognising different epitopes of the antigen (76, 185, 190). The capture antibody is firstly assembled on sensing surface, usually by non-covalent chemistry, followed by the antigen which is sandwiched between the capture and primary antibody. A secondary antibody, conjugated with an enzyme binds to the primary one leading to color development (76, 78, 92, 94, 185, 190, 191). In this type of ELISA, the antigen should be a large molecule with at least two distinct physically separated epitopes (92, 190). In terms of selectivity, the sandwich ELISA is one of the most precise techniques, among other ELISA protocols, such as direct or the indirect ELISA, as two antibodies are used for different epitopes of the antigen. However, this higher selectivity is accompanied by higher cost of reagents, and more is time spent on the protocol (78). The competitive ELISA is based on the competition between an unlabelled and a labelled antibody for binding to the antigen. In this method, a known amount of a target antigen (similar to the analyte of interest) is added to the sample and the color development is inversely related to the presence of the analyte of interest. The presence of the analyte leads to competition between the analyte and the added antigen, which prevents the formation of the colorimetric product, while the absence of the analyte means no competition and therefore produces a colorimetric signal (185, 190). Despite of this type of ELISA is more suitable for small molecules, it can be developed for any kind of analyte (76, 185).

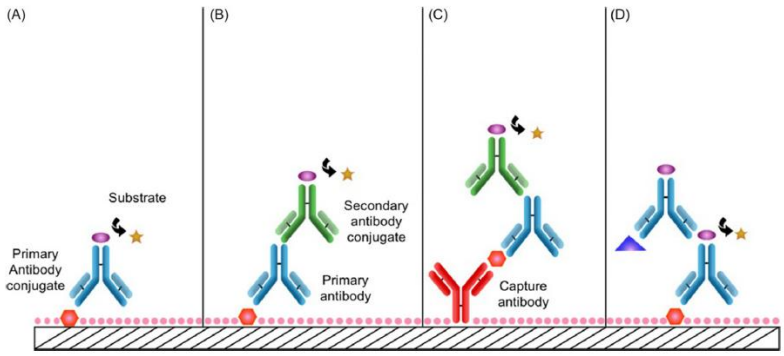

Figure 2-14. ELISA formats. Direct ELISA (A), indirect ELISA (B), sandwich ELISA (C) and competitive ELISA (D). Taken from (78).

Overall, biosensors present an interesting approach in several areas, highlighting its importance in disease diagnostics, namely cancer, especially the ones designed in a PoC format (1, 5). Although PoC devices are not intended to replace clinical tests, they have gained an increasing interest in the last decade, particularly for diagnostic purposes as they could offer a simple and rapid preliminary screening, even outside the laboratory (5, 155). Until now, several diagnostic tests for cancer biomarkers are available on the market providing a rapid and non-invasive detection (6).

2.5. Cancer biomarkers detection by colorimetric paper analytical devices

Colorimetric PADs are a cheap, fast, and simple test for the PoC of several molecules as cancer biomarkers with several advantages. Paper substrates allow the use of small sample volumes and do not require pretreatment of the samples. The PADs usually have a long shelf life and do not need to be refrigerated during storage, which is suitable for developing countries. Finally, as a naked eye result is provided by colorimetric transduction, there is no need of sophisticated equipment for readout (146).

PADs are suitable for qualitative and semi-quantitative analysis, helping in cancer screening. Even sensors with a qualitative response, providing instant results based on a color change, can be used to reduce cancer cases in low- and middle-income countries. These PADs are also relevant for detection of viruses, parasites and other agents, which were crucial in the recent pandemic period of covid-19 (72).

Despite the advantages and promising future of PADs, there are still some shortcomings that need to be addressed before PADs can be commercialised. The limitations mainly relate to manufacturing methods, reading equipment, legislation, sensitivity and accuracy. Most of the available fabrication

methods for paper patterning are expensive and require training personal which is not available in low- and middle-income countries (72). Some physical inherent properties of paper, as pore size, porosity, surface area, wettability, permeability and capillary flow rate, could not be rigorously controlled and will affect device performance in parameters such as fluid flow, color uniformity and reagents immobilisation (24). Regarding this, challenges in the design of new paper-based biosensing devices are related with the selection of papers with specific properties as appropriate porosity, paper purity, filtration speed or pore surface hydrophobicity (43), parameters that will affect retention and evaporation of samples and reagents (41). For this reason, physical and chemical treatments should be employed in order to reduce these batch-to-batch variations (24). The fabrication of hydrophobic barriers on μPADs is other important factor in PADs production that sometimes require costly equipment and skilled personnel (129). When visual colorimetric detection is applied to PADs, lack of reproducibility and sensitivity could be a drawback, leading to the need of the development of more precise and sensitive detection methods (5). Colorimetric readouts can lead to incorrect interpretation of results by untrained end-users and impact in color development due to environmental conditions (29). Accuracy of results can be improved by the combination with artificial-intelligence-based analysis (72). When the target biomarker is present at high concentrations, the sensitivity is not a problem, and the assay is capable to discriminate the patients from the healthy people. Nevertheless, in some diseases as cancers, biomarkers are at low concentrations, especially at early stages. In that case, a highly sensitive assay is mandatory (24). Alternative materials could be applied in sensitivity and selectivity enhancement approaches to allow a detection of trace levels biomarkers and better target recognition with discrimination from interfering substances (1, 24). Silver and enzymes, for example, have been used to amplify the signal of AuNPs (146). Additionally, and as it was already referred in this thesis, a significant number of PADs only enable qualitative or semi-quantitative responses, which is a major drawback of these devices. This can be overlapped by the development of new readout techniques (1) as electrochemistry or optical techniques as fluorescence, used to improve LODs on colorimetric PADs and to enable quantitative measurements. Nevertheless, we need to be conscious that these techniques require higher costs and complexity (5, 145). For example, luminescent labels have been used for fluorescent, chemiluminescent or electrochemiluminescent detection, leading to lower LODs when compared with colorimetric detection. However, these labels require specific readers, increasing the cost and complexity of the assay (24). Selectivity is also a crucial factor as complex samples are often analysed by these type of sensors with possible interference from the components of the matrix (5). As the diagnosis of a complex disease as cancer is generally a process

requiring the measurement of several parameters, the capability of the device to simultaneously detect several parameters, should be deliberated (5). To achieve this, different designs have been applied as strip arrays, star shape or multiple parallel channels. Still, it should be known that multiplex assays could suffer from lack of specificity due to cross-reaction, especially with complex samples (1, 24). Stability is other essential factor for sensor feasibility once an ideal device should be designed to be a long shelf-life, maintaining their stability even under less appropriate storage conditions (5, 24). Environmental factors such as temperature, pH and humidity could impact the quality of the PAD regarding to its stability (24). The activity of the biological molecules (e.g. antibodies, enzymes, redox probes) stored in cellulose pores should be preserved. For this reason, some natural materials have been replaced by alternative materials, as aptamers or other artificial receptors, with high stability (24). Furthermore, the naked eye observation of a colorimetric assay response could lead to subjective interpretation of the results. For a quantitative colorimetric assay, a clear color change should occur. Sometimes signal amplification strategies and an adequate tool should be used to evaluate the signal by digitalizing the color and providing numeral data (24). External factors as light conditions while capturing results should be considered as it can influence their quality. Also, a dry and a wetted paper should have differences regarding to color perception, so this factor should be considered. Other limitation of colorimetric PADs is related with less appropriateness for impaired and color-blind people (159, 162).

In view of the above, and although a number of PoC systems have been developed over the last decade, most of them have either not been commercialised or have not taken hold in the market due to a lack of integration and automation (24, 138). Also, despite LFAs and dip-sticks have been successfully commercialized, there are only few examples of μPADs in the market (5).

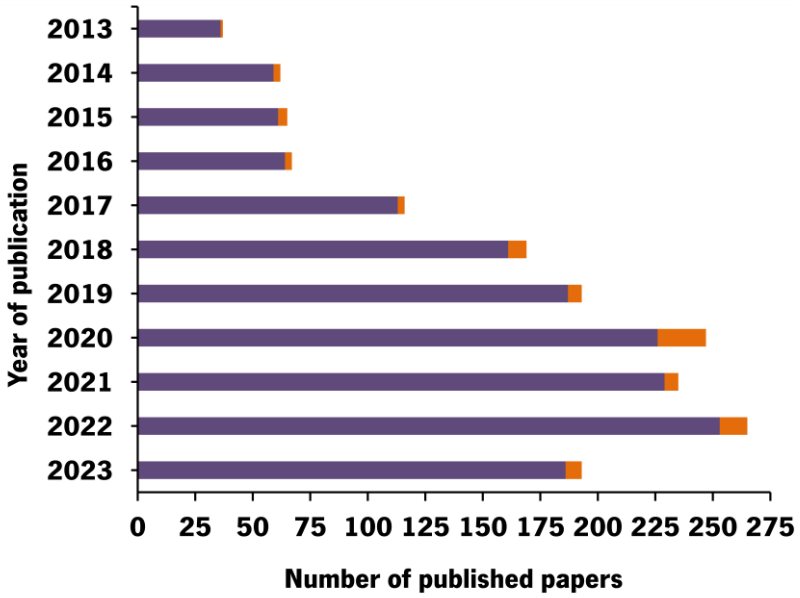

Figure 2-15. Number of papers describing colorimetric PADs (purple bar) and colorimetric PADs for cancer biomarkers detection (orange bar), published on last decade (183).

Figure 2-15 represents the number of scientific papers reporting colorimetric PADs (purple bar), highlighting the ones applied to cancer biomarkers detection (orange bar), published since 2013. Data included papers from the last decade, since 1st January 2013 to 1st December of 2023, from ISI WEB OF KNOWLEDGE, using the keywords "colorimetric AND paper-based" and "colorimetric AND paper-based AND cancer".

It can be noticed that colorimetric PADs have been increasing, being the ones applied to cancer a minority but still growing over the years. It seems that since 2020 this growing tendency has been stabilized. Although it appears that year 2023 had a decrease in the publications, no conclusions can the taken as the year is not over and search includes papers published until 1st of December.

Focusing on cancer screening and diagnosis and on the purpose of this thesis, several biosensors were already reported for CA15-3 detection, in which different REs as antibodies (10, 21, 192), MIPs (60, 122, 193), aptamers (15) were coupled with different signal transduction approaches, such as CM (192), SPR (23, 121), fluorescence (15, 20), ECL (123), SERS (127) and electrochemistry (10, 21, 60, 193).

In the next chapters, the sensors developed for cancer biomarkers detection over the course of this PhD will be presented. For these sensors, cellulose paper was used as substrate, in which different molecules were assembled as REs, and colorimetric detection was selected for signal transduction.

Chapter 3

Nanocellulose-based biosensor for colorimetric detection of glucose

Chapter 3 describes the production of carboxyl-NC by TEMPO-mediated oxidation of microcrystalline cellulose (MCC) and its use for surface modification of cellulose paper. Glucose was selected as target based on epidemiological data that suggests that high levels of glucose have been related to an increased risk to develop BC. GOx and ABTS were used as RE and colorimetric system, respectively, to develop and enzymatic sensor for glucose colorimetric detection on a paper substrate modified with carboxyl-NC.

Part of the content of this chapter was published in Sensing and Bio-sensing Research:

Neubauerova, K., Carneiro, M. C. C. G., Rodrigues, L. R., Moreira, F. T. C., & Sales, M. G. F. (2020). Nanocellulose- based biosensor for colorimetric detection of glucose. Sensing and Bio-Sensing Research, 29, 100368. doi:10.1016/j.sbsr.2020.100368.

3. Nanocellulose-based biosensor for colorimetric detection of glucose

3.1. Introduction

Nanocellulose (NC) materials are among the different products that may be obtained from cellulose by combining proper mechanical, chemical, and enzymatic treatments (194). They display outstanding properties, such as high surface area, mechanical strength, high thermal and chemical durability, or film-forming capacity (195-197). NC have a highly crystalline structure, with a rod-like shape ranging 2–50 nm width and 100–2000 nm length (198, 199).

The most popular process for producing NC is acidic hydrolysis (200), employing typically concentrated sulphuric acid (201, 202) and/or hydrochloric acid (203, 204). In sulphuric acid-based hydrolysis, sulphate ester groups are introduced on the surface of the NC. This leads to the formation of highly stable NC suspensions, because negatively charged sulphate groups are attached to the surface of the NC. However, sulphuric acid is strongly oxidizing, and sometimes causes the degradation of cellulose. Unlike sulphuric acid hydrolysis, hydrochloric acid hydrolysis yields.

The TEMPO-mediated oxidation is an alternative promising procedure, which can produce nanocrystals with modified surface in one step. TEMPO radicals catalyse oxidation of hydroxyl groups and after system supported by NaClO-KBr components converts oxidized aldehydes into final charged carboxyl groups (205-207). The use of this technique was attracting by many investigations since 1994, showing that only the primary alcohol groups of polysaccharides were oxidized, whereas the secondary hydroxyls remained unaffected (208).

For cellulose, the TEMPO-mediated oxidation was applied to different types of cellulose, ranging from cotton to wood pulp, cell cellulose, rayon, and cellulose III (204, 209-213). These studies led to the preparation of a series of products, ranging from water-soluble polyuronic acid to partially derivatized cellulose products.

According to previous results (205, 206), TEMPO-mediated oxidation was applied to microcrystalline cellulose (MCC) and a pre-treatment method of first oxidation was devised to prepare water-soluble polyuronic acid in high yield, which was dependent on the reaction temperature during first and second oxidation. In literature (214), the relationships between the amount of NaClO was optimised and either carboxylate or aldehyde content in oxidated NC. The carboxyl group content increased remarkably to 0.68 mmol solid $^{-1}$ with the addition of at least 5 mmol of NaClO g MCC $^{-1}$. The oxidation of primary alcohol groups in cellulose, catalysed by TEMPO, has been recently proposed as a more selective, faster, and better-controlled method (215, 216).

Due to its remarkable characteristics, NC is one of the most attractive cellulose-based nanomaterial used in biosensors and biomaterials applications (114, 217-219). Cellulose and NC have been widely used as a support material for proteins/enzymes immobilisation (215, 220-227), making use of optical or electrical transduction schemes (114, 168, 194, 228-230), due its outstanding characteristics of these materials. Besides, specially NC shows a high surface area promoting an easy analyte immobilization (194).

Glucose is a monosaccharide, metabolized by glycolysis to produce energy (30) in the form of adenosine triphosphate (ATP) molecules, through oxidation of carbon bonds (231). Several studies reported a positive correlation between some types of cancer (e.g. gastrointestinal, urinary, and reproductive system cancers) and diabetes. Epidemiological data suggest that people with high levels of glucose have an increased risk to develop BC (232, 233) and BC patients with higher glucose levels have poor prognosis (234). Also, it is known that diabetic patients diagnosed with cancer have lower survival rates when compared with people with a normal glucose metabolism (235). Barone et al. found that the coexistence of diabetes with cancer increases the mortality in about 40% (236). High glucose levels, insulin resistance, hyperinsulinemia and obesity are common conditions in diabetics that can increase the risk of neoplastic transformation and progression of pre-existing cancer, as they are associated with chronic inflammation and injury to the immune system. Hyperglycaemia in cancer is explained by the need of cancer cells to maintain continuous and uncontrolled proliferation, for which they require high levels of energy and substrates. Tumour cells are able to increase glucose levels by improving the expression of glucose membrane transporters (30, 235). This excess of glucose leads to the formation and accumulation of glycation end-products in the cells which promotes cell damage leading to the activation of inflammation processes in the cells, and activation of immune cells as macrophages and neutrophils, thus increasing the production of oxygen free radicals. However, glucose metabolism is differentially regulated in cancer cells and in normal cells (235, 237). Normal cells, produce energy through mitochondrial oxidative phosphorylation, in aerobic conditions. However, when oxygen is not available, cells obtain energy through glycolysis (238). In 1920, Otto Warburg discovered that cancer cells have a different metabolism to normal cells, as they produce ATP more efficiently under aerobic conditions through glycolysis, a phenomenon also known as aerobic glycolysis. The Warburg effect is thus defined by the fact that cancer cells produce a lot of lactate, despite the accessibility of oxygen (239). While in normal healthy cells glucose is fermented and converted to pyruvate to form ATP with the participation of oxygen in the Krebs cycle, cancer cells convert pyruvates to lactic acid and use glucose to synthesise DNA, RNA, proteins and lipids to

maintain their proliferation (30, 235, 240). The increased production of lactic acid and accumulation of H^+ ions in cancer cells drops the pH of the extracellular matrix, thus leading to the death of normal cells and increasing collagenases activity, facilitating tumour cells migration (30, 231, 235, 237). As Warburg effect is considered a hallmark of cancer, glucose can be a promising cancer biomarker and inhibition of glycolysis could be an interesting alternative strategy for cancer treatment (30, 240).

Several LFAs have been widely used for glucose analysis in urine (241). However, this procedure is rather complex, because it uses a porous membrane with specific antibodies or proteins immobilised in lines (5). Besides, LFAs show other concerns, as it is based in a "one-step" assay, in which the sensory surface is not easily washed and, consequently, may suffer from interference sample components that pre-block the strips. Beyond that, these assays demonstrate a qualitative and semi-quantitative nature (241). In addition, sometimes it is necessary to label the antibody to increase the sensitivity, losing the one-step concept, becoming a more complicated and expensive assay, especially accounting the needs of a very selective antibody.

A similar tool to LFA using cellulose as a support material is the well-known dipstick based sensing system (242). When the dipstick gets in touch with the sample (urine or other physiological fluid), a color change in the stick is generated (168, 242-244). This method is simple but offer a response of semi-quantitative nature, thereby limiting the accuracy of the analytical data generated.

Some REs have also been employed in PADs, including enzymes (245). Enzymatic biosensors use enzymes as biological RE (246-250) and offer highly selective responses. In the case of preparing of enzyme-based biosensor, it is essential to ensure that enzymes are available to catalyse the intended reaction and must be stable under the normal reaction conditions of the biosensor (247, 248). Several enzymatic assays, with different enzymes immobilised on the cellulose paper surface and aiming to detect different analytes have been reported in the literature. These include glucose (245), lactate (251), stearate (252), catechol (253), phenol (254), among others.

The main issue concerning the preparation of enzymatic based-cellulose sensors is related to the enzyme immobilisation on paper substrates. Several techniques have been reported in the literature for this purpose (255), mainly based on adsorption (256) and covalent attachment (257, 258). Adsorption is a simple methodology but hinders the typical binding capacity of enzymes for being immobilised randomly on a solid cellulose support. In addition, the enzymes are sensitive to harsh conditions as pH and temperature, leading to some concerns in terms of sensor reliability. Other methodologies include chemical cross-linking (259), thin film entrapment (255), and microencapsulation (260). These increase the effectiveness of enzyme immobilisation but may limit

the accessibility of the substrate and increase the complexity of the assay development and associated costs.

This work combines the TEMPO-oxidation of MCC to produce carboxyl-NC and their application in the development of colorimetric based test-strips for glucose. The MCC oxidation is optimised, as well as the integration of the GOx within the cellulose/NC-based substrate, and the ability to generate color in the presence of H_2O_2. Overall, this works reports for the first time the integration of NC with enzymatic biosensor, for glucose detection in urine samples in diabetes.

3.2. Experimental section

3.2.1. Reagents

Microcrystalline cellulose was obtained from Biochem Chemopharma. TEMPO (2,2,6,6-tetramethyl piperidine-1-oxyl radical), ABTS (98%), EDC (99%), MES monohydrate (2-(*N*-morpholino) ethanesulfonic acid monohydrate, $C_6H_{13}NO_4S{\cdot}H_2O$, 99%) and GOx HPS 300 (activity 260.3 U mg^{-1}) from SCKISUI and uric acid were supplied by Sigma Aldrich. Sodium hydrogen carbonate ($NaHCO_3$, > 99%), sodium chloride (NaCl), hydrochloric acid (0.5 M) and hydrochloric acid (37%) were purchased from Panreac. Sodium hypochlorite solution (NaClO, ca. 10% active chlorine, 15% solution) was obtained from Carlo Erba, sodium carbonate (Na_2CO_3) and L-ascorbic acid were supplied by Riedel-de-Haen. Glucose (dextrose monohydrate, $C_6H_{12}O_6{\cdot}H_2O$) Alfa Aesar. Sodium hydroxide (NaOH, solid pellets) was purchased from Eka. NHS (> 97%), HRP (150 U g^{-1}) and creatinine were obtained from Fluka. Urea was supplied by Fragon. Ethanol (96%) was purchased from José Manuel Gomes dos Santos. PBS tablets were obtained from Amresco, dissolved in Mili-Q water and pH was changed to 7.2. Purified Milli-Q water was used for all the experiments and analysis. All chemicals were used without any prior purification.

3.2.2. Pre-treatment of microcrystalline cellulose

MCC was pre-treated according to literature (206). Two different protocols were used for this purpose: 1 g MCC was added to 13 mL HCl (37%), stirred and hydrolysed at 45 °C for 30 min or 1 g MCC was added to 10 mL HCl (37%) and hydrolysed at 100 °C for 15 min. After acid hydrolysis, the dispersion was washed and centrifuged three times at 12000 rpm. The last wash was carried out in a dialysis membrane with distilled water until a neutral pH was reached. The supernatant solution was sonicated for 15 min to obtain NC. The resulting MCC residue was filtered. NC was precipitated in ethanol, filtered, and dried in an oven at 60 °C.

3.2.3. TEMPO-oxidation of nanocrystals

TEMPO-mediated experiments were carried out as previously published with minor modifications (205) and the pictures of the resulting materials at intermediate stages are shown in Figure 3-1.

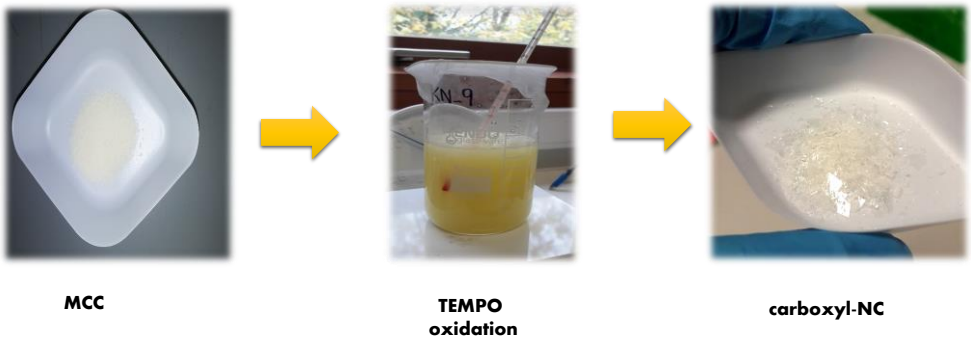

Figure 3-1. Synthesis of the carboxyl-NC by TEMPO oxidation of MCC.

The first oxidation was carried out by dispersing 1 g of MCC in carbonate buffer solution (75 mL, pH = 10.83) in a sonicator (15 min) and adding TEMPO (30 mg) and KBr (0.32 g) to this suspension, which was kept at 30 °C. The sodium hypochlorite solution (15%, 6 mL) was then added to the resulting suspension, which was mechanically stirred. The pH was kept at 10 to prevent strong degradation of the water-soluble polymer. After 5 h of stirring, the reaction was terminated by adding 20 mL of ethanol, which reacted with the remaining TEMPO. The reaction mixture was acidified with 0.5 M HCl to pH 3 (to remove K^+ cations) and then centrifuged to remove the remaining insoluble microcrystalline material. The water-soluble NC in the supernatant was precipitated by adding an excess of ethanol (up to 400 mL), followed by centrifugation. The precipitate was washed with ethanol, centrifuged several times and finally dried in an oven at 45 °C. The remaining MCC was washed with ethanol and dried in the oven at 45 °C and served as starting material for the next oxidations. The second and the third oxidation procedures consisted in repeating the previous experiments.

3.2.4. Nanomaterial characterisation

3.2.4.1. Conductometry

The carboxyl content of oxidized NC samples was determined by conductometric titration (205). Dried NC samples (30-40 mg) were resuspended in 15 mL of 0.01 M HCl solution. After 10 min of sonication and stirring, the suspension was titrated with 0.01 M NaOH. According to

(205), the content of carboxyl groups in the material was expressed in the form of degree of oxidation (DO), as given by the following equation:

$$DO = \frac{162 \times C \times (V2 - V1)}{w - 36 \times C \times (V2 - V1)} \quad \textbf{(Equation 1)}$$

where V_1 and V_2 are the amount of NaOH (in L), c is the NaOH concentration (mol L^{-1}), and w is the weight of dried sample (g). The value of 36 corresponds to the difference between the molecular weight of an anydroglucose unit (AGU) and that of the sodium salt of a glucuronic acid moiety.

3.2.4.2. Fourier-transform infrared spectroscopy

The NC and the MCC were analysed via FTIR spectroscopy to evaluate the chemical modifications. The resulting spectra were used to determine the structural characteristics of the NC.

Infrared spectra were recorded on a FTIR Thermo Scientific spectrometer (Nicolet iS10) with an ATR (attenuated total reflectance) accessory, having a diamond crystal. Spectra were analysed from 400 to 4000 cm^{-1} wavenumber, with a 2 cm^{-1} resolution, and an accumulation of 150 scans, after background collection.

3.2.4.3. Transmission electron microscopy

Dried oxidized NC was dissolved in water (0.01% w/v) and sonicated for 15 min. A drop of this suspension was deposited on the electron microscope grid and negatively stained with phospho-tungstic acid for 10s. The excess of liquid was removed by a filter paper. The grids were observed in a TEM Zeiss, Model EM902 A.

3.2.5. Colorimetric assay

3.2.5.1. Binding of glucose oxidase to the nanocellulose

3.2.5.1.1. Glucose oxidase adsorption

An oxidized carboxyl-NC (20 mg) was dispersed in 10 mL of 50 mM MES buffer with 500 mM NaCl buffer (pH 5.0) and kept stirring for 24 h at room temperature, before use. Then, 2.5 µL of carboxyl-cellulose was casted on the cellulose surface. After, a solution of GOx (2.0 mg mL

$^{-1}$) previously dissolved in PBS, was drop-casted on the modified cellulose paper with the NC. The sensor was let dry at room temperature and stored in the fridge at 4°C before use.

3.2.5.1.2. Covalent attachment of glucose oxidase

The carboxyl groups of the carboxyl-NC were activated using EDC/NHS. To this end, 12 mg of NHS (10 mM) and 8 mg of EDC (4 mM) were added into the well-dispersed mixture of carboxyl-NC (20 mg) in 10 mL of 50 mM MES and 500 mM NaCl buffer (pH 5). The solution was stirred for 24 h at room temperature. The excess of reactants was removed by precipitating of the activated carboxyl-NC in ethanol. The precipitate was centrifuged, cleaned with ethanol and oven-dried to eliminate ethanol residues. The activated material was dispersed in 12 mL of PBS (pH = 7.2) containing 20 mg of GOx. This dispersion was stirred 24 h at room temperature. Then, 2.5 μL of the previous solution was drop-casted in the cellulose paper.

3.2.5.2. Colorimetric assay

3.2.5.2.1. Carboxyl-nanocellulose and glucose oxidase concentration optimisation

For glucose detection, oxidized-NC (0.01-20 mg mL $^{-1}$, 2.5 μL) was adsorbed on a cellulose paper substrate. The next stage consisted of the immobilisation of GOx. The concentration of the enzyme was studied within 0.001 and 0.5 mg mL $^{-1}$, by using 2.5 μL of the enzyme solution. For this purpose, the enzyme was casted on the cellulose/carboxyl-NC surface and let dry at room temperature. Then, 22.5 μL of a solution consisting of different concentration of glucose (0.001 to 100 mM, 1.2 μL), PBS (pH = 7.2, 18.9 μL), ABTS (5 mM, 1.2 μL) and HRP (150U g $^{-1}$ solid, 1.2 μL), was dropped on the filter paper substrate with, containing the carboxyl-NC (261) (Figure 3-2). The color of each test-strip was monitored for periods of 3, 5 and 10 min of incubation. Resulting color was compared with color of the blank sample containing only glucose without enzyme.

Pictures of the results were obtained using a smartphone camera. However, light conditions highly influence quality and reproducibility of the acquired images and thus the feasibility of results. Thus, the pictures were taken in controlled light conditions and a fixed focal distance.

Image J software (version 1.4.3.67) have been used to analyse the results. A square tool has been used to select a constant area for the measurements. Several parameters were analysed

as RGB. The average of RGB channel image provided the best results in terms of linearity when plotted against glucose concentration and was used for analysis.

3.2.6. Selectivity assay

The selectivity of the system is a crucial parameter for the analysing system when it is expected to be applied under real conditions. For this reason, the selectivity of the sensing system was further evaluated by incubating different interfering molecules, present in urine samples, onto the test-strips. Glucose (19.2 mM) plus ascorbic acid (0.01 M), glucose (19.2 mM) plus acid uric (0.06 mg mL^{-1}), glucose (19.2 mM) plus creatinine (12 mM) and glucose (19.2 mM) plus urea (0.2 mg mL^{-1}). Assays were prepared in PBS and dropped on the filter paper previously described in the section 3.2.5. Colorimetric assay. Images of the results were captured, and ImageJ was used to obtain the parameter values and calculate the associated errors.

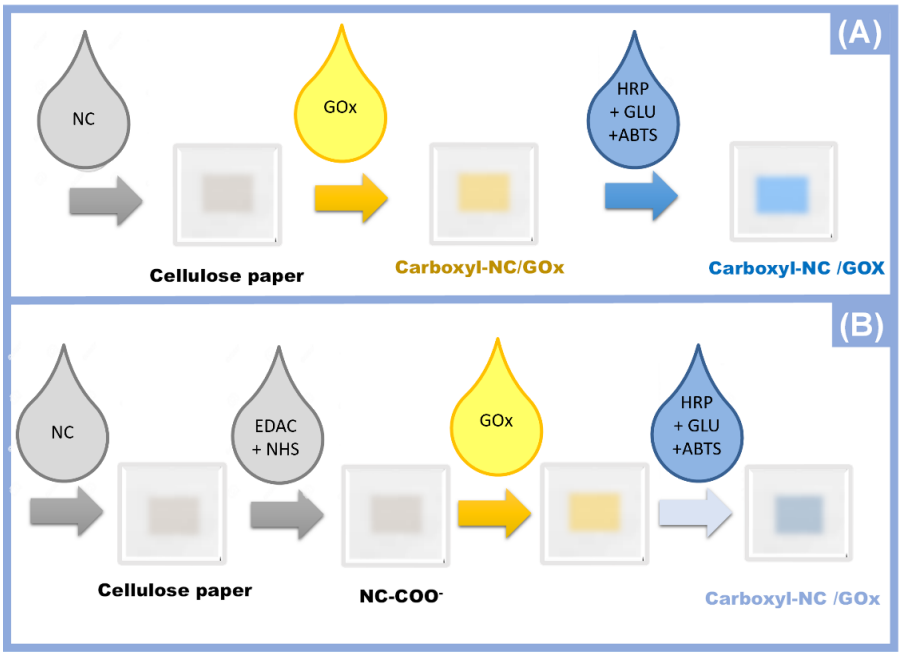

Figure 3-2. Test-strip based colorimetric assay produced by casting on the cellulose substrates the indicated solutions, and binding GOx either by adsorption (A) or by covalent bonding (B).

3.3. Results and discussion

3.3.1. The oxidation of microcrystalline cellulose

The oxidation of raw cellulose by means of the TEMPO reaction is often incomplete. On the other hand, pre-treated cellulose can give larger amount of totally oxidized water-soluble polyglucuronans (206). Thus, the oxidation of MCC by TEMPO reaction may be more effective by establishing sequential oxidative reactions. In general, at least two oxidation stages were applied herein, in

which the oxidized material was removed from the solution and the remaining MCC material was further subjected to a second oxidation stage. A third oxidation was also processed to show if this would further enhance the oxidative yield or the properties of the final material.

Herein, MCC was oxidized with sodium hypochlorite, combining catalytic amounts of potassium bromide and TEMPO radicals, under various conditions, as described in Table 3-1. The effect of the number of sequential oxidative procedures and the concentration/volume of sodium hypochlorite, on the NC weight yield was tested by using four different samples, named A to D. Sample A was prepared according to the procedure described in (206), by using 13.4 mmol of hypochlorite per gram of MCC. The weight yield in the first round of oxidation was reasonable (13%), but in the second round it drops to only 3%. The efficiency of the oxidation of MCC to NC was further optimised by adding a higher concentration of hypochlorite (24 mmol hypochlorite per gram of MCC) at once or in several rounds. In sample B, the entire volume of hypochlorite was added at the beginning of each oxidation reaction. Compared to sample A, the weight yield in the first oxidation round was similar, but the second oxidation gave a higher yield (5 times more, equal to 15%) and the third oxidation gave a yield of 11%. For samples C and D, the same amount of hypochlorite was added sequentially, divided into three and six rounds, respectively. If one compares the single and multiple additions of hypochlorite, the effect is obvious. The NC yield increased significantly in all 3-round oxidations when a smaller amount was added several times. Overall, the best results were obtained for samples C and D, which achieved the highest yields for all oxidations of MCC. The process of sample D yielded the most oxidized material.

It is obvious that the efficiency of the MCC oxidation using the TEMPO-NaClO-KBr system to produce water-soluble NC depends positively on the increasing amount of hypochlorite, up to a limiting value when the cellulose structure would be fully destructed. Moreover, multiple addition of the smaller volume of reagent into the solution provided higher yield, because there is more often fresh reagent capable of starting new oxidative reactions. After these results, subsequent studies used sample D as a support material for the enzyme immobilisation.

Table 3-1. The effects of amount and adding of sodium hypochlorite on weight yield of functionalised CNC.

Sample	Oxidation procedure	Total volume of NaClO (ml g^{-1} MCC)*	Sequential addition of NaClO (ml)*	Amount of NaClO (mol g^{-1} MCC)	Weight yield (%)***
A	1st	6**	2	0.013	13
	2nd				3
B	1st	24	24	0.054	16
	2nd				15
	3rd				11
C	1st	24	8	0.054	25
	2nd				23
	3rd				13
D	1st	24	4	0.054	28
	2nd				30
	3rd				29

**Partial adding every 30 min, followed by adjustment to pH = 10*

***According to procedure of Li.. (206)*

****Weight yield was calculated from actual amount of material*

3.3.2. Characterisation of the materials

3.3.2.1. Fourier-transform infrared spectroscopy

TEMPO-oxidation reaction of primary alcohol groups was evaluated by FTIR spectroscopy, searching evidence of the presence of carbonyl or carboxyl acid functional groups. The infrared spectra of initial raw MCC and carboxyl- NC are shown in Figure 3-3.

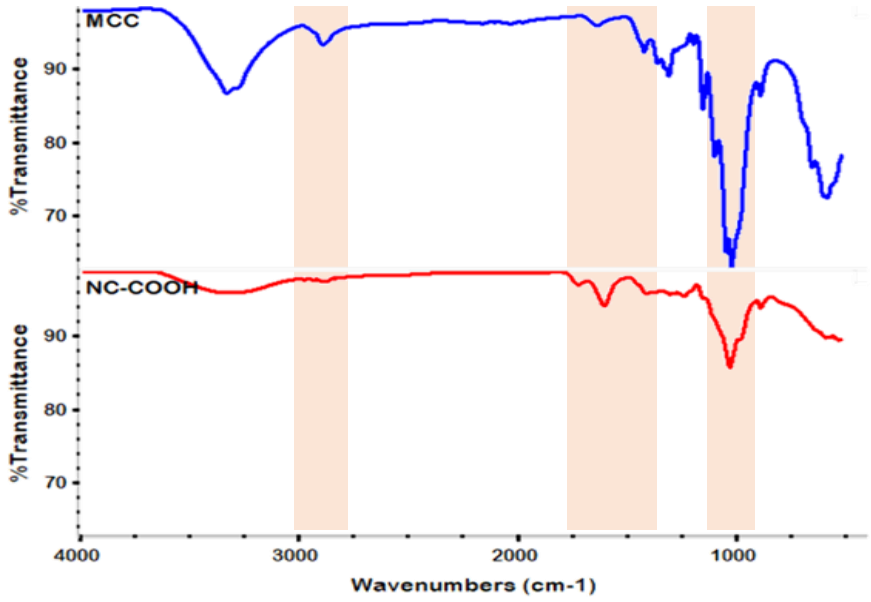

Figure 3-3. FTIR Spectra of pristine MCC (top) and NC-COOH (bottom), signalling the wavenumbers areas with the major differences between these (in pink).

Overall, the FTIR spectra of pristine MCC contains a strong peak around the 3500 cm^{-1} region, attributed to the O-H stretch of cellulose. This peak was an indicator of high concentration of alcohol groups (ROH) in cellulose. The strong peak at 1060 cm^{-1} was assigned to the stretching of the C-O bond in the cyclic structure of glucose. This band is related to groups of secondary alcohol and secondary ether functions (262).

After TEMPO oxidation, a new relevant peak appeared at 1730.9 cm^{-1}. It corresponded to the C=O stretching vibration of carboxyl groups in their acidic form. Consistently, the peak at 1611.2 cm^{-1} was assigned to the presence of anionic forms of carboxylic acids. Moreover, the peak was signalling the stretching vibration of C-O shifted to a higher wavenumber (herein 1037.1 cm^{-1}), as expected. Finally, the stretching vibration of C-H at 2896 cm^{-1} was of lower intensity and the band at 3333 cm^{-1} was broader, also signalling the presence of the carboxylic acid groups.

When compared to the pristine MCC, the combination of these peak changes in the FTIR spectra confirmed the oxidation of primary hydroxyl groups by TEMPO (205-207, 214, 215), leading to the formation of carboxyl-NC. Overall, peaks in obtained spectra demonstrated that some hydroxyl groups of the D-glucose cyclic unit were converted into carbonyl groups successfully, leading to the formation of carboxylic or aldehyde groups.

3.3.2.2. Conductometric assay

The carboxylic content in the oxidized NC was evaluated by acid/base conductometric titration. As shown in Figure 3-4. There are three stages of conductivity that are also described, in the literature (205-207). First, a decrease of conductivity was observed, which revealed the titration of the excess of HCl present in the solution. The concentration of H^+ decreased because reaction with HO^- resulting in forming water (a non-ionic specie that cannot change the conductivity of the titrated solution), and the concentration of Na^+ increased (due to the increasing addition of NaOH). As H^+ has a higher intrinsic conductivity than Na^+, the conductivity signal dropped with the increasing NaOH concentration, until a minimum value at which the strong acid was consumed. This minimum value was V_1 in Equation 1. The second stage of this titration was signalled by a more or less steady conductivity signal against the addition of NaOH and corresponded to the titration of the carboxylic acid groups. Then the HO^- being added is shifting the H^+ from the carboxylic groups to form water, also leading to the formation of the corresponding conjugated base that had an anionic form ($-COO^-$). Thus, the concentration of H^+ was decreasing and the signal should be decreasing as well. However, this was compensated

by an increasing amount of Na^+ and $-COO^-$, which justifies that no significant change was observed. The end of the carboxylic acid group titration signalled V_2 in Equation 1. The third stage of the calibration started after V^2. Only with increasing amounts of added Na^+ and HO^- did the conductivity increase, as all acids in the solution had previously been neutralized and no acid/base reaction took place.

Considering all titrations, the results indicated that the water-soluble, oxidized cellulose samples had about 0.7 to 0.8 mmol g^{-1} of carboxyl content. The results were reproducible between samples and did not appear to be affected by the different optimisation of the processes when considering samples D. From this, it was assumed that the average degree of oxidation was 15%, which is a considerable level of oxidation reported in the current literature.

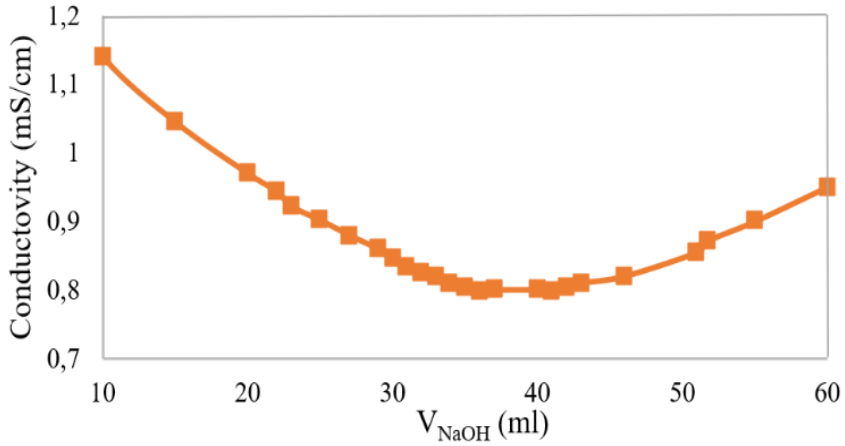

Figure 3-4. Conductometric titration curve of NC-COOH.

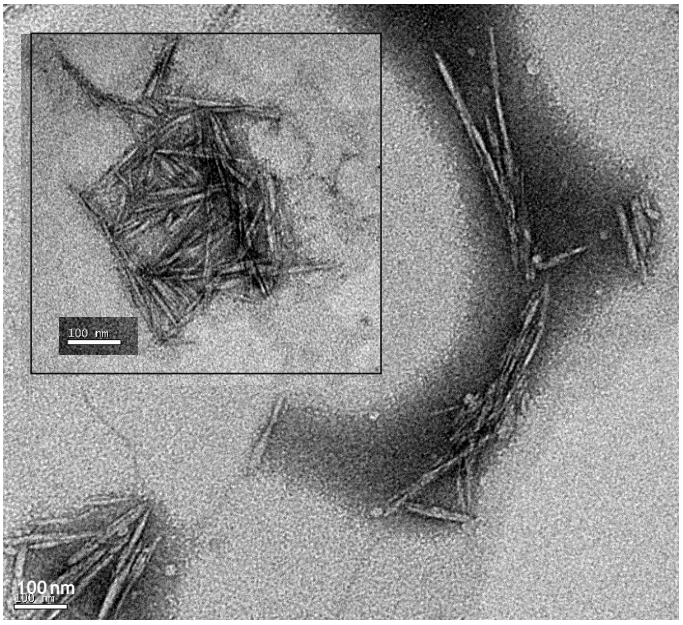

Figure 3-5. TEM images of carboxyl-NC material obtained after TEMPO oxidation of MCC.

3.3.2.3. Transmission electron microscopy

The morphological analysis of all samples was made by TEM, in which the presence of nanowhiskers in the solution was confirmed Figure 3-5 indicates that there is a large poly-dispersity in the distribution of both the length and the width of the whiskers. Indeed, their length ranged from around 50 nm to more than 300 nm, with an average size of 100 nm. Regarding their width, valued from 5 to 20 nm were measured, but most of them are close to 20 nm.

Overall, the size and the structure obtained herein are in agree with the literature (263, 264), in which *Nie et al.* (264) also reported the presence of NC after TEMPO oxidation. They obtained a similar nanowhiskers, in terms of shape and size, with about 250–300 nm long and 10–20 nm width.

3.3.3. Glucose sensing system

The use of carboxyl-NC material as a suitable support for a sensing system was tested herein using the conventional glucose enzymatic-based assay. Briefly, glucose was used as substrate, GOx acted as the enzyme that catalyses the selective oxidation of glucose, and HRP and ABTS were employed colorimetric system for the detection of the products that signalled indirectly the oxidation of glucose. Overall, this is a well-known reaction and is employed herein to develop a test-strip for glucose.

3.3.3.1. Glucose oxidase concentration study

GOx (2 mg mL^{-1}) was prepared in PBS solution and drop-casted (2.5 μL) on a filter paper surface and let dry at room temperature. The enzymatic response was observed against different concentrations of glucose (22.5 μL), ranging from 0.1 to 10 mg mL^{-1}, previously prepared in PBS pH 7.4. The results obtained under the different GOx concentration are shown in Figure 3-6. In these, each GOx concentration was tested against glucose concentrations ranging from 1.5 to 25.6 mM.

In general, it was obvious that higher concentrations of glucose and higher concentrations of GOx resulted in more intense blue colors, which was expected. However, given the purpose of developing a test-strip, it was also important that the color change occurred in the form of a gradient. This gradient meant that the absorption of GOx into the carrier was more reproducible, ensuring more reliable analytical data. The color change as a function of concentration was

more apparent when using 2.0 mg mL $^{-1}$ GOx (260.3 U mL $^{-1}$), which is why this concentration was selected for further studies.

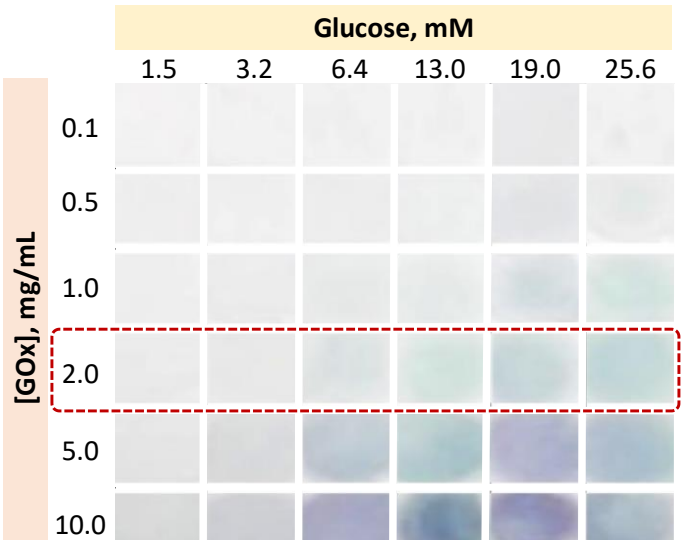

Figure 3-6. Digital images of the calibration curves of glucose using GOx adsorbed to the test-strip.

3.3.3.2. Time effect

Considering that the reaction is of enzymatic-nature, it was very important to monitor the color of the test-strip within time. In general, as enzymatic reactions are quick, the colors on the test-strip appeared immediately after dropping of reagents on the material and these were evolving fast within time. After 6 min, most of test-strips turned dark purple, depending on the concentration of glucose and GOx. For the higher concentrations of glucose and GOx, the purple color on the paper was observed since the very first moments, indicating that the reaction reached its maximum extent under those conditions. Therefore, the reaction was followed at different intervals. According to obtained results, the ideal time for analysing the colors ranged from 3 to 5 min since the beginning of the reaction. A period of 3 min was set for the subsequent tests, allowing a shorter period of reaction, and leading to suitable detectability features (Figure 3-7).

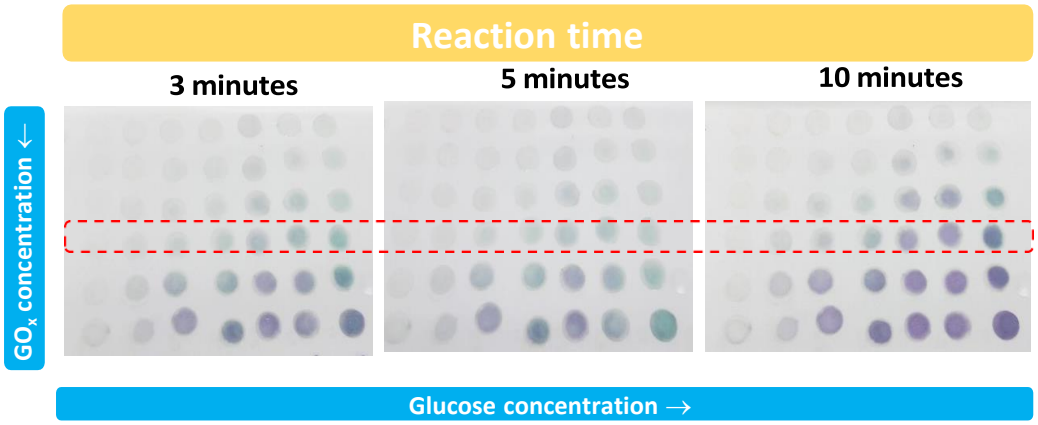

Figure 3-7. Dependence of concentration of GOx and an amount of glucose with the time.

3.3.3.3. Sensing system bound by adsorption to the oxidized nanocellulose

While the chemical system for glucose detection is well-known, information about the effect of the carboxyl-NC on the color gradients or concentration ranges of detection is missing. In general, it was expected that the presence of carboxylate groups on a cellulose substrate would enhance its binding efficiency and create a suitable environment for GOx activity. In terms of binding efficiency, a regular cellulose substrate would establish interactions with GOx via hydrogen bridges only. When cellulose is doped with carboxyl-NC these interactions could be enhanced by the presence of multiple –COOH groups, which would intensify the hydrogen bridges and establish ionic interactions with multiple positive points existing in the external surface of GOx. Thus, different tests-trips were prepared by casting different amounts of NC-COOH on the cellulose substrate, ranging from 0.010 to 20 mg mL^{-1} and let to dry after casting. These studies were made by keeping the previously defined concentrations, having 2.0 mg mL^{-1} GOx and 3 min for the reaction to take place. Figure 3-8 summarizes the results obtained from different concentrations of glucose, ranging from 1.5 to 25.6 mM.

When compared to the results obtained without carboxyl-NC the observed colors were more homogenously distributed along the whole surface of the test-strip and the gradient color change was improved by the presence of the carboxyl-NC. Overall, this confirmed that the presence of carboxyl-NC affected positively the results obtained by improving the color features of the glucose detection.

However, there was not a great difference among the different test-strips prepared with increasing amounts of carboxyl-NC. This was probably linked to the saturation of carboxyl-NC

adsorbed on the cellulose support for the selected concentration range. Thus, an intermedium concentration of 5 mg mL $^{-1}$ was selected for subsequent studies, considering reproducibility and cost purposes. This would ensure highly reproducible strips at a lower cost than those employing the highest concentration tested.

Comparing the analytical performance of test-strips prepared without carboxyl-NC and with 5 mg mL $^{-1}$ carboxyl-NC a linear trend was observed in both by plotting (R+G+B)/3 against glucose concentration. The presence of carboxyl-NC yielded improvements in terms of lower limit of linear range, decreasing the observed value from 6.4 to 1.5 mM. Moreover, the slope increased in about 50% by the presence of carboxyl-NC, increasing the slope value from 1.0 to 1.5 a.u/mM. Additionally, the operational features in terms of lower limit of linear demonstrated improvements starting 1.5 mM with NC and 6.4 mM for the biosensor without NC.

Overall, these results confirmed that the loading of GOx on the test-strips and its catalytic activity were more controlled by the presence of carboxyl-NC.

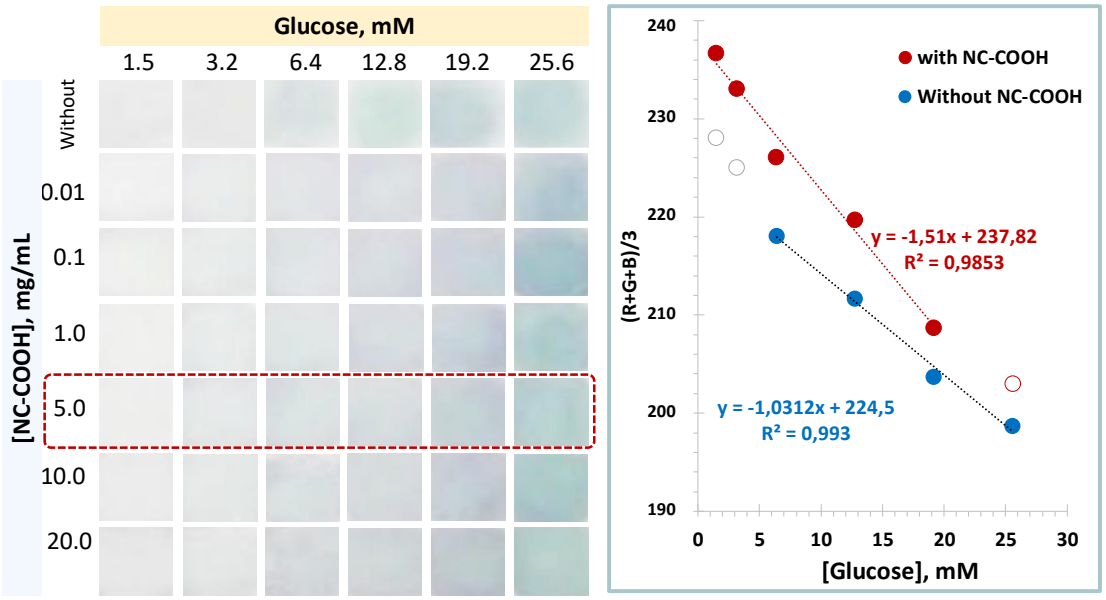

Figure 3-8. Digital images of the test-strips in the presence of different glucose concentrations using ABTS as colorimetric indicator, prepared with different concentrations of carboxyl-NC (left) and the analytical calibration curves plotting the color coordinates collected against the glucose concentration (right, the carboxyl-NC assay corresponds to 5 mg mL $^{-1}$ of NC-COOH).

3.3.4. Sensing system covalently bound to the oxidized nanocellulose

The possibility of attaching covalently GOx to the test-strip was also explored herein, aiming to increase the stability of the final device. This was made by employing EDC/NHS chemistry. In this, the carboxylate groups in the carboxyl-NC matrix were activated and underwent subsequent

covalent binding to the amine groups exposed in the outer surface of GOx. The concentration of GOx bound to the activated carboxylic groups ranged from 0.01 to 20 mg mL^{-1}.

The results obtained are shown in Figure 3-9. Comparing with the adsorption assay, covalent immobilisation showed much more intense colors that lead to much more sensitive readings. The slope of the 3.5-times higher, increasing from 1.5 to 5.3 a.u/mM. As expected, this increase in sensitivity was also linked to a narrower concentration range of linear response, ranging from 1.5 and 12.8 mM.

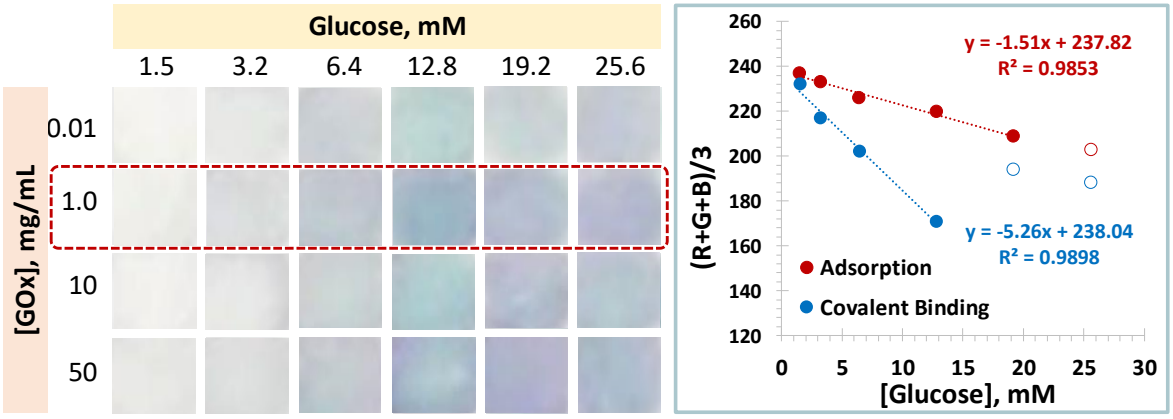

Figure 3-9. Digital images of the test-strips in the presence of different glucose concentrations using ABTS as colorimetric indicator, prepared with different concentrations of GOx covalently bound (left) and the analytical calibration curves plotting the color coordinates collected against the glucose concentration (right, the carboxyl-NC assay corresponds to 1 mg mL^{-1} GOx).

Overall, the method described herein is an expeditious and low-cost approach that may be further explored in the analysis of glucose in urine. Normal levels may reach up to 150 mg L^{-1}, meaning that normal urine samples may require 10× dilution prior to analysis with the test-strip. Moreover, urine samples shall not have intrinsic color that may interfere with this determination.

3.3.5. Selectivity assay

Ascorbic acid, uric acid, creatinine, and urea were incubated onto the paper substrate simultaneously with glucose and compared with glucose incubated alone. It can be seen in Figure 3-10 that the response of the paper test-strip was not affected by other interferents as the variation of the tested interfering species is low (less than 10%) comparing to glucose value. Ascorbic acid and uric acid showed a slightly positive variation (4.6% and 5.3%, respectively) whereas creatinine and urea revealed a low negative variation (8.3% and 9.9%, respectively), over the glucose value.

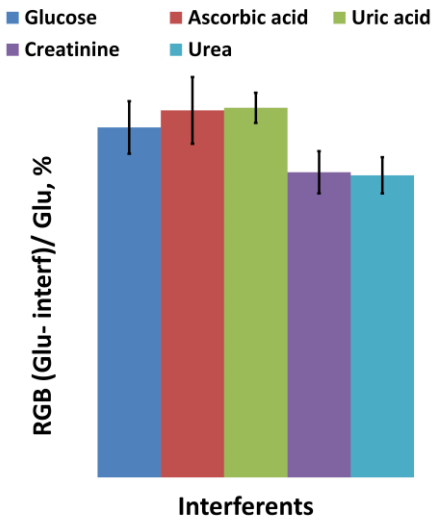

Figure 3-10. Evaluation of interfering species variation in comparison with glucose.

3.4. Conclusions

This work reports on the oxidative modification of MCC to produce water-soluble cellulose derivatives that can improve the use of test-strips using cellulose substrates as carriers. Different conditions were applied. Overall, it was possible to achieve better properties of the cellulose substrate material by using an appropriate ratio of TEMPO/hypochlorite and an appropriate number of successive oxidative procedures.

The use of carboxyl-NC to improve cellulose substrates requiring enzyme binding was further tested. It was found that modified NC exhibited better color distribution and improved the process of glucose detection in terms of analytical performance.

Overall, the proposed enzymatic test-strip showed good characteristics in terms of simplicity, reaction time, price and applicability and is a promising tool for PoC analysis. In addition, this device opens up possibilities for multiplex analysis by using different chromogenic reagents. By utilizing the inherent capability of the H_2O_2 producing oxidase, it can be extended to the detection of a wide range of analytes of interest in the food, health, and environmental fields.

Chapter 4

Paper-based enzyme-linked immunosorbent assay for fast cancer antigen 15-3 detection in point-of-care

This chapter focused on the development of a sensor by adapting the standard ELISA protocol to a paper substrate. CA15-3 was selected as target as it is overexpressed in 90% of BCs, being one of the biomarkers approved BC diagnosis, as well as follow-up of cancer patients during treatment. Detection signal results from a colorimetric reaction based on the oxidation of the TMB substrate by a peroxidase enzyme.

Part of the content of this chapter was published in Microchemical Journal:
C.C.G. Carneiro, M., Rodrigues, L. R., Moreira, F. T. C., & Goreti F. Sales, M. (2022). Paper-based ELISA for fast CA15–3 detection in point-of-care. Microchemical Journal, 181, 107756. doi:10.1016/j.microc.2022.107756.

Part of this chapter was presented as a poster in 31st anniversary world congress on biosensors, Live and On-demand:
Carneiro, M. C. C. G., Rodrigues, L. R., Moreira, F., & Sales, M. G. F. (26-29 july, 2021). Poster P5.054: Paper-based ELISA for rapid protein detection.

4. Paper-based enzyme-linked immunosorbent assay for fast cancer antigen 15-3 detection in point-of-care

4.1. Introduction

CA15-3 is a transmembrane glycoprotein that is overexpressed in 90% of BCs (37) and is one of the biomarker approved not only for BC diagnosis, but also for follow-up of cancer patients during treatment (23, 59, 92). ELISA is the most used technique for detection of CA15-3 in serum but this methodology involves long incubation times and multiple washing steps (265). Regarding this, new screening devices with rapid response and high sensitivity and selectivity such as biosensors are needed (266). Biosensors meet the requirements for PoC analysis as they are easy to use, fast responding, have high sensitivity and specificity and offer the possibility of multiplex detection (9, 26). There are several biosensors reported for CA15-3, involving equipment-based transduction (10, 23, 121).

Colorimetric assays can provide instrument-free PoC analysis (41) being particularly attractive for environmental and cost reasons when cellulose paper is used as a substrate (155). PADs have therefore experienced exponential growth in the last decade (27, 81) and are suitable alternatives for cancer diagnosis compared with actual methods (267). A quantitative result can be provided by colorimetric PADs by using simple readout devices as smartphones to capture the results (1, 24, 41, 124, 125, 159, 161, 162, 268), which are then analysed using adequate software to calculate optical parameters using as RGB or HSB coordinates that can be used for biomarker quantification (159).

Scientists tried to overcome the disadvantages of the traditional ELISA by replacing the conventional 96-well plate with cellulose paper substrates and developing the P-ELISA which can be used as a PoC device, being particularly important in resource-poor settings (94, 185, 186). It takes advantage of the high specificity of conventional ELISA, but in a fast procedure performed in less than 1h and requiring small amounts of samples and reagents (1-10 μL), which lowers the cost of the test.

There are several reports of colorimetric PADs for various cancer biomarkers, not only proteins (CEA (19, 27, 129, 269, 270), p16 (271), HPV 16/18 E6 oncoprotein (272), cytochrome c (273)) but also for nucleic acids (miRNA-21 (171)) and other molecules (citrate (140)). Most of them are based on immunoassays that include the enzymatic reaction of HPR with TMB as chromogenic substrate (142, 182).

As far as we know, this method has never been reported for the detection CA15-3 in paper substrate. This paper reports on the development of a colorimetric P-ELISA for CA15-3. Based on a sandwich

immunoassay on a cellulose substrate, which was modified and optimised accordingly. The detection is performed by a colorimetric reaction based on the oxidation of the TMB substrate by a peroxidase enzyme, HRP, in the presence of H_2O_2. The color development on the paper substrate can be visualized and recorded in the ImageJ software for further analysis, allowing the concentration of the analyte of interest to be determined. The characterisation and application of the test-strip is also presented.

4.2. Experimental section

4.2.1. Reagents and solutions

All chemicals were of analytical grade and water was ultrapure Milli-Q laboratory grade. Sodium phosphate dibasic dihydrate was acquired from Panreac. Sodium dihydrogen phosphate dihydrate was from Scharlau. Sodium Hydroxide was obtained from EKA. Potassium periodate was from May&Baker. APTES was obtained from Acros Organics. Glucose monohydrate was purchased from Alfa Aesar. Bradford reagent was from BioRad. TMB Liquid Substrate System for ELISA and BSA were purchased from Sigma Aldrich. Tween20 was acquired from Merck. Cormay® serum HN was from PZ Cormay®. CEA was obtained from EastCostBio. CA125 was from Hytest. CA15-3 from host human (reference MBS536585) was purchased from MyBioSource. Capture antibody (Mucin 1 monoclonal antibody Vu-2G7, reference SC-69644) was acquired from Santa Cruz Biotechnology and detection antibody (Recombinant monoclonal antibody to MUC1 labelled with HRP, reference EPR1023) was from Abcam.

Stock solutions of proteins and antibodies were prepared in phosphate buffer (PB), having 0.081 M Na_2HPO_4 and 0.019 M NaH_2PO_4, with pH 7.7. Whatman® quantitative filter paper (ashless, Grade 40, 110 mm diameter, 210 μm thickness, 8 μm pore size) was used as substrate.

4.2.2. Apparatus

FTIR and thermogravimetric analysis (TGA) were used to characterise the cellulose paper at consecutive stages of sensor assembly. FTIR spectra were recorded using a Nicolet iS10 spectrometer from Thermo Scientific, coupled to an ATR accessory with a diamond crystal. All spectra were acquired after background correction from 400 to 4000 cm^{-1} with a resolution of 8 cm^{-1} and 250 scans. Data analysis was performed using OMNIC 9 software. TGA measurements were made on and Hitachi TGA DTA/7200, using ≈5.4 mg paper samples in an aluminum holder at a heating rate of 5ºC per second, from 30 to 500ºC, under a nitrogen atmosphere at 300 mL min^{-1}. A homemade dark box (Figure 4-1A and Figure 4-1B) was used for picture collection. A

cardboard box (19 cm width × 13.5 cm height × 13.5 cm depth) was painted inside and outside with a black spray ink. An aperture (2 cm × 1 cm) was made on the top of the box where a smartphone lens exactly fits for image acquisition. A light-emitting diode (LED) tape (high luminosity, 4000K, 50/60 Hz, DC12V) was stacked on the inside, covering all the four faces of the box.

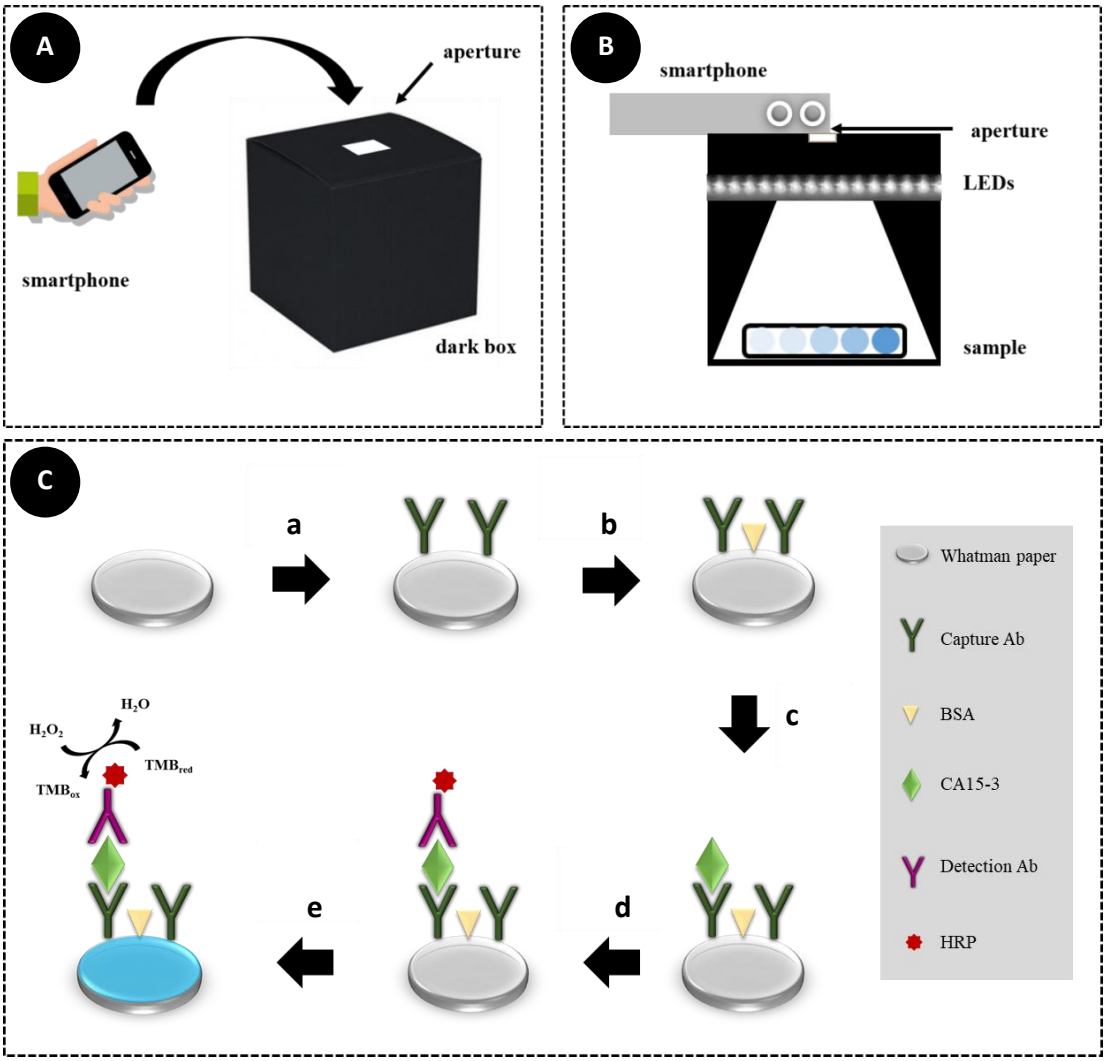

Figure 4-1. Outside (A) and inside (B) view of the dark box for image acquisition. Steps of the sensor construction (C). Covalent immobilisation of capture antibody (a), blocking step with BSA (b), incubation with CA15-3 antigen (c), incubation of detection antibody labelled with HRP (d) and color development with TMB solution (e).

4.2.3. Paper pre-treatment: washing and functionalisation

Whatman® filter paper circles (area ≈ 95 cm^2) were soaked in 8% NaOH solution in a horizontal shaker for 1 h to remove contaminants. They were then washed several times with ultrapure water to remove the NaOH content. The pH of the washed solution was measured with an indicator paper until a neutral value was reached. The paper circles were then dried in an oven at 60 °C.

The cellulose substrate was first modified to allow subsequent antibody binding (159). For this purpose, silanization with APTES and oxidation with potassium periodate was tested.

Silanization was performed by immersing the paper in a 10% APTES (230) solution in ethanol:water (95:5, v/v) and shaking horizontally for 2 h at room temperature. The paper was then washed with fresh ethanol:water solution to remove unbound silanes and thermally treated in an oven at 80 °C for 2 h.

Oxidation of cellulose was carried out with periodate functionalisation, as described in (86). Potassium periodate was employed in a solution of 3.1×10^{-3} M prepared in water (protected from light by aluminium foil and prepared daily). The filter paper was immersed in 50 mL of potassium periodate and allowed to react at 65 °C for 2 h to produce aldehyde functions allowing covalent binding of an antibody. After this reaction, the filter paper was washed twice with water and dried at 60 °C.

The chemical changes on the cellulose surface were then monitored by FTIR. To determine which functionalisation (APTES or KIO_4) provided the best binding to proteins/antibodies, the functionalised paper was incubated with 1% BSA for 30 min, washed with 1 mL PB, and subjected to Bradford reagent to detect the bound amino groups ($-NH_2$) of BSA on the cellulose-oxidized surface.

4.2.4. Assembly of the paper-based sandwich enzyme-linked immunosorbent assay

Whatman® paper was cut into small circles of 8 mm diameter with a hole puncher. The minimum volume of reagent solution required to ensure a uniform and complete coverage of the entire paper circles was investigated using red food coloring.

A sandwich ELISA is the principle of the assay used in this work and each step is represented in Figure 4-1C.

For covalent immobilisation of capture antibody on the aldehyde-modified paper circle, a solution containing monoclonal antibodies (3 µL, 161 µg mL^{-1}) against CA15-3 antigen was added and let to incubate at 37 °C in the oven for 10 min. Then, any remaining aldehyde functions and non-specific binding regions of the antibodies were blocked by addition of BSA solution (3 µL, 1%). After incubation for 10 min at 37 °C, a washing and a drying step were followed. At this stage, the paper circles were ready to detect CA15-3.

After each incubation, a washing step was performed with 1 mL of PB. Washing steps between the incubation steps are crucial to remove unbound material from the sensor surface, which could increase background noise. Despite washing, the drying steps proved to be essential in this assay. For this reason, washing and drying steps were carried, after each incubation step and before the next one, as follows. Washing buffer (PB, 1 mL) was allowed to pass through the circle paper with the aid of a Pasteur pipette. An auxiliary filter paper was positioned under the reaction paper circle to absorb the excess of washing buffer and the paper was allowed to dry at 37 °C in the oven for 15 min. At this stage, the paper circles were ready to detect CA15-3.

4.2.5. Detection of cancer antigen 15-3

The detection ability of the test-strips was tested by incubating CA15-3 antigen standard solutions with different concentrations (from 2 to 2000 U mL $^{-1}$) prepared in PB. The control was made by incubating only PB solution and this was considered the background signal. After finishing the incubation time, the test-strips were washed to remove unbounded target, and dried.

Antigen binding was detected by adding HRP-labelled antibody (5 µg mL $^{-1}$) to the test-strips. It recognises the CA15-3 previously bound to the capture Ab and forms a sandwich structure. After this interaction, the paper was washed and allowed to dry. Color development was achieved by pouring 5 µL of a ready-to-use redox indicator solution of TMB onto each reaction paper. A multichannel micropipette was used for this step to ensure the same reaction time for all test-strips. A color change from colorless to blue immediately occurred on the paper zone and images were immediately captured in the dark box (Figure 4-1A and Figure 4-1B).

4.2.6. Quantitative data and sample analysis

Quantitative data were obtained by capturing images with a smartphone and analysing them with ImageJ software. The coordinates of the RGB and HSB color systems were considered with the aim of obtaining a linear trend as a function of concentration. HSB system was chosen to optimally represent the absence or presence of the protein proportional to its concentration.

The performance of this paper-based assay was evaluated in Human Cormay® serum. Thus, various concentrations of CA15-3 (from 2 to 2000 U mL $^{-1}$) were added into Cormay® serum aliquots using a 100-fold dilution of serum.

4.2.7. Selectivity assay

Since it is assumed that the sensor will be used under real conditions, selectivity is a crucial parameter to be evaluated. The selectivity of this sensor system was evaluated by incubating various interfering molecules normally present in human serum samples. For this purpose, CA15-3 (25 U mL $^{-1}$) plus glucose (1 mg mL $^{-1}$), CA15-3 (25 U mL $^{-1}$) plus CEA (0.25 ng mL $^{-1}$), and CA15-3 (25 U mL $^{-1}$) plus CA125 (0.35 U mL $^{-1}$), prepared in PB, were incubated on the filter paper.

4.2.8. Carboxy-nanocellulose modification of the sensor surface

At least, we want to verify if a modification of the sensor surface with carboxy-NC synthesized in a previous work, Chapter 3, enables the improvement of its performance. This was tested after the optimisation of all the above described parameters, and the previously selected functionalisation was replaced by carboxy-NC. For this purpose, 3µL of a carboxy-NC solution (5 mg mL $^{-1}$) was incubated onto the paper surface after the washing step with NaOH. The solution was able to dry on the paper for 10 min at 37 °C. After that, the sensor was constructed as previously described. The effect of NC was evaluated, comparing one and three layers of nanomaterial deposited on the paper surface.

4.3. Results and discussion

4.3.1. Chemical modification of the paper substrate

Cellulose consists of glucose units with (1-4) bonds arranged in linear polymer chains. The dominant chemical functions are the hydroxyl groups, which are targeted in the subsequent chemical modification of cellulose.

NaOH was used in this work for pre-treatment of cellulose. The process of cellulose treatment with sodium hydroxide is commonly known as mercerization and leads to chemical and morphological modifications on cellulose. The immersion of cellulose on high NaOH concentrations (7-8 wt.%) causes the Na^+ penetration on intracrystalline spaces. This process is usually finished with a washing step in water or an alcohol and leads to the transformation of cellulose I into cellulose II (274, 275).

Physical adsorption is often used to immobilise antibodies on substrates because it is simple. However, this process can cause antibodies to desorb in the washing steps. In addition, cellulose has a limited number of functional groups on its surface, which hinders adsorption binding. Therefore, covalent bonding can improve the stability of the final test-strip (84, 88), which has been

attempted herein by aminated silanes or carbonyl modification. In one approach, silane modification was tried. Alkoxysilanes such as APTES react with -OH groups on the cellulose surface to form a stable coating (276) containing -NH_2 groups on the outer surface that promote antibody binding.

In another approach, carbonyl modification with potassium periodate was tried. This reaction cleaves the C–C bonds between the - OH vicinal groups and oxidizes each carbon to form aldehyde functions (–C=O). Subsequently, the amine groups of the antibodies can bind to the aldehyde groups of the cellulose paper by nucleophilic addition to form an imine (84, 88, 277, 278).

The above mentioned chemical modifications were followed by FTIR analysis (Figure 4-2A and Figure 4-2B). As expected, the characteristic hydroxyl groups of cellulose were observed in all samples. These are in the range 3660 to 2900 cm^{-1} and are assigned to O–H stretching and C–H stretching (279). The silane modification was not detectable in the FTIR spectra because the absorption region around 1000 cm^{-1} already has low transmittance due to the intense C–O vibrations. However, the presence of the amine groups of APTES was further confirmed by the Bradford test on the surface of the paper. As for the oxidation of cellulose by periodate, the appearance of a differential absorption peak at around 1720 cm^{-1} indicated the presence of a carbonyl group C=O corresponding to stretching in aldehyde groups, according to the reaction between the glucose units and periodate.

These chemical modifications were followed by thermogravimetric analysis. Thermal stability and degradation profile of (i) raw paper, (ii) NaOH-washed paper, (iii) APTES-modified paper and (iv) KIO_4-modified paper was evaluated for this purpose, obtaining degradation curves of the cellulosic material (Figure 4-2C and Figure 4-2D). The greatest weight loss occurred at about 300 to 380 °C (Figure 4-2C), which can be attributed to the decomposition of cellulosic and non-cellulosic materials. Raw paper, NaOH-washed paper, APTES-modified paper, and KIO_4- modified paper exhibited peak temperatures (Figure 4-2D) at 341 °C (weight loss of 94.4%), 356 °C (weight loss of 91.0%), 358 °C (weight loss of 83.7%), and 343 °C (weight loss of 87.9%), respectively. When comparing raw paper with NaOH-washed paper, this one is thermodynamically more stable (peak temperature shifted from 341 °C to 356 °C) due to the conversion of cellulose I into cellulose II, thus confirming its modification (275).

Regarding the functionalisation step, NaOH-washed paper started to decompose around 325 °C and ended at about 375 °C (ΔT= 50 °C), while the temperature of thermal decomposition of oxidized cellulose (KIO_4-modified paper) shifted to lower temperatures and lower intensities,

proceeding more slowly as it started to decompose at 305 °C and ended at 360 °C (ΔT= 60 °C) (277).

The chemical modifications of cellulose paper were further followed by the Bradford assay. It results in a higher number of bound antibodies, each paper circle modified with APTES and periodate was incubated in 1% BSA for 30 min, washed with PB, and incubated with a conventional protein dye, Bradford reagent. Bradford assay is based on binding of Coomassie Brilliant Blue G-250 to proteins which causes a shift in the absorption peak of the dye, observed by naked eye (280). This binding is based on the electrostatic interaction between the sulphonic groups from the reagent and the basic amine groups from the proteins (281). In the presence of amino groups (from antibodies and proteins), the Bradford reagent changes color from brown to blue, which intensity is proportional to the to $-NH_2$ content on the surface.

Since the APTES-modified cellulose had amine groups on its surface, the main difference between the control and the paper with BSA was taken into account when selecting the better modification. The stability of protein binding was also monitored in this assay as the BSA was allowed to interact with the modified cellulose substrates and was conveniently washed out before Bradford reagent was added. Thus, non-specific binding events of low stability were eliminated by washing. The data were presented in the form of the HSB coordinates, reflecting the observed color change. As can be seen in the images from Figure 4-2E and corresponding bar charts from Figure 4-2F, the highest difference was obtained with periodate modification, thus indicating that a greater amount of protein was present on the KIO_4-modified cellulose paper.

Overall, considering the Bradford assay data and the FTIR/TGA results, the oxidation with potassium periodate appears to be more effective than APTES modification for further binding of proteins (or antibodies) and was selected for further experimentation. The efficiency of the bound antibodies in recognising the target protein was evaluated by optimising the conditions for binding CA15-3.

4.3.2. Optimisation of the assay conditions

In order to achieve good sensitivity and consistent results, the effects of several variables were analysed using the paper-based ELISA method. First, the minimum reagent volume required to cover the entire paper surface was analysed. Then, parameters that could affect the results of the immunoassay were evaluated, including the composition of the wash buffer, the washing procedure, the concentration of capture and detection antibodies, the concentration of blocking

agent, the number of washing steps between incubations, the temperature of the incubation and drying steps and the effect of functionalisation. During the optimisation experiments, different conditions were tested and the HSB values extracted from the ImageJ analysis were compared. The condition that showed the greatest difference between a negative control and a positive result was selected for further testing.

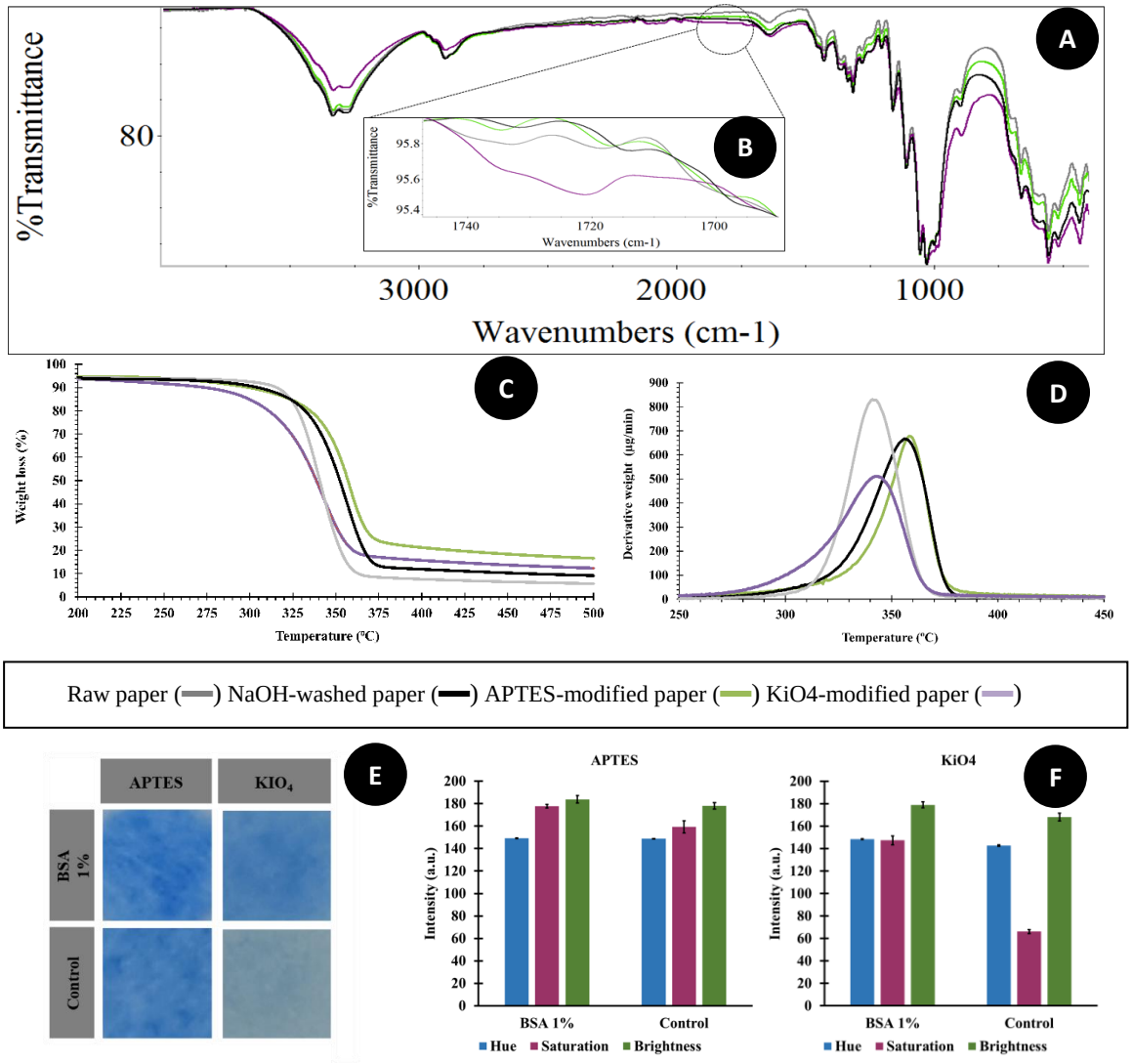

Figure 4-2. Characterisation of paper substrate before and after washing treatment and functionalisation. FTIR spectra (A) and zoom at 1720 cm^{-1} (B); TGA (C) and DTG (D) spectra; pictures of paper test-strip after Bradford assay in APTES-modified or KIO_4-modified paper incubated with buffer vs BSA (E). HSB coordinates of the several modifications (F). In (C) and (D).

4.3.2.1. Minimum reagent volume optimisation

The choice of minimum reagents was important from the point of view of cost and reproducibility. Some reagents are quite expensive, and their use should be kept to a minimum. On the other hand, using larger volumes than necessary to cover the paper circles means that

some of the reagent does not contact the substrate paper, resulting in non-reproducible data. The results illustrated in Figure 4-3 show that 3 µL of solution covers the entire paper surface, while lower volumes do not. Higher volumes provided comparable results to 3 µL but would result in higher costs for the entire test-strip assembly. Therefore, a volume of 3 µL was chosen for all reagents added for further experiments.

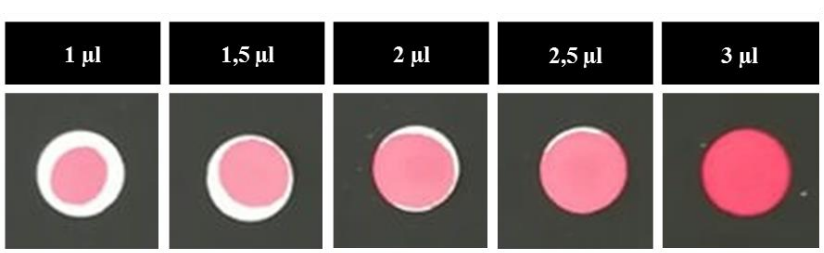

Figure 4-3. Photographs of paper circles with different volumes of food coloring for reagent volume optimisation

4.3.2.2. Buffer composition

Washing steps between incubations are important to remove unbounded materials that could cause background signals. Not only the amount of buffer but also its composition should be studied. Washing only with buffer (129, 186) and buffer with Tween20 (27, 42, 86, 94, 142) has been reported. Figure 4-4 shows that when the papers were washed only with PB, a higher difference is observed in terms of observed color (Figure 4-4A). The HSB values in the bar graphs (Figure 4-4B) between control and protein change more when PB is used, especially for coordinate saturation. Further experiments were performed using PB only after it was shown.

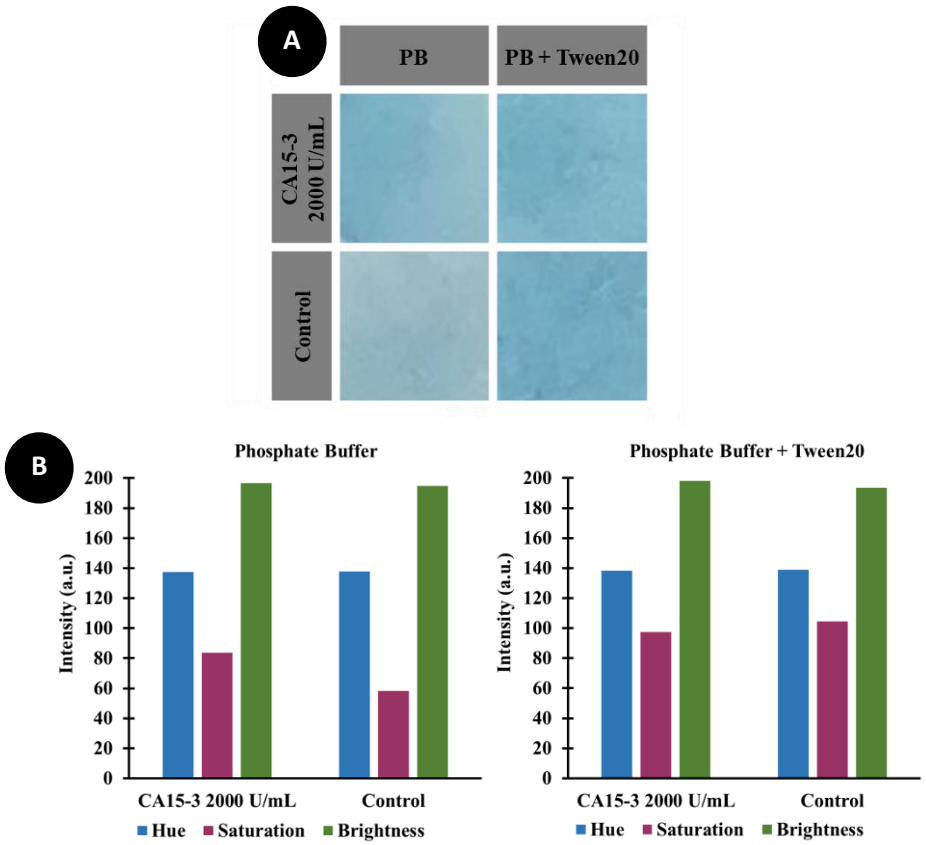

Figure 4-4. Photographs (A) and respective bar charts (B) of saturation values from optimisation of the composition of washing buffer (PB vs PB with Tween20).

4.3.2.3. Capture and detection antibody concentration

Three different concentrations (1.61, 16.1 and 161 μg mL $^{-1}$) of capture antibody were tested for a common target protein concentration of 2000 U mL $^{-1}$ CA15-3. Basically, the higher the amount of antibody on the periodate-modified paper, the higher the sensitivity of the test, but there is a concentration above which it is useless to add more antibody. Changes are not significant, and the test would only become more expensive. Although minor differences were found between the different concentrations, it seemed evident that 161 μg mL $^{-1}$ gave the largest difference between the control and the positive result (Figure 4-5). Therefore, solutions with an antibody concentration of 161 μg mL $^{-1}$ were selected for further studies.

Detection antibody was also tested at three different concentrations (0.5, 5.0, and 50-μg mL $^{-1}$) for a target protein concentration of 2000 U mL $^{-1}$ CA15-3. The results obtained are shown in Figure 4-6. While 0.5-μg mL $^{-1}$ showed hardly any color and 50-μg mL $^{-1}$ showed a very intense color with almost no difference between negative and positive results, 5-μg mL $^{-1}$ showed a large

difference. The color of the blank sample was very light and appeared greenish, while the color of the positive sample was a clear blue. This condition was therefore selected for further testing.

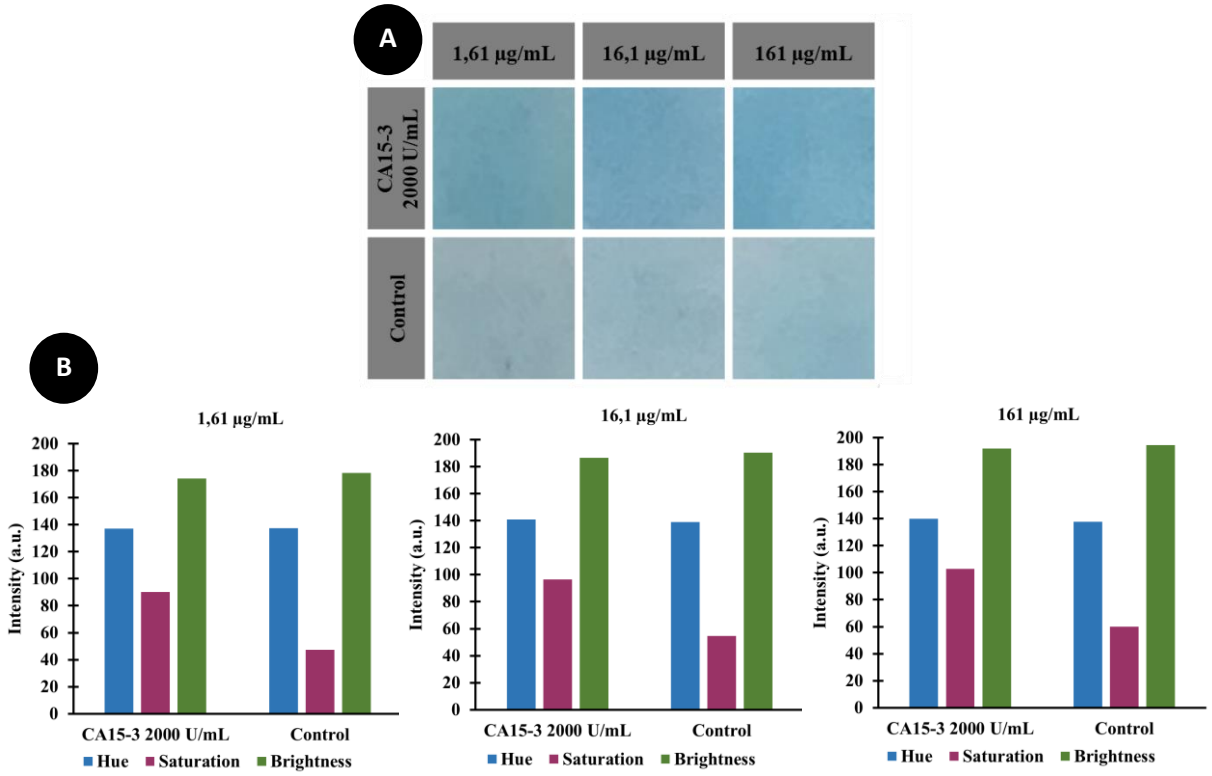

Figure 4-5. Photographs (A) and respective bar charts (B) of saturation values from capture antibody concentration optimisation with 1.61, 16.1 and 161 µg mL $^{-1}$.

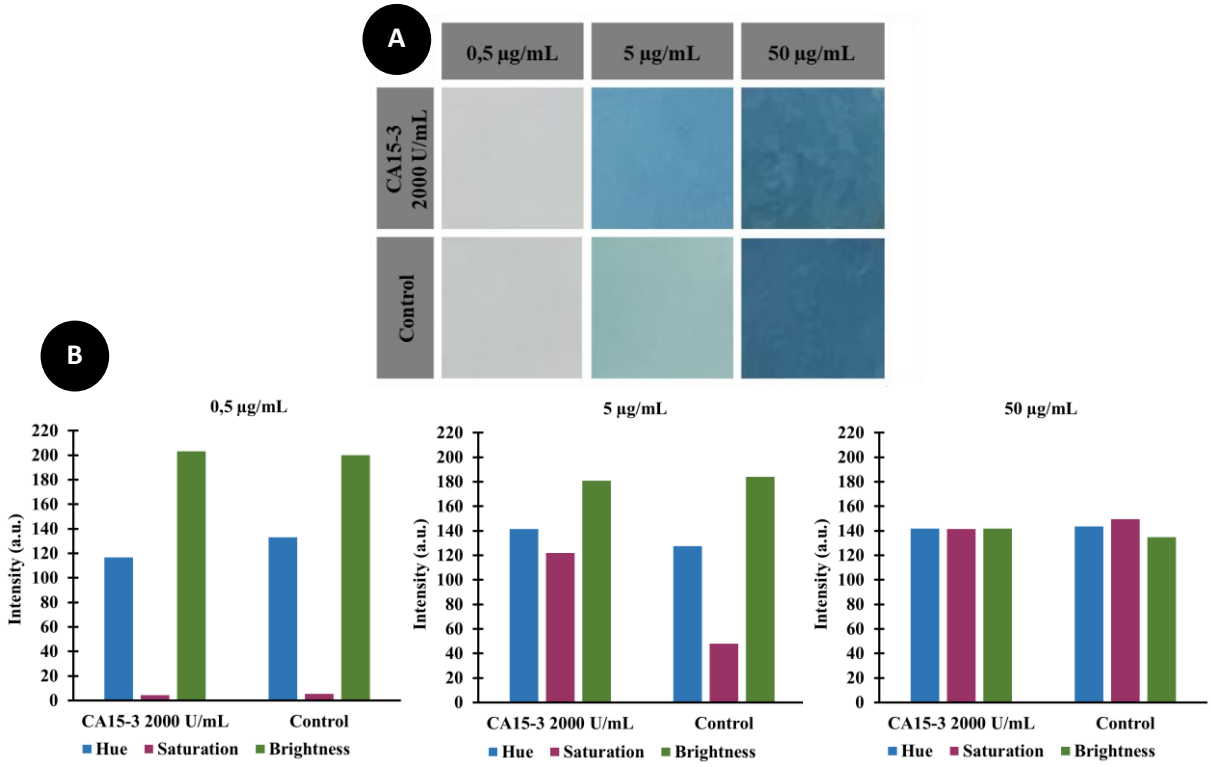

Figure 4-6. Photographs (A) and respective bar charts (B) of saturation values from detection antibody concentration optimisation with 0.5, 5 and 50-µg mL $^{-1}$.

4.3.2.4. Blocking agent concentration

BSA is frequently used in ELISA as a blocking agent to prevent non-specific bindings of other molecules (e.g. proteins, antibodies) to the surface (282). Absence and presence of BSA as blocking buffer was evaluated in three different concentrations (0.1, 1 and 10%). Results are shown in Figure 4-7. Increasing concentrations of BSA provided higher background signals in negative controls. It has already been reported in a previous work that some BSA formulations (including globulin or endotoxin) used for blocking step cause high background signals (282). Despite that, it was also reported that some antibodies used in ELISA can cross-react with BSA (283). Nevertheless, due to the occurrence of a considerable background signal at controls, possibly resulting from the facts described before (interference from BSA formulation and/or antibodies cross-reaction), 1% of BSA was selected as the best concentration for the blocking step since it provided a more pronounced difference between the control and a positive result.

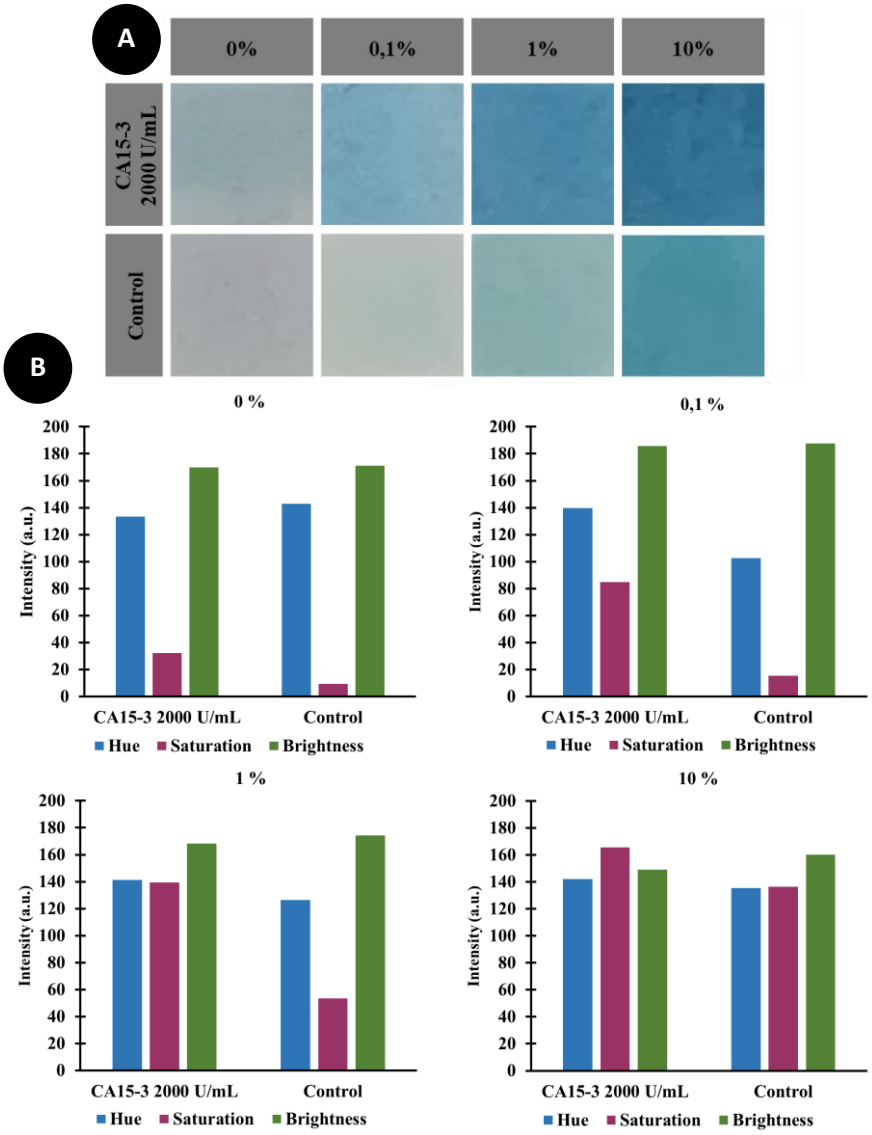

Figure 4-7. Photographs (A) and respective bar charts (B) of saturation values from blocking agent concentration optimisation with 0, 0.1, 1 and 10% of BSA.

4.3.2.5. Number of washing steps

As already stated, the washing step in ELISA assays is crucial to reduce background signals provided from unspecific bindings. Besides the composition of the washing buffer, already optimised, the number of washing steps (no washing *versus* one washing step with 1000 µL of PB *versus* three washing steps with 1000 µL of PB) was also tested (Figure 4-8). No washing results in highly colored papers due to background signal from unbounded or unreacted reagents and a small difference between the positive result and the negative control. One washing step led to a higher difference between the papers and was proved to be efficient in the removal of unbounded reagents. Finally, three washing steps showed a small difference between papers, when compared with only washing step, and leads to an increase in HSB values of negative control. This may be due to the fact of the excessive wash can promote the removal of more capture antibody, thus promoting nonspecific bindings and increasing the background signal. Therefore, only one washing step with 1000-µL of PB was selected for further assays.

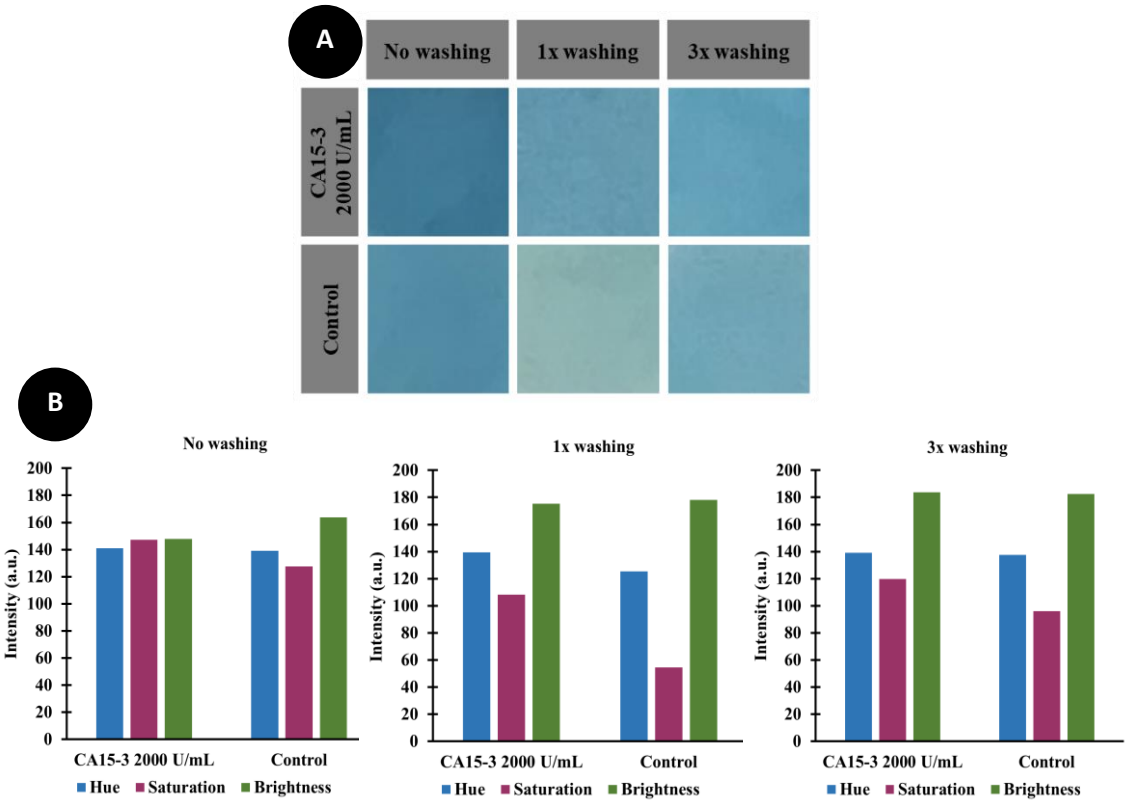

Figure 4-8. Photographs (A) and respective bar charts (B) of saturation values from number of washing steps optimisation, including no washing, one washing step with 1000-µL of PB and three washing steps with 1000-µL of PB.

4.3.2.6. Incubation and dry temperature

Temperature of incubation and drying steps have been mentioned as important factors in the assay performance. Incubation and drying at room temperature (21 °C) were tested against 37 °C (Figure 4-9). Room temperature provided very colorful papers but seemed to promote unspecific response in the negative control as it shows higher HSB values, especially on saturation parameter, compared to the positive result. Thus, 37 °C was selected as the best condition.

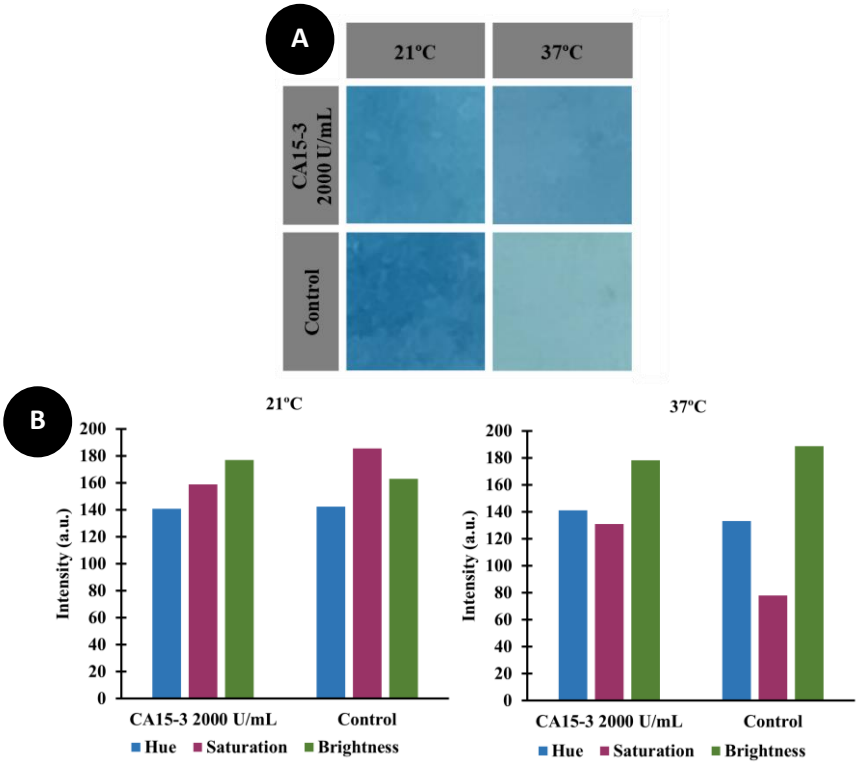

Figure 4-9. Photographs (A) and respective bar charts (B) of saturation values from incubation and dry temperature optimisation with 21 °C and 37 °C.

4.3.2.7. Effect of functionalisation

The effectiveness of the functionalisation step with KIO_4 was already showed through the characterisation by FTIR, TGA and Bradford assay. However, it is important to assess if this step is or not essential to the performance of the assay. Results (Figure 4-10) showed that paper without functionalisation exhibits no significant differences between control and positive result, hence justifying the need to functionalise to assure a proper capture antibody mobilization and further recognition of the target protein.

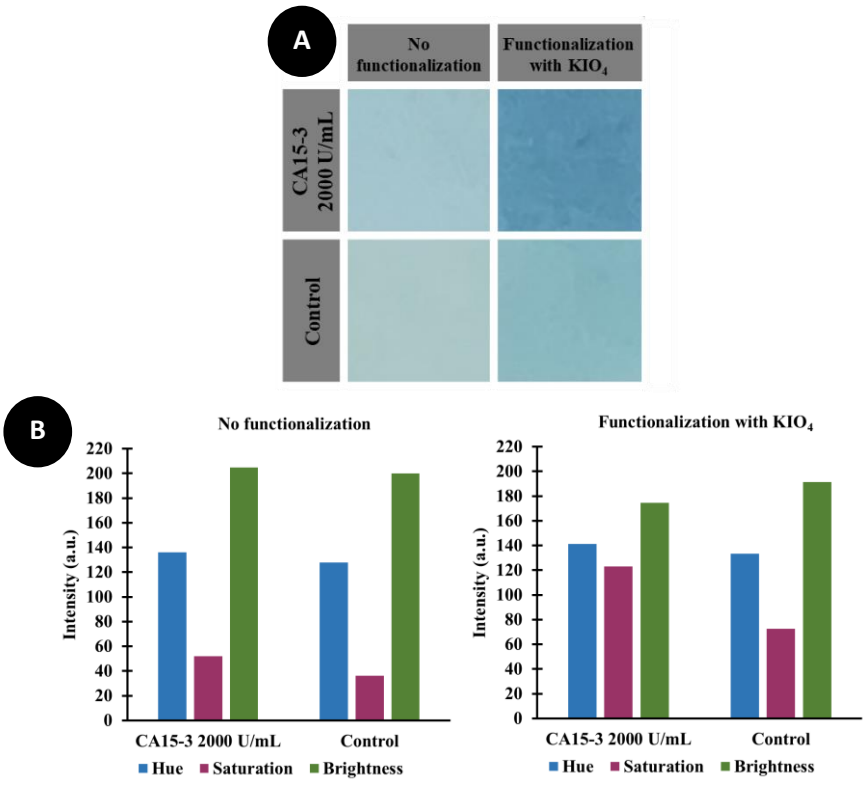

Figure 4-10. Photographs (A) and respective bar charts (B) of saturation values from papers without functionalisation and with KIO_4 functionalisation.

4.3.3. Main analytical features

The intensity of the blue color of oxidized TMB depends on the amount of peroxidase enzyme catalysing the reaction. This is determined by the amount of HRP-labelled antibody bound to the target analyte. When CA15-3 is present in the sample, the HRP coupled to the detecting antibody allows the colorless TMB to oxidize to TMB^+, resulting in a blue color complex that is visible to the naked eye. Therefore, the intensity of the blue color of the oxidized TMB is proportional to the CA15-3 present in the sample.

It is worth noting that the background signals for blank paper circle could come from residual HRP-marked Ab that remain on the sensor surface. This is because the blocking agent could not completely block the reactive sites, making these sites available for the HRP-labelled antibody. Moreover, the HRP-labelled antibody used as the detection antibody could also bind to the capture antibody. These results are consistent with previous paper-based ELISA assays using colorimetric detection, which also showed color development in negative samples (269).

Figure 4-11A displays the sensor color change with increasing concentrations of CA15-3 (from 2 to 1100 U mL^{-1}) after HRP reaction with TMB. The data obtained showed a linear trend in hue

values against logarithm concentration, corresponding to Hue = 3684.3 × log(CA15-3, U mL $^{-1}$) + 125098m with R-squared > 0.997 (Figure 4-11B). Each data point represents an average of three independent experiments, and the error bars indicate the standard deviation (SD).

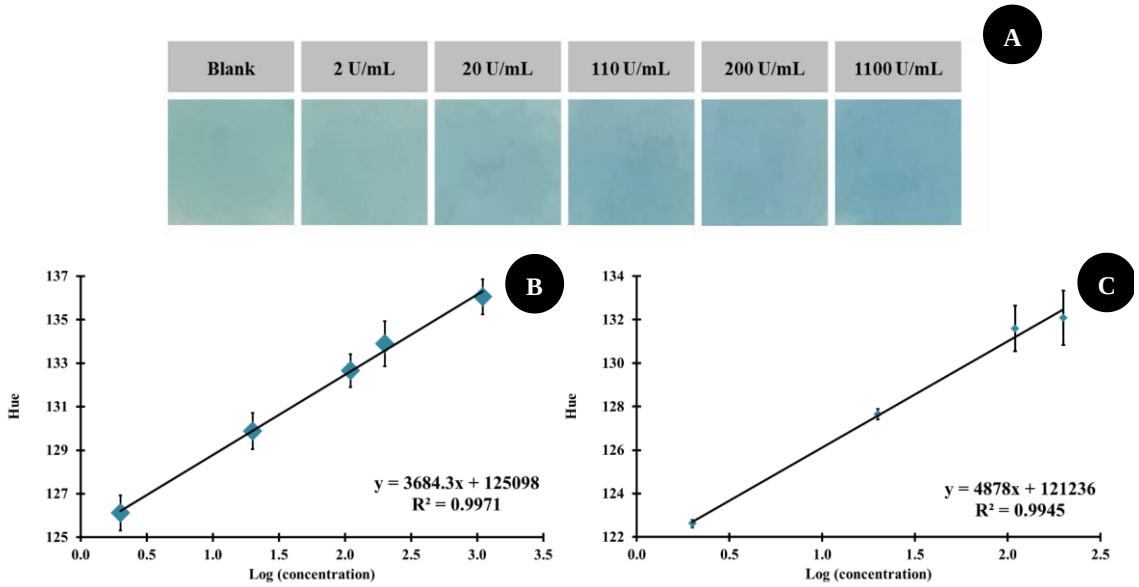

Figure 4-11. Pictures of the colorimetric sensor showing the color change with increasing concentrations of CA15-3 (from 2 to 1100 U mL $^{-1}$) prepared in PB, after HRP reaction with TMB (A) and respective calibration curve of hue values extracted from the photographs vs logarithmic concentration (B). Calibration curve of the sensor incubated with a 100-fold dilution of Cormay® serum spiked with CA15-3 (from 2 to 200 U mL $^{-1}$) (C). Equations from calibration curve are shown.

4.3.3.1. Spiked serum samples

Figure 4-11C demonstrates the sensor response for the detection of CA15-3 in Cormay® serum. It showed a linear trend in hue values against logarithm concentration, corresponding to Hue = 4878 × log(CA15-3, U mL $^{-1}$) + 121236 (R-squared > 0.994). Compared with the experiments in PB, we obtained similar linearity but a narrower linear range (from 2 to 200 U mL $^{-1}$). The assay was performed in triplicate. Each data point represents the average of the assays, and the error bars indicate SD. Thus, it was confirmed that this P-ELISA can be used to detect CA15-3 in human serum with good performance.

4.3.3.2. Selectivity assay

Glucose, CEA and CA125 were incubated simultaneously with CA15-3 on the paper substrate and compared with CA15-3 incubated alone. It can be seen from Figure 4-12 that the response of the paper test-strip was not significantly affected by other interfering factors, as the deviations of the tested interfering species compared to the CA15-3 value were 1.6%, 7%, 12.1% (all below

15%), respectively. The test was performed in triplicate and the data are presented as mean ± SD.

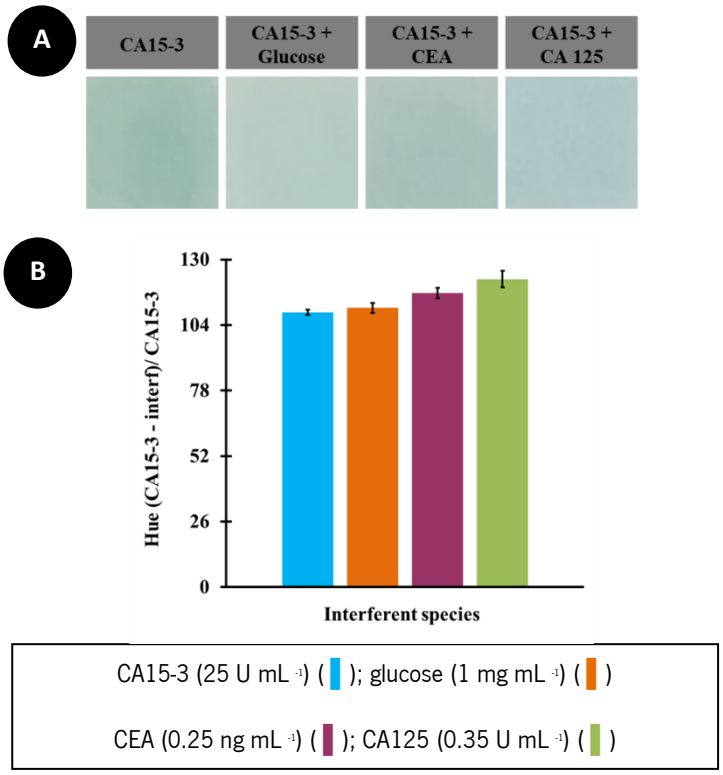

Figure 4-12. Selectivity study based on comparison of the response of CA15-3 incubated alone or mixed with interfering species. Photographs (A) and respective bar chart (B) with mean ± SD.

4.3.3.3. Carboxy-nanocellulose modification of the sensor surface

Despite the good performance obtained in the reported sensor, we want to verify if the modification of sensor surface with a carboxy-NC synthetized in a previous work (284) provide any improvement.

It is expected that the presence of -COOH groups on cellulose surface provided by carboxyl-NC enhance its binding efficiency to the primary antibody, thus increasing the colorimetric signal. However, results in Figure 4-13 shown that neither one nor three layers of carboxy-NC improved the performance of the sensor as it was not possible to visually distinguish between the different concentrations of protein. This highlighted that each system has its own characteristics, and each sensor needs to be carefully optimised considering each parameter that can affect the sensor performance.

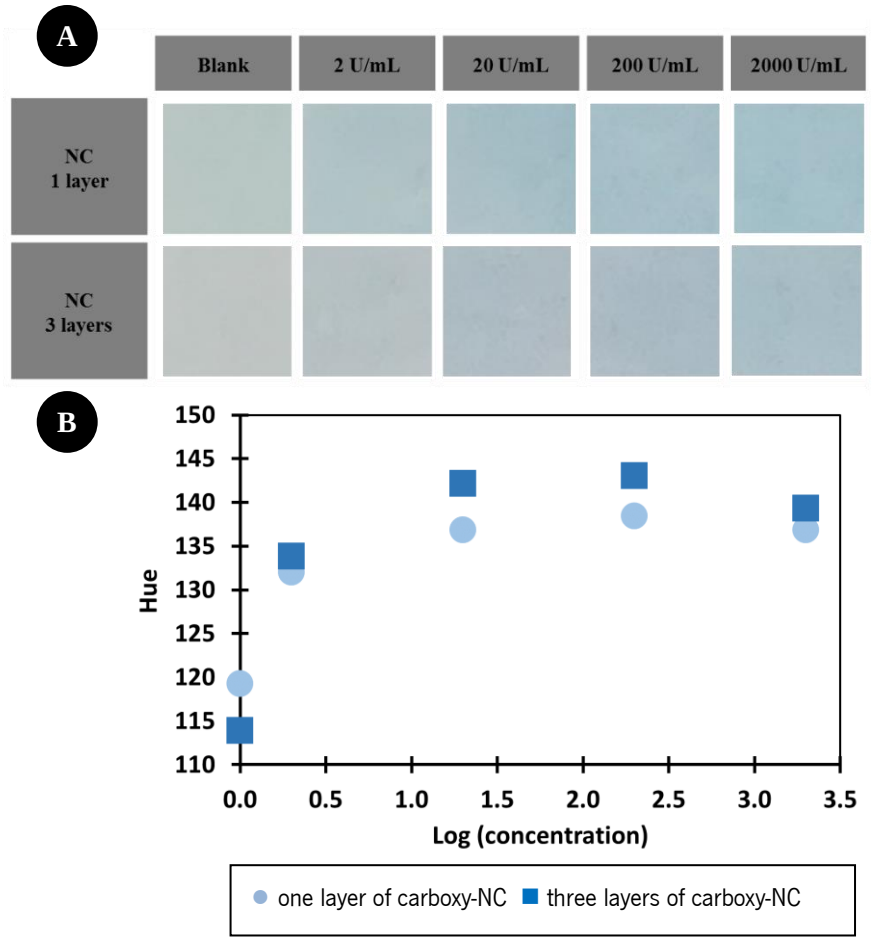

Figure 4-13. Photographs (A) and calibration curve (B) of the effect of sensor functionalisation with carboxy-NC

4.4. Conclusions

The biosensing strips described here are a rapid and sensitive method for the detection of cancer proteins on a paper substrate, consisting of a sandwich ELISA method on a surface-modified cellulose filter paper with colorimetric detection based on TMB oxidation.

The combination of an inexpensive and biodegradable substrate such as filter paper with simple colorimetric detection makes this sensor suitable for PoC detection of cancer biomarkers such as the CA15-3 protein. In addition, colorimetric detection as a transduction method allowed the qualitative result to be obtained with the naked eye, and data analysis with the ImageJ made it possible to determine the color coordinates and extrapolate the target concentration by comparison with a calibration curve. A good correlation coefficient was obtained with both buffer and human Cormay® serum (R^2 >0.99), suggesting that the sensor is suitable for clinical practice. In addition, the sensor proved to be selective for the target analyte as it was not significantly affected by other interfering

molecules. A major disadvantage of colorimetric sensors is their lack of sensitivity and high LODs. In this work, however, CA15-3 could be detected in the clinical range without the need for lower LODs. The entire test (including the construction of the sensor) can be performed in approximately 2 h, which is shorter than the duration of a conventional ELISA. The target can be detected in 35 min (Table 4-1).

Table 4-1. Reagent's volume and reaction time for the detection of CA15-3 using the reported paper-based sensor.

Reagents	Volume (µL)	Time (min)
Sample	3	10
Washing buffer	1000	-
Dry Step	-	15
Detection antibody	3	10
Washing buffer	1000	-
Dry Step	-	15
Revealing step (TMB)	5	-

The short incubation times used for the assay may be due to the high surface-to-volume ratio and porous structure of cellulose. These properties of cellulose also allow the use of a low volume of reagents and samples, which is an advantage of the P-ELISA over the conventional ELISA.

Despite the advantages of this simple and rapid detection of CA15-3, there are still costs associated with the use of antibodies as detection elements. A future improvement could therefore be to replace natural antibodies with other synthetic biomimetic materials, such as molecularly imprinted polymers or aptamers.

Chapter 5

Paper-based biomimetic test-strip for cancer antigen 15-3 with colored readout

Chapter 5 focused on the replacement of the antibody in paper-based ELISA protocol described in Chapter 4 by a MIP. The target and colorimetric system used were the same of the previous work.

Part of the content of this chapter was published in Microchemical Journal:

C.C.G. Carneiro, M., Rodrigues, L. R., Moreira, F., & Goreti F. Sales, M.. Paper-based biommimetic test-strip for CA15-3 with colored readout. Microchemical Journal. 2024;196:109640.

5. Paper-based biomimetic test-strip for cancer antigen 15-3 with colored readout

5.1. Introduction

Several biosensors were already reported for CA15-3 detection, in which different REs as antibodies (10, 21, 192), MIPs (60, 122, 193) or aptamers (15) were coupled with electrochemical (10, 21, 60, 193) or optical (15, 121, 192) signal transduction approaches.

The previous work (192) reported a paper-based colorimetric immunosensor for CA15-3. Despite the well-established role of antibodies as REs and their unquestionable selectivity for their targets (22), they still present some issues regarding their cost and stability (23). For that reason, researchers are searching for new REs, namely synthetic ones, as MIPs or aptamers (1, 24). The purpose of this thesis was to produce colorimetric sensors for cancer biomarkers, on paper substrates, and using synthetic REs. After proving the applicability of colorimetric detection onto a paper substrate for glucose in Chapter 3 and demonstrating the performance of P-ELISA for CA15-3 in Chapter 4, it is time to adapt the procedure developed on the previous chapter, replacing the antibody by a MIP. MIPs were originally developed for sample purification and pre-concentration of analytes, but they are also used as REs for various biomarkers (105, 175). Their recognition ability is due to the complementary cavities formed during their production and allows their use as replacements for natural antibodies in ELISA, leading to biomimetic enzyme-linked immunosorbent assay (B-ELISA). MIPs as alternatives to natural receptors can help overcome these drawbacks by improving sensor performance, shortening reaction time and increasing selectivity and sensitivity (105).

The first B-ELISA was published in 2000 (285). It is cheaper, more stable, and easier to produce, and has lower batch-to-batch variability than conventional ELISA approaches (103, 104, 107). Various approaches have been used to integrate MIPs into ELISA assays, which include direct polymer growth on the substrate, including 96-well microplates (286) or paper substrates (104, 287-291), or fabrication of MIP NPs to coat the substrates (103).

In general, paper is a versatile substrate for the growth and immobilisation of MIPs (104), and the inclusion of MIPs as REs in PADs has led to new advances in low-cost and highly selective analytical devices (105). Paper-based MIPs have been developed for various molecules (e.g. disease biomarkers, metal ions, pesticides or pollutants) (105), with CL being the main detection mode. Color detection provides a simple visual readout that can provide qualitative or semi-quantitative data. Quantitative

data is also possible, although colorimetric detection usually has low sensitivity and some non-specific adsorption (105).

As we know, no one has used this for glycoprotein recognition yet. This paper therefore presents a B-ELISA method for the detection of CA15-3, combining traditional ELISA (detection method) with MIP (detection element) and paper as substrate.

5.2. Experimental

5.2.1. Reagents and solutions

All chemicals employed in the present work were of analytical grade and water was ultrapure Milli-Q laboratory grade.

Sodium phosphate dibasic dihydrate and sodium chloride (NaCl) were acquired from Panreac (Spain). Sodium dihydrogen phosphate dihydrate was from Scharlau (Australia), while sodium hydroxide (NaOH) was sourced from EKA (Brazil). APTES and 3-aminophenylboronic acid monohydrate (3-APBA) 98% were both from Acros Organics (United States). As chromogenic substrate we relied on TMB liquid Substrate System for ELISA and HRP (275 U mg^{-1}) from Sigma Aldrich (Germany). Dopamine, in the form of 3-hydroxytyramine chloride was purchased from Merck (Germany). Ammonium persulfate (APS) was acquired from Analar Normapur (Belgium). N,N,N',N'-Tetramethyl-ethylene diamine ≥ 99% (TEMED) was obtained from Fisher Chemical (United States). Triethoxyphenylsilane (TEPS) < 98% was acquired from Fluka (United States). Hydrogen peroxide (H_2O_2) 35% was purchased from Labchem (United States). Absolute ethanol 99.8% was purchased from Riedel-de-Haën (United States).

Whatman® quantitative filter paper (ash-free, grade 40, 110 mm diameter, 210 μm thickness, 8 μm pore size), from Sigma Aldrich (Germany), was used as substrate.

CA15-3 from human host (reference MBS536585) was purchased from MyBioSource (United States). The detection antibody (recombinant monoclonal antibody against MUC1 labelled with HRP, reference EPR1023) was purchased from Abcam (United Kingdom).

Stock solutions of proteins and antibodies were prepared in PB (0.081 M Na_2HPO^4 and 0.019 M NaH_2PO^4, pH=8.5).

5.2.2. Apparatus

Scanning electronic microscopy (SEM) and TGA were used to characterise modified cellulose paper. SEM images were acquired on FEI Quanta 400FEG ESEM/EDAX PEGASUS X4M

instruments with gold sputter coating. TGA measurements were performed with ≈1.5 mg of sample, using a platinum holder from 30 to 1000 °C under a nitrogen atmosphere of 40 mL min^{-1}.

A homemade darkroom (19 cm width × 13.5 cm height × 13.5 cm depth) with a light-emitting diode strip (LED) (high luminosity, 4000K, 50/60 Hz, DC12V) covering the four sides of the chamber was used for image acquisition.

5.2.3. Methodologies

The complete process of synthesis and detection of the protein consists of 6 main steps and is shown in Figure 5-1. Before the imprinting step, the Cellulose Whatman® paper was washed and functionalised. Then 3-APBA was polymerised on the surface of the paper (Figure 5-1A) to react with the glycosylated CA15-3 protein. In the imprinting stage, the polydopamine layer is formed by polymerisation of dopamine in the presence of CA15-3 (MIP) or in its absence (NIP) to produce a control material (Figure 5-1B). The template was removed (Figure 5-1C) and CA15-3 was allowed to bind the formed cavities (Figure 5-1D). For the color development, the HRP was incubated (Figure 5-1E), adsorb to the proteins present and then the substrate TMB was allowed to react with H_2O_2 (Figure 5-1F).

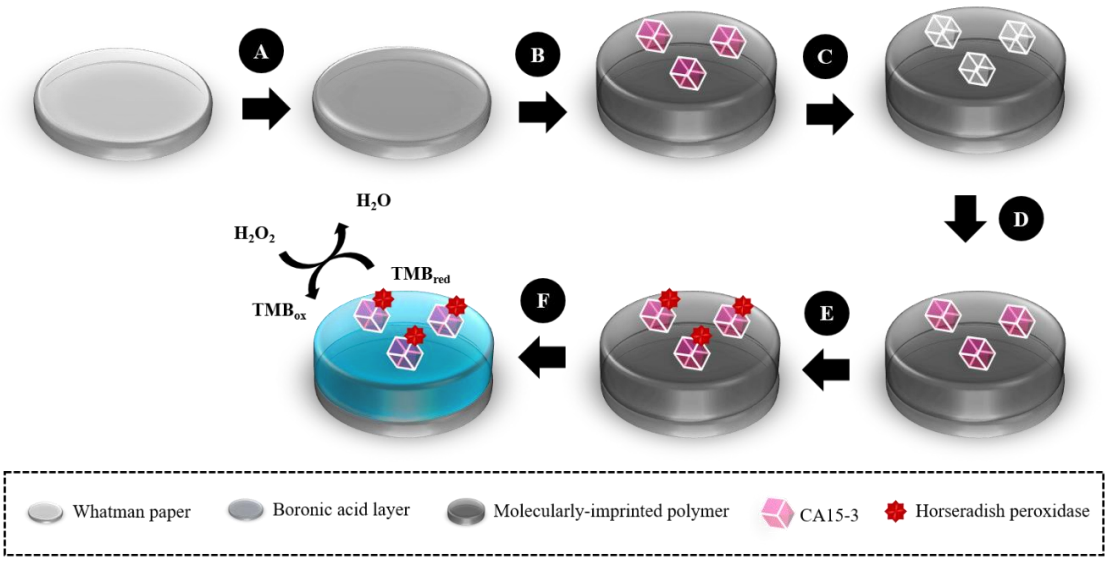

Figure 5-1. Schematic representation of the sensor construction. Production of a first layer of polymerisation with 3-APBA (A), production of MIP (B), removal step (C), rebinding step (D), HRP incubation (E), and color development with TMB solution (F).

5.2.3.1. Synthesis of biomimetic material

Prior to MIP production, the papers were first washed to remove impurities and functionalised

to obtain functional groups. A circular Whatman® filter paper (area ≈ 95 cm^2) was immersed in H_2O_2 (5M) for 2 h in a horizontal shaker. It was then soaked in water to remove unreacted products. A silane coupling technique was then applied by immersing the paper in 50 mL of a 10% silane mixture (APTES:TEPS, 1:1) prepared in absolute ethanol for 2 h at room temperature in a horizontal shaker. The paper was then thermally treated at 80 °C for 2 h. It was then rinsed with ethanol to remove unbound silanes and dried again. It was then stored in a desiccator until use.

After the washing and functionalisation steps, the cellulose paper was cut into 8 mm circles with a hole punch and modified with poly-APBA by polymerising the monomer APBA (1×10^{-4} M), using APS (1×10^{-6} M) and TEMED (1×10^{-6} M) as catalysts. These components were mixed in equal proportions and incubated on the paper circles for 2 h at room temperature in 48-well plates in a horizontal shaker. Each paper was washed with 3 mL PB (pH=8.5) and dried at 37 °C for 15 min. MIPs were then prepared using CA15-3 as the template molecule, dopamine as the functional monomer, and TEMED and APS as catalysts. A solution containing dopamine (1×10^{-4} M) and CA15-3 (at a final concentration of 100 U mL^{-1}) was incubated on the surface of cellulose paper for 1 h with stirring and protected from light. During this step, the protein was bound to the APBA layer with its boron groups (on the outer surface) and the vicinal hydroxyl groups of the glycoprotein. A solution containing APS and TEMED (1×10^{-6} M) was then added and stirred for a further hour. In parallel, a NIP was prepared. The solution added to the paper filter circles in a 48-well plate and incubated for one hour at 25 °C with horizontal shaking to obtain a uniform polydopamine film around the paper substrate. Polymerisation was then continued for a further 2 h without shaking. Finally, the papers were washed with PB to remove unreacted components and dried at 37 °C for 15 min. All solutions used for the polymerisation mixture were freshly prepared and purged with nitrogen.

To remove the template, the NIPs and MIPs were incubated with sodium chloride (0.1 M) (292) for 2 h with horizontal shaking to allow imine cleavage. Then the papers were washed with PB and left in the wells with PB for 1 h. Finally, the obtained MIPs with specific binding sites for CA15-3 were washed with PB and dried at 37 °C for 15 min.

5.2.3.2. Colorimetric protein detection

Under the optimised experimental conditions, calibration tests were performed with 5 µL CA15-3 antigen standards (from 3 to 1000 U mL^{-1}) prepared in PB, pH=8.5. The standards were

added to the paper filters and incubated at 37 °C for 10 min. As a negative control, PB was added to a paper filter instead of CA15-3, to obtain a background signal. After incubation, the papers were washed with PB to remove unbound target protein and dried at 37 °C for 15 min. In the final step of the sensor construction and before color development by adding a chromogenic substrate, incubation with HRP is essential because it reduces H_2O_2 and oxidizes TMB, resulting in a blue color. Since the optimum pH of HRP is 7 (293) and we intend to work at physiological conditions, PB with a pH of 7.4 was used to prepare the HRP solutions. In this step, 5 μL of HRP solution (50 μg mL^{-1}) was incubated at 37 °C for 10 min. Subsequently, the papers were washed with PB and dried at 37 °C for 15 min.

A ready-to-use redox indicator solution of TMB (150 μL) was added to each paper in a 48-well plate. Let them react in the dark for 5 min. The papers were removed from the plate, the excess reagent was removed with absorbent paper and the images were immediately taken in the homemade darkroom.

5.2.3.3. Real samples assay

To test the developed sensor in the presence of real samples, CA15-3 standards (from 3 to 1000 U mL^{-1}) were added to aliquots of foetal bovine serum (FBS) using a 1000-fold dilution of the serum and incubated on the sensing paper circles.

5.2.3.4. Selectivity assay

The selectivity of the sensor was evaluated by incubating various interfering molecules that may be present in human serum samples. These include CA15-3 (250 U mL^{-1}) plus CEA (0.25 ng mL^{-1}), CA15-3 (250 U mL^{-1}) plus CA125 (0.35 U mL^{-1}), CA15-3 (250 U mL^{-1}) plus glucose (1 mg mL^{-1}) and CA15-3 (250 U mL^{-1}) plus IgG (0.1 mg mL^{-1}), prepared in PB, and incubated on the sensor surface.

5.2.3.5. Analysis of results

To obtain quantitative results, images were analysed using ImageJ software. Several parameters were evaluated, and the average value of each parameter was transferred to an Excel workbook for further analysis. The YIQ system was used, where Y represents luminance and I and Q represents chrominance. The Y and Q-channels were chosen because they are best suited to describe the absence/presence of the protein, being proportional to its concentration. Y is given

by the equation Y=0.229R+0.587G+0.114B and represents the grey scale. Q is given by the equation Q=0.211R-0.523G+0.312B (294) and represents the quadrature. R stands for red coordinates, G for green and B for blue coordinates.

During the optimisation steps, the difference between the Q values of NIP and MIP control (incubated with buffer) and the Q values of NIP and MIP incubated with CA15-3 was calculated. The condition where $MIP_{control}$-MIP_{CA15-3} gives a higher value than $NIP_{control}$-NIP_{CA15-3} was selected and used for further experiments.

5.3. Results and discussion

5.3.1. Characterisation techniques

5.3.1.1. Thermogavimetric analysis

Modification of cellulose paper substrates with sensor materials was evaluated by thermal degradation at TGA (Figure 5-2). As expected, the degradation profile of the cellulose paper shows a maximum degradation rate after 320 °C, leaving a residual solid of 5.6 % at 500 °C. The addition of silanes to the cellulose substrates changes the thermal stability of the material, as silanes remain stable at higher temperatures. This reduces the proportion of the material that can be subjected to degradation, leaving a residual amount of 18.7 % at 500 °C. The subsequent steps lead to the formation of MIP or NIP materials, including poly-APBA and polydopamine on the silane-cellulose composite, which in the case of MIP also contains CA15-3. Overall, the MIP and NIP polymer layers are unstable and undergo thermal degradation mainly at temperatures between 275 °C and 365 °C, which is associated with the decomposition of the cellulosic materials. The fact that the degradation profile of all samples was similar agrees well with the similar chemical composition of all sensor materials and the fact that CA15-3 is present only in an extremely low percentage. Nevertheless, it is important to highlight that the NIP sensor was formed to a higher extent before template removal than the MIP with template. This essentially indicates that the polymer film NIP was formed to a higher extent because CA15-3 hindered the polymerisation of the polydopamine film on the MIP, justifying the lower residual amount of NIP (11.3 % at 1000 °C) corresponding to the pure silane composition. Removal of CA15-3 from the MIP film changed the residual amount of MIP from 15.4 to 18.1 %, confirming the presence of the protein. However, the same procedure to remove NIP resulted in a higher percentage weight loss, with the residual amount increasing from 11.3 to 17.9 %. Since NIP does not contain any protein to be removed, this change is likely due to

the loss of the polymeric network, that was not firmly attached to the sensor film. In general, the TGA information confirms the formation of the imprinted film and the effects of removal on the modified cellulose substrates, resulting in sensing materials that contain similar a percentage of polymer above the silane/cellulose composite.

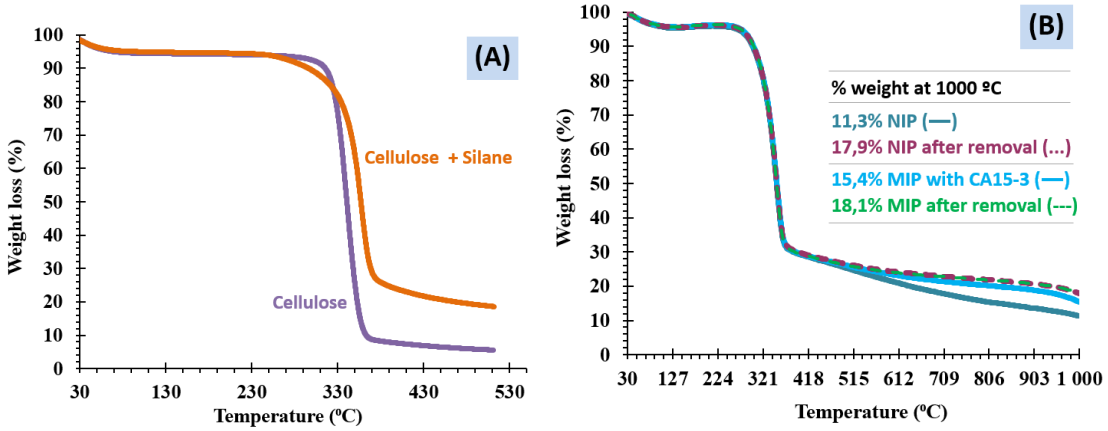

Figure 5-2. Thermogravimetric analysis of cellulose paper with or without silane modification (A) and the cellulose paper with silane modified with MIP/NIP polymerisation, including stages before and after template removal (B).

5.3.1.2. Scanning electronic microscopy analysis

The morphology of the bare and modified cellulose substrates was characterised using SEM. Figure 5-3 shows magnification images of the cellulose paper showing the typical microfibers of cellulose (A), which were also modified with polydopamine in the form of NIP (B) or MIP (C). The images show that the cellulose fibers have been coated with polydopamine during the polymerisation step, resulting in an increase in fiber diameter (B and C) compared to the naked cellulose separator (A). Higher magnification images show the polydopamine fibers and the rough polymeric surface in MIP (F) compared to bare cellulose (D) and to NIP (E), which is still smooth (287). This roughness suggests that the presence of the template on MIP led to a different structural polymer growth. Nevertheless, the embossed voids on MIP cannot be observed because the dimensions of these binding sites are below the resolution limit of the technique.

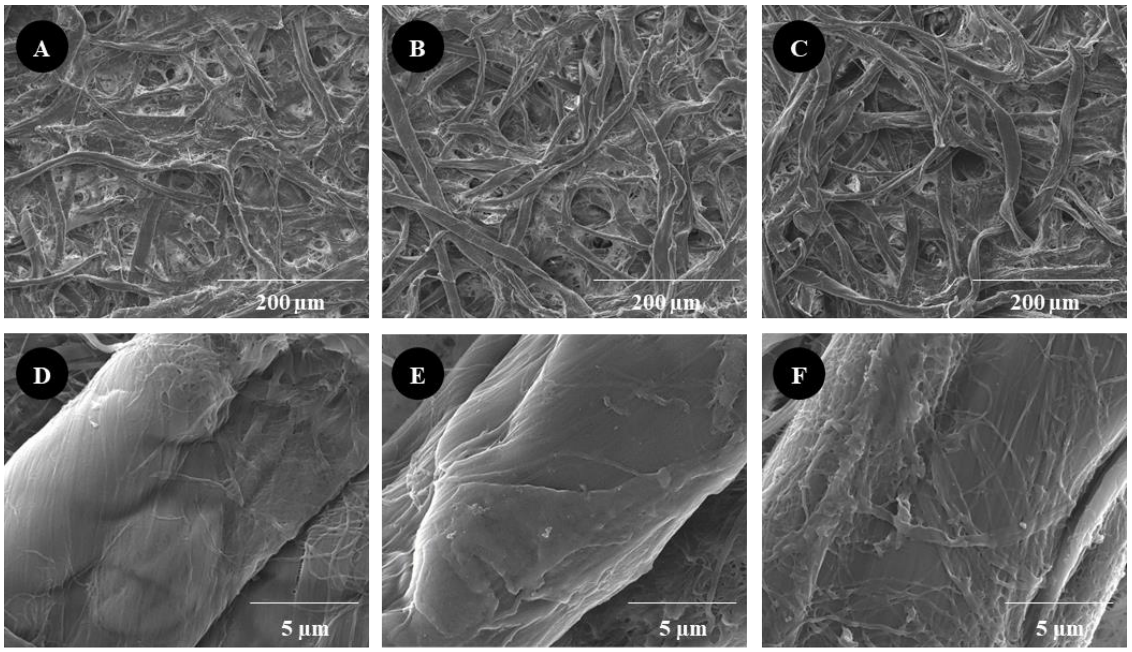

Figure 5-3. SEM images of bare paper (A), NIP (B) and MIP (C) with 500× magnification and bare paper (D), NIP (E) and MIP (F) with 15000× magnification.

5.3.2. Synthesis of the biomimetic material

The biomimetic material was assembled as shown in Figure 5-1, where a cellulose substrate was modified with silane chemistry, resulting in the interaction of the template with boronic acid and subsequent polymerisation with dopamine to form the MIP layer.

An important aspect of any chemosensor is reproducibility, which depends first on the homogeneity of the starting material. Therefore, all paper substrates were washed with H_2O_2 before any further modification. H_2O_2 is a strong oxidising agent that is said to oxidise impurities, increasing their solubility in water. It also adds hydroxyl groups to the paper surface, which helps to increase the efficiency of subsequent chemical modifications with involving covalent hydroxyl bonds (as in silane chemistry) (289). Physical adsorption would also be possible as an immobilisation technique for any intended biological RE, but desorption of the molecules may occur during the washing steps. Therefore, cellulose was modified with silane chemistry by incubating the paper in silanes. Binding to the vicinal hydroxyl groups of the cellulose (treated with H_2O_2) and cross-linking through the porous structure of the cellulose provided stable chemistry of the silane/cellulose matrix (84, 88). Next, 3-APBA was incubated on the silane/cellulose composite followed by the protein (in the case of the MIP), to undergo the reversible reaction between boronic acid (in 3APBA) and the cis-diol groups (in glycoproteins) (118). This stage corresponds to the formation of a template-monomer complex in a pre-polymerisation solution, giving rise to a cyclic bromate ester. This ester is easily

reversed by a change in pH/ions, releasing the protein as needed. The stability and suitability of this complex is critical, as this stage establishes the functional groups to which CA15-3 will bind after contact with the MIP in the sample.

The subsequent addition of a monomer/cross-linker and an initiator allowed the formation of the MIP film (105). In this work, dopamine was considered as the monomer. It is a small molecule containing catechol and amine functional groups that self-polymerise in a weak alkaline pH (295). Its polymerisation is based on the oxidation of catechol group to quinone and further reaction with amine groups and other catechols and quinones, allowing the formation of a biocompatible and hydrophilic polymeric film. This polymer is highly reactive towards amine and thiol groups, which has advantages for covalent binding of target biomolecules for sensing purposes (296). To our knowledge, the first polydopamine-based MIP was reported for nicotine sensing (116), but since then dopamine has been used in the preparation of MIPs as REs for sensing of macromolecules, including proteins (296).

Removal of the template was the next step, a critical step in molecular imprinting. Efficient template removal should be performed to create the imprinted sites and allow subsequent rebinding of CA15-3 present in the sample. In addition, residual template molecules should be minimised as they are responsible for background signals (286). Template removal was optimised by incubating NIPs and MIPs under different conditions that affect the reaction between the diol and phenylboronic acid and the conformation of the protein, while the effects on the polymer surface should be minimal. In this work, water (113) or sodium chloride (0.1 M) (292) or acetic acid (10%) and sodium dodecyl sulphate (SDS, 1%) (297) or acetic acid (3%) and Tween-20 (0.1%) (115) were tested, under the same experimental conditions (temperature and time). This study was made by checking how the color of the MIP/NIP sensor paper changes between the control solution and the CA15-3 standard solution of 2000 U mL^{-1} to check the effect of removal conditions upon the sensitivity of the system. The collected images and the analytical output are shown in Figure 5-4. The results showed that the use of a detergent with acetic acid was undesirable, and the use of water or sodium chloride gave similar results, but with the naked eye, sodium chloride ($\Delta_{MIP-NIP}$= 2.90) was slightly better than water ($\Delta_{MIP-NIP}$=2.58), due to the greater difference between the results of the control and the protein detection.

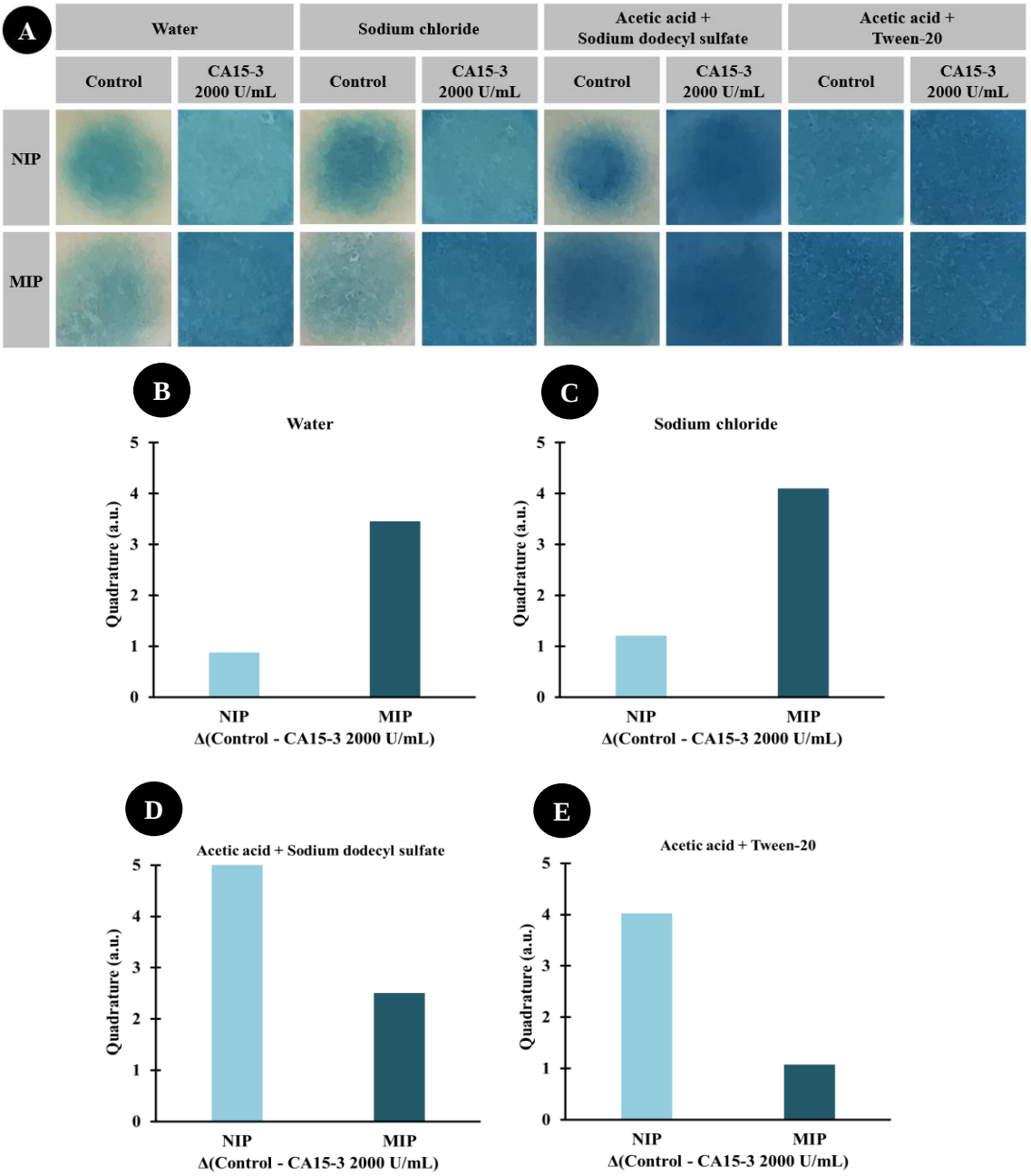

Figure 5-4. Photographs of NIPs and MIPs with different removal solutions (A). Respective bar charts with Q values for removal with water (B), sodium chloride (C), acetic acid + sodium dodecyl sulfate (D) and acetic acid + tween-20 (E).

5.3.3. Colorimetric protein detection

The presence of CA15-3 was detected by a color change from colorless to blue because the incubation of HRP was followed by addition of a ready-to-use peroxidase substrate with TMB. The more intense the blue coloration, the more HRP was bound to the sensor surface. This meant that HRP was bound to CA15-3 by non-specific protein-protein interactions. This also meant that this HRP-biomarker interaction was more intense than any interaction of HRP with polydopamine.

Because this interaction was non-specific, a larger amount of HRP would also result in color development as it binds to different sites on the sensor than the protein CA15-3. Therefore, the best experimental conditions should be optimised.

This principle was confirmed by testing different conditions for color development, as shown in Figure 5-5. The incubation of a TMB solution in PB on the sensor papers did not lead to any color development, either on the NIP or on the MIP. The same applies to the sensor paper incubated with CA15-3 standard solution (1000 U mL^{-1}), which remained colorless. This shows that the peroxidase substrate is stable with TMB and this substrate is not oxidised in the absence of HRP. As with conventional ELISA methods using antibodies, incubation of an antibody labelled with HRP was also attempted for CA15-3. It showed a good response with a higher value for ΔMIP than for ΔNIP, but this condition also gave high background signals. This was certainly due to the non-specific adsorption of the antibody to the polymeric material, as the epitope region of the antibody corresponds to only a small part of the antibody and the control tests do not contain CA15-3. This was also confirmed by the more intense color obtained in the control test of NIP (compared to MIP) where CA15-3 was not present. This confirms that the MIP surface is less susceptible to non-specific adsorption. The higher color intensity of the MIP signals compared to the signals from NIP in the presence of CA15-3 proves the selective response of the MIP surface to CA15-3. Incubation of HRP alone (5 µg ml^{-1}), not in combination with an antibody, was subsequently tested. This condition resulted in a significant reduction in background signal compared to antibody binding, as no color was obtained in controls. MIP incubated with CA15-3 also showed a good (color intensive) response, which was also significantly higher than the response obtained with NIP. Increasing the amount of HRP (to 50 µg mL^{-1}) showed a very weak response to the MIP control, but the signal of the paper incubated with CA15-3 also had a blue color. Since the $\Delta_{MIP}/\Delta_{NIP}$ ratio is higher at the highest HRP concentration, the following tests were performed with 50 µg mL^{-1} HRP.

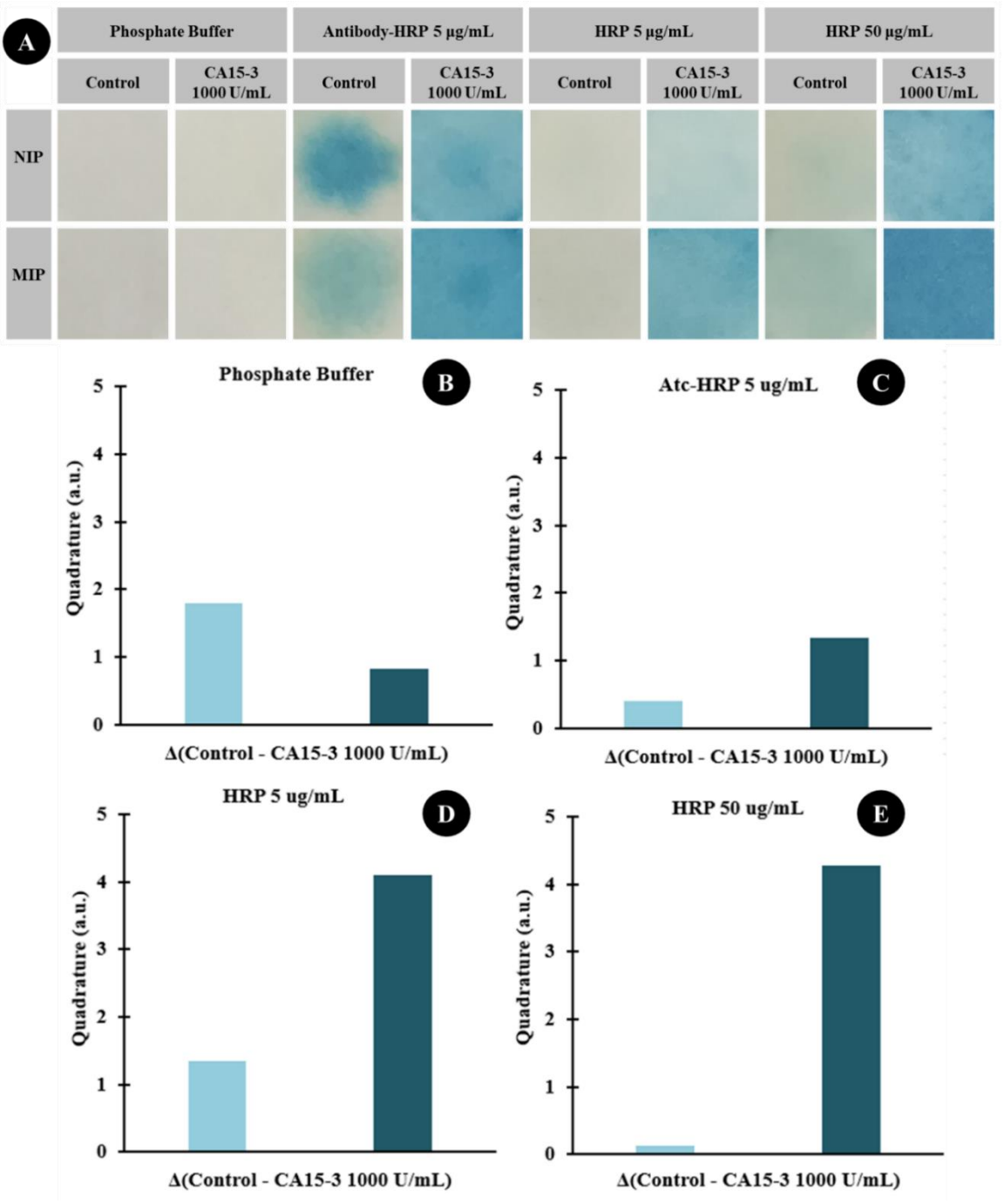

Figure 5-5. Photographs (A) of NIPs and MIPs with PB, antibody-HRP or HRP. Respective bar charts with Q values for PB (B), antibody-HRP 5 µg mL $^{-1}$ (C), HRP 5 µg mL $^{-1}$ (D) and HRP 50 µg mL $^{-1}$ (E).

From another point of view, the volume of the solution used was important for the homogeneity of the sensor surface and the sensitivity of the response, as shown in Figure 5-6. In the previous tests, 3 µl CA15-3 solution (or buffer) and then 3 µl HRP solution were incubated on each paper circle. The results showed that only high concentrations of CA15-3 could lead to color development under these conditions and that no color was visible to the naked eye at lower concentrations. For this

reason, higher volumes (4 and 5 µL) were tested. Incubation of 4 µL or 5 µL CA15-3 and HRP solutions resulted in an increase in colorimetric reaction intensity with increasing concentration of CA15-3. It was also found that not only MIPs can also recognise lower concentrations of this protein, but also NIPs can adsorb some targets. However, the recognition capacity of the MIP surface is obviously greater than the adsorption that occurs on NIPs. Five microlitres were selected for further investigation as this gave the best linear response, as shown in Figure 5-6 (B to C). Under this condition, the quadrature signal of the sensor was saturated for concentrations > 500 U mL^{-1}, which by far includes the CA15-3 values > 30 U mL^{-1} that are clinically important in BC.

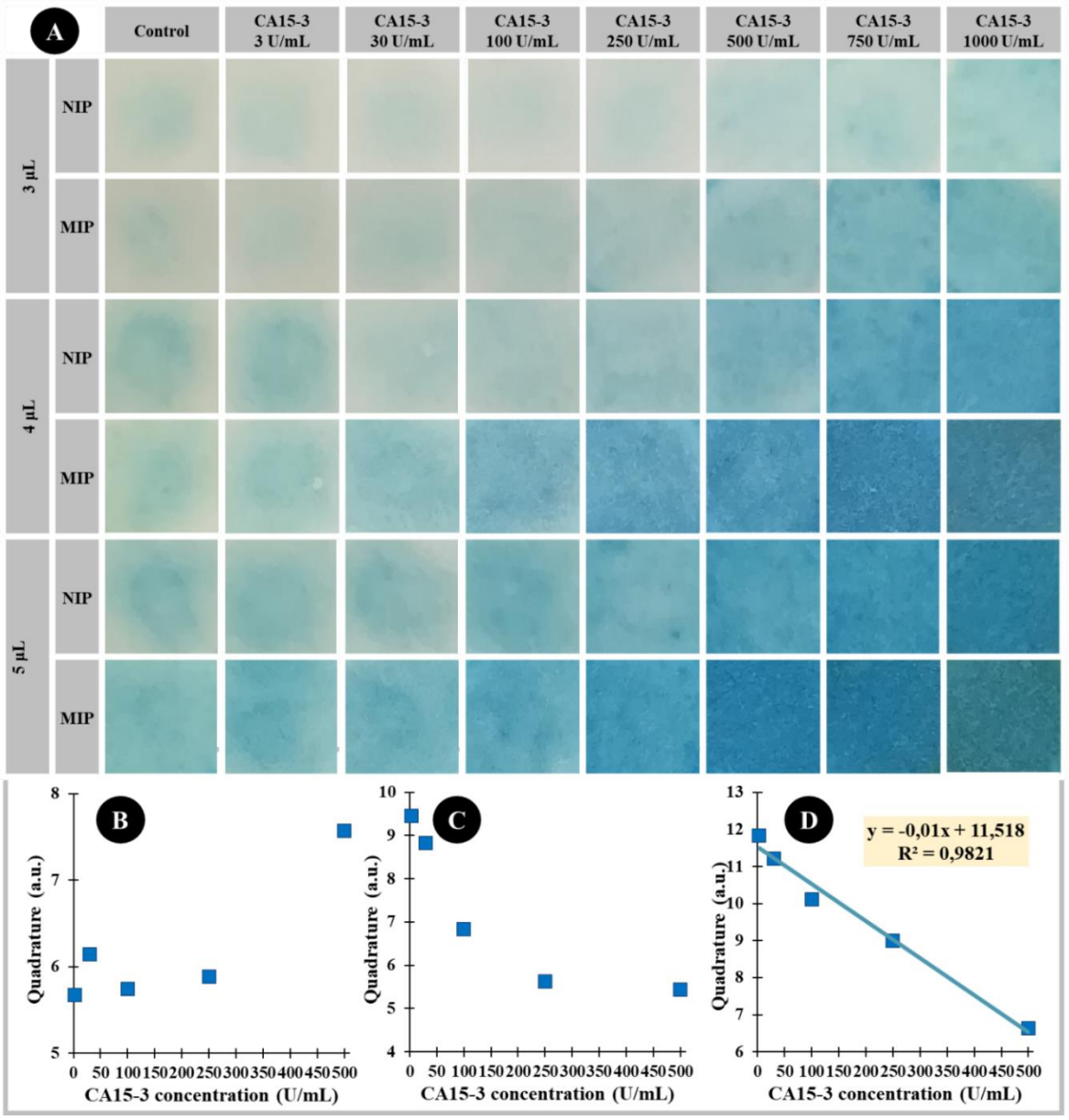

Figure 5-6. Photographs (A) of NIPs and MIPs with 3, 4 or 5-µL of standard solution and HRP solution. Calibration curves with Q values of MIPs with 3 (B), 4 (C) or 5 (D) µL of standard and HRP solutions.

5.3.4. Biomimetic enzyme-linked immunosorbent assay calibration

Figure 5-7 shows the images of the paper sensors incubated in different concentrations of CA15-3, from 3 to 500 U mL^{-1}, in buffered solutions. The average points obtained from triplicate measurements of each data point were plotted against grey intensity or Quadrature. The error bars included correspond to the SD. The linear regression equation of the MIP was Grey intensity = -0.0858 × CA15-3 U mL^{-1} + 149.44 (R-squared 0.9892) or Quadrature = -0.0102 × CA15-3 U mL^{-1} + 11.032 (R-squared 0.9794). The NIP showed no linear response.

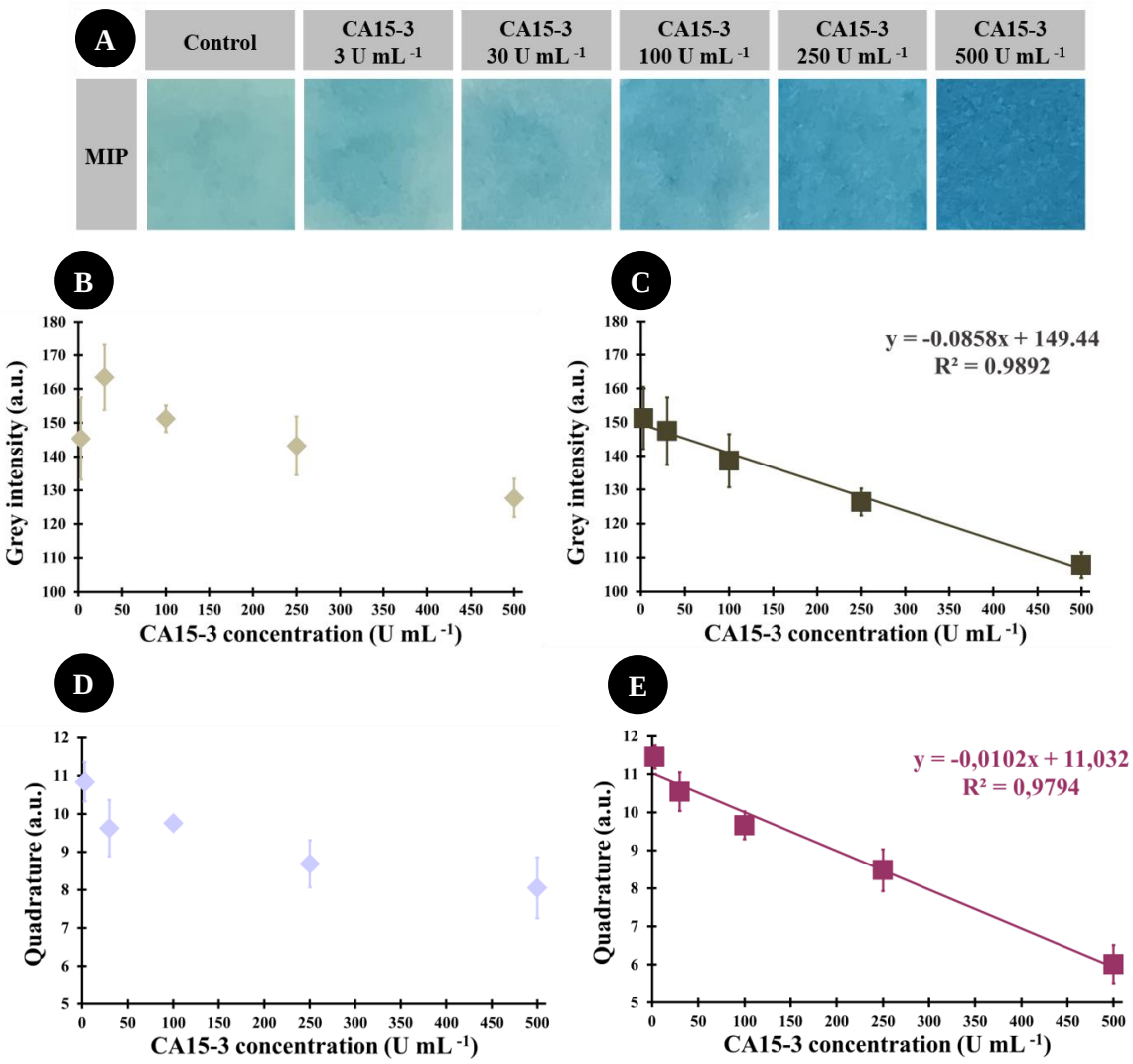

Figure 5-7. Photographs of buffer calibration in MIP (A). Calibration curve based on grey intensity for NIP (B) and MIP (C). Calibration curve based on quadrature values for NIP (D) and MIP (E).

5.3.5. Selectivity

Selectivity is a crucial parameter to be investigated when evaluating the performance of a biosensensor to assess whether it can be used in real-world conditions. The selectivity assay was

performed by incubating CA15-3 solutions prepared alone or in the presence of a possible interfering substance. Assays were made triplicate and data was expressed as mean ± SD. Figure 5-8 shows the mean values in terms of percent signal change compared with CA15-3 alone. CEA (1%) and CA125 (5.5%) resulted in small differences in grey scale compared with the effect of glucose (10.4%) and IgG (11%). Overall, the effect of the four interfering species tested in this assay was negligible with error values equal or below 11%. The results show that the MIP surface has highly selectivity for CA15-3 compared to the interfering molecules tested. This is mainly due to the presence of the imprinted cavities for CA15-3. These results suggest that these sensors could be used to detect CA15-3 in complex matrices.

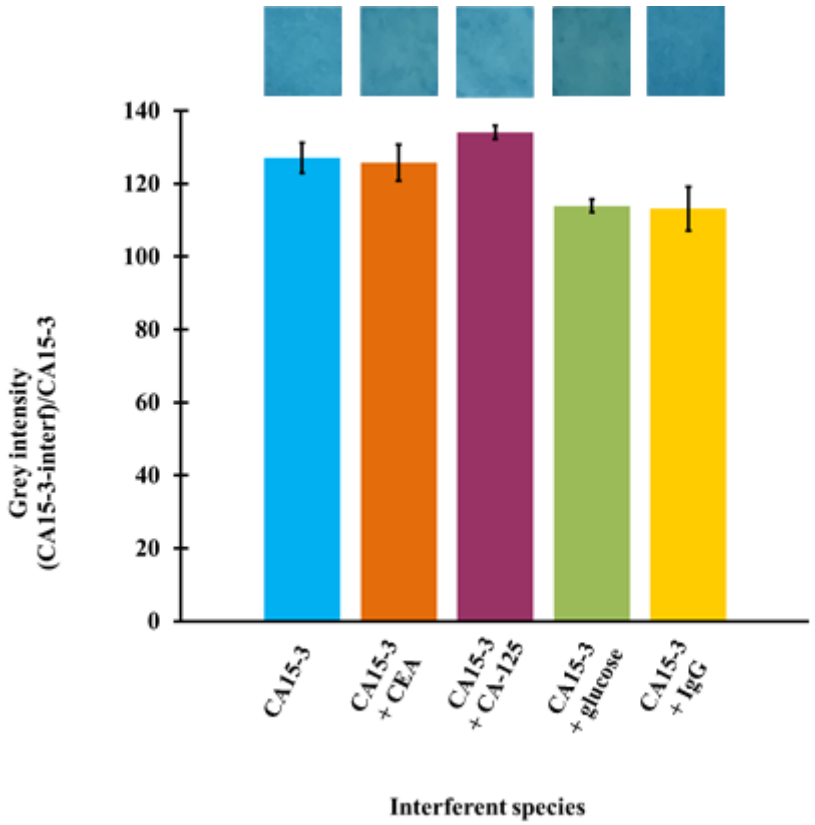

Figure 5-8. Images and the respective bar chart of selectivity study based on comparison of the response of CA15-3 (250 U mL^{-1}) incubated alone or mixed with interfering species as CEA (0.25 ng mL^{-1}), CA125 (0.35 U mL^{-1}), glucose (1 mg mL^{-1}) and IgG (0.1 mg mL^{-1}).

5.3.6. Biomimetic enzyme-linked immunosorbent assay in serum samples

Figure 5-9 shows the sensor response for the detection of CA15-3 in FBS. Calibrations were performed in a background medium of serum to achieve an analytical level of communication that

is well matched to the composition of the sample. For this purpose, the standard samples of CA15-3 contained real serum in their composition. As with the buffered solutions, calibrations were performed in triplicate and data are reported as mean ± SD. The overall behaviour showed a linear trend for both the grey-scale and the quadrature values as a function of CA15-3 concentration (U mL^{-1}), corresponding to grey value = -0.0956 × CA15-3 U mL^{-1} + 158.05 (R-squared 0.997) and quadrature = -0.0098 × CA15-3 U mL^{-1} + 11.006 (R-squared 0.9903). Compared with the experiments with buffer, the slope values were similar, as was the range of the linear response. The results obtained indicate that this sensor can be used for the detection of CA15-3 in serum samples.

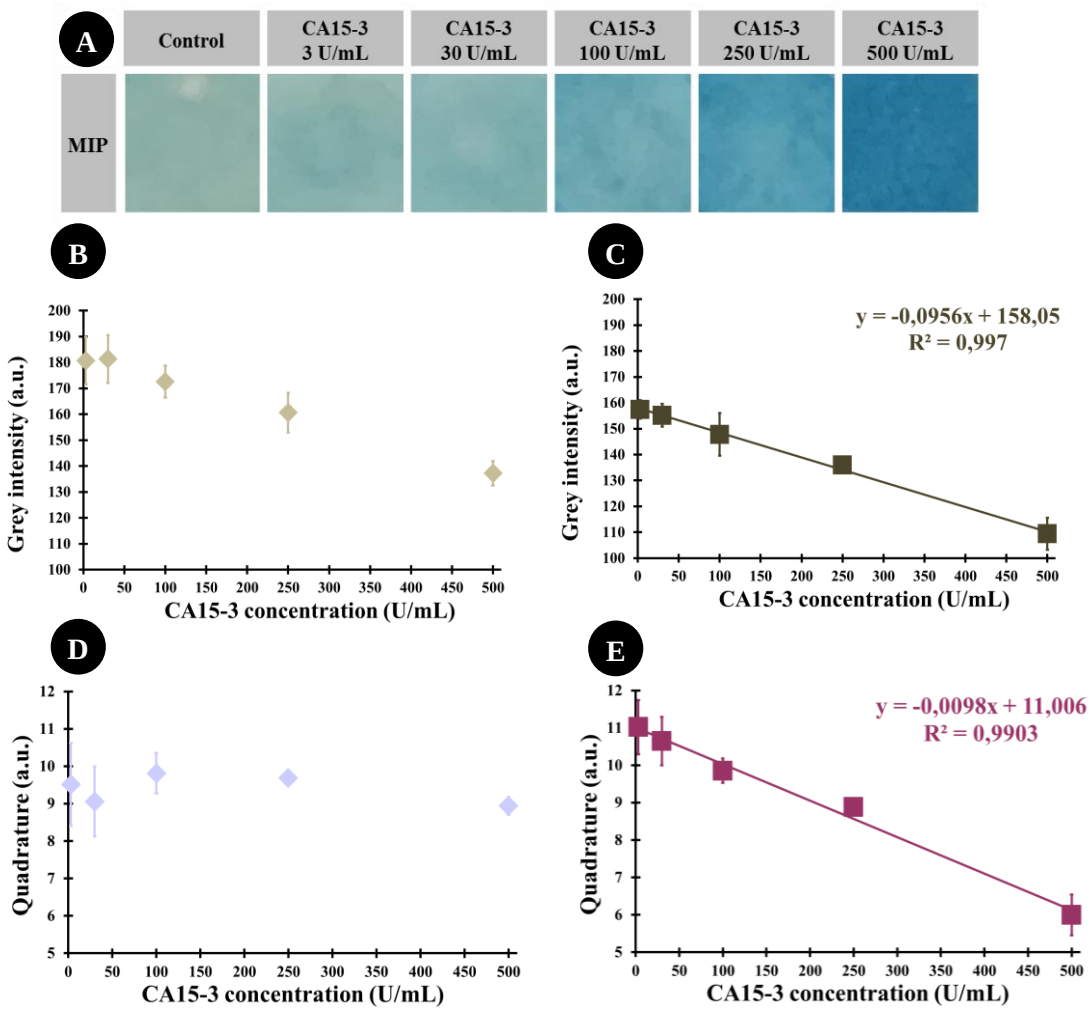

Figure 5-9. Photographs of FBS calibration in MIP (A). Calibration curve based on grey intensity for NIP (B) and MIP (C). Calibration curve based on quadrature values for NIP (D) and MIP (E).

5.4. Conclusions

The combination of MIPs, paper and ELISA has already been reported, but only for small molecules (104, 287-290). As we know, no one has yet used this for the detection of (glyco)proteins (Table 5-1). Nevertheless, several biosensors for CA15-3 have been described using different REs and transduction systems. Most of the mentioned works have LODs between 0 and 2 U mL^{-1} (10, 21, 60, 121, 122, 192, 193), but some of them can actually reach a very low LOD, such as the work by Wu et al. (LOD = 2.56×10^{-5} U mL^{-1}) (15). Despite the high sensitivity of this work, the fluorescence signal emitted by the sensor requires a fluorometer, which may be a limitation. In addition, some of them report very narrow linear ranges (e.g., 0.1–20 U mL^{-1} (21), 0.25 to 10 U mL^{-1} (193), 0.25-14 U mL^{-1} (15)), which might not be very useful in clinical practice because the CA15-3 cut-off is 30 U mL^{-1}.

This work demonstrates that it is possible to assemble a MIP material on a paper substrate that can selectively bind target proteins of interest, in this case CA15-3. This underlines the increasing attention given to MIP-based sensors, as they are easy to fabricate, robust, stable, and inexpensive. Their incorporation into PADs provides a versatile tool that can be used in a variety of situations. The use of an ELISA-like system was also presented as a simple approach to identify the presence of bound CA15-3. The results confirmed the need for HRP, but the presence of an antibody for this purpose (as within the conventional ELISA) was not required. The paper-based B-ELISA showed good linear correlation over a wide concentration range (3 to 500 U mL^{-1}) and the selectivity of the developed sensor was very high.

The advantages of using cellulose paper as ELISA substrate for CA15-3 were already demonstrated in a previous work (192), but antibodies were used as REs. In the present work, we maintain the choice of cellulose paper as substrate and colorimetric substrate for the transduction system, but we would like to highlight the outstanding advantages of using a MIP instead of an antibody as detection element. If we compare the traditional ELISA (in 96-wells) with the P-ELISA, we can find that the latter has outstanding advantages such as portability, ease of use, and rapid response due to the use of paper as a substrate and is also more cost-effective because it does not require the use of natural antibodies. In terms of analytical performance, both works achieved very similar linearity ($R^2 \approx 0.99$) when the sensors are calibrated with serum samples. Despite the advantages, the B-ELISA takes more time, which is due to the steps associated with the MIP design. The proposed approach can be easily extended to other glycoproteins that need to be monitored at the PoC, as a screening test in the physician's office or in countries that do not have easy access to healthcare facilities.

Table 5-1. Published works for molecular imprinting polymers combined with colorimetric detection on a paper substrate.

Target	Analyte recognition	Colorimetric detection	Linear range	Limit of detection	Reference
Bisphenol A	$ZnFe_2O_4$-@MIP membranes	TMB	0.01 to 1 μM	6.18 nM	(287)
Tetrabromobisphenol A	Copper-based metalorganic framework (MIP/HKUST-1)	TMB	0.01 to 10 ng g^{-1}	3 pg/g	(288)
Sulfamethoxazole	MIP	Diazotization reaction + naphthyl ethylenediamine dihydrochloride	0 to 3 and 3 to 10 ppm	0.24 ppm	(298)
Thiacloprid	MIP-capped metal-organic frameworks	TMB	0.1 to 1.2 and 1.2 to 10 μM	0.04 μM	(299)
Kanamycin	metal–organic framework/MIP chip (FZS@CPBA@MIP)	ninhydrin-aminoglycoside antibiotic	0.1 to 25 mg L^{-1}	4.69 μg L^{-1}	(300)
Carbaryl	B-ELISA	TMB	0.001 to 1 mg L^{-1}	0.007 mg L^{-1}	(104)
	Mesoporous silica-platinum NPs coated with a MIP (MSN-PtNPs@MIP)	TMB	0.002 to 20.00 mg kg^{-1}	15 ng g^{-1}	(301)
Cd (II)	Ion imprinted polymers (IIPs)	dithizone	1 to 100 ng mL^{-1}	0.4 ng mL^{-1}	(289)
	MIP	TMB	0 to 300 ppb	0.1 ppb	(302)
17β-estradiol	MIP grafted paper	chromogenic substrate	-	0.25 μg L^{-1}	(290)
CA15-3	B-ELISA	TMB	3 to 500 U mL^{-1}	3 U mL^{-1}	This work

Chapter 6

General conclusions and future perspectives

This chapter discusses the general conclusions of this thesis and presents some future perspectives.

6. General conclusions and future perspectives

6.1. General conclusions

Early diagnosis of cancer, even before appearance of symptoms is the key for a better prognosis and selection of proper treatment, which can reduce morbidity and mortality caused by cancer cases. Analysis of the composition of biological samples and determining the concentration of certain analytes can provide valuable information about patient's health condition that can be useful for an accurate and timely diagnosis and an appropriate therapeutic selection. Available detection methods for biomarkers are usually highly sensitive and specific but not ideal for routine diagnosis and involve complex and costly procedures, sophisticated equipment, requiring a lot of time and resources, which limits its accessibility and results in a delay in disease diagnosis. Therefore, rapid, simple, and low-cost methodologies are needed.

Paper is a versatile substrate, being used in the development of PADs, that meet the requirements of a PoC device. Thus, PADs represent an emerging and attractive alternative to conventional methodologies. Colorimetric PADs have been used for the detection of several analytes, as cancer biomarkers in different types of samples. However, despite the amount of published works using PADs for colorimetric detection of biomarkers and the current evolution in this field, its application in real life is still very limited. Thus, more research is still needed to identify and address several drawbacks related to PADs and provide strategies to overcome them. These efforts may enable to improve the performance of PADs and address its successful translation into commercialization.

This work reported new approaches for paper-based biosensing devices, to be applied as cancer screening methodologies.

In general, a well-established methodology, ELISA, was applied at a paper substrate for a cancer biomarker detection. Different RE were used and all of them showed to be capable of monitoring the target analyte with good sensitivity and selectivity, with response in the clinical range, using a colorimetric transduction of the signal. All the results were captured with a camera smartphone and analysed with ImageJ software to obtain the color coordinates. This combination of PADs and smartphones should progress to get better qualitative and quantitative signals and to provide a preliminary on-site disease screening that can be performed outside the laboratory or the hospital, as in remote locations.

The first biosensor developed herein mainly focused on the enzymatic detection of an unspecific molecule, glucose, onto a cellulose paper, as proof of concept for colorimetric detection on paper

substrates. In collaboration with an Erasmus colleague, Katrin Neubauerova, it was developed carboxyl-NC, through TEMPO-mediated oxidation of microcrystalline cellulose. The synthetized material was then deposited onto cellulose paper, with the aim to increase the superficial area and improve further immobilisation of biomolecules. In this work, GOx was used as RE and a colorimetric response was obtained based on oxidation of ABTS as chromogenic substrate. The sensor showed a good linear response between 1.5 and 13.0 nM of glucose and it was proved that the carboxyl-NC improved the sensor performance, by enhancing the homogeneity of the colorimetric response, as well as the linear response.

Then, a traditional RE commonly used in ELISA, an antibody, was incorporated in a paper-based biosensor for colorimetric detection of CA15-3, as a BC biomarker. ELISA-sandwich format was used for sensor assembly and the colorimetric reaction was consequence of TMB oxidation. This sensor displayed good linearity between 2 and 2000 U mL^{-1} and was successfully tested in serum samples, testifying its applicability in complex samples and being a suitable tool for cancer screening. This methodology presents advantages over the traditional ELISA, performed in solution using well-plates, namely the fast response due to the short incubation times, which are the consequence of the high surface-to-volume ratio and porous structure of cellulose and the facility in washing steps. Moreover, it presents a lower cost, due to the used of less amounts of reagents and samples, related with the use of cellulose paper as substrate. At least, we should highlight the portability of the system as it does not require special instrumentation to read the results.

Considering the previous work, the latter one aimed to replace the antibody by an artificial RE, namely a MIP, to reduce the cost of sensor production and improve its performance. CA15-3 was kept, as target, as well as the cellulose paper substrate and the colorimetric response based on TMB oxidation. This sensor presented a good linear response between 3 and 500 U mL^{-1}, with successful application in serum samples. In addition to all the above advantages mentioned for paper-based ELISA over the ELISA performed in solution, this device takes benefit of using a MIP instead of an antibody as RE, as it lowers the cost of the assay. Also, as far as we know, it was the first B-ELISA developed in paper substrate for a high molecular weight molecule, namely a protein. Despite the linear range of the developed biomimetic sensor is shorter than the obtained for the immunosensor (3 to 500 U mL^{-1} in comparison to 2 to 2000 U mL^{-1}), the sensor still operates under the significant clinical range, being able to distinguish patients who have low levels (< 30 U mL^{-1}) of CA15-3 from these that have higher values (> 30 U mL^{-1}), which can be indicative of a poor prognosis and of the presence of metastasis.

Summing up, this work developed new PADs for colorimetric detection of cancer biomarkers that can

be used on cancer screening. From a practical perspective, the developed sensors were able to distinguish form lower to higher concentrations of CA15-3, working at the clinical values. The biomarker herein studied was CA15-3 whose high concentrations (> 30 U mL $^{-1}$) are associated with a poor prognosis in patients with invasive BC and can be an indicative factor to search for metastases. However, as CA15-3 has not enough selectivity and sensitivity in early BC diagnosis, it should be combined with other parameters, as other cancer biomarkers (e.g. CEA) to increase the prognostic value. Moreover, the concept behind the biomimetic paper-based sensor may be extended to any other biomarkers, from cancer or not.

Despite the evident advantages of biosensors in biomarkers detection, it is dubious to say that this kind of devices could one day replace the conventional methodologies. However, at least, the detection of abnormal levels of cancer biomarkers by sensing devices is a useful and attractive approach to complement the data provided by conventional methodologies to provide accurate diagnosis and select an effective therapy. Patients with positive results for a cancer biomarker in a screening test should further perform more specific tests to determine the cancer type, as well as the stage of the disease and select the adequate protocol for treatment.

6.2. Future perspectives

In a near future, paper-based sensors for cancer biomarkers like the ones developed throughout this thesis, can be optimised to be PoC devices for cancer screening or diagnosis.

In the described sensors some important tests remained to be done, namely test the sensors against biological samples of cancer patients and recovery studies. The mentioned tests are of major relevance to understand the behavior of the sensor in a real-world context. Despite we understand their importance, they were not performed due to ethical issues and lack of time.

Furthermore, if we intent to commercialize the sensors for cancer screening or diagnosis, several factors need to be considered.

In addition to the above mentioned tests (real samples from cancer patients and recovery studies), automatization of the steps for sensor construction in a large-scale is of greater importance for sensor commercialization. This could be achieved, for example, by automatic pipetting of reagents and samples, as well as apply a faster and practical strategy to wash the sensors between incubations. This automatization steps will allow to reduce the time spent for sensor construction, as well as improve the variability between sensors, by reducing the errors in the several steps of sensor construction. Finally, factors as stability of the sensor and storage conditions should be evaluated. At

least, to use this sensor in the field, proper conditions to acquire the results should be guaranteed in order to not affect assay sensitivity and repeatability. In the described works, a homemade darkroom was constructed to capture the photographs under controlled conditions, namely light intensity, and focal distance. For that reason, a portable and robust darkroom can be constructed, where a smartphone can be coupled to capture the results. In this smartphone, several software can be used to calculate the color coordinates and a specific one can be developed to automatically convert these values to the concentration of the detected target, given a real-time response.

Regarding the complexity of cancerous process and the wide range of available biomarkers, the development of future biosensors for cancer detection should consider a panel of analytes in a multiplex device, enabling the detection of several analytes at the same time, using the same biologic sample.

Despite the good performance obtained in Chapter 5 with a MIP being used as an alternative to antibodies as RE, other synthetic REs (e.g., and aptamer) with promising recognition ability for cancer biomarkers could be tested.

Chapter 7

References

7. References

1. Mahmoudi T, de la Guardia M, Baradaran B. Lateral flow assays towards point-of-care cancer detection: A review of current progress and future trends. TrAC Trends in Analytical Chemistry. 2020;125:115842.
2. Ferlay J, Ervik M, Lam F, Colombet M, Mery L, Piñeros M, et al. Cancer Today: International Agency for Research on Cancer; 2020 [Available from: https://gco.iarc.fr/today/home.
3. Shankaran DR. Chapter 8 - Nano-Enabled Immunosensors for Point-of-Care Cancer Diagnosis. In: Mohan Bhagyaraj S, Oluwafemi OS, Kalarikkal N, Thomas S, editors. Applications of Nanomaterials: Woodhead Publishing; 2018. p. 205-50.
4. Organization WH. Cancer [Available from: https://www.who.int/news-room/fact-sheets/detail/cancer.
5. Carrell C, Kava A, Nguyen M, Menger R, Munshi Z, Call Z, et al. Beyond the lateral flow assay: A review of paper-based microfluidics. Microelectronic Engineering. 2019;206:45-54.
6. Tothill I, Altintas Z. Molecular biosensors: promising new tools for early detection of cancer. Nanobiosensors in Disease Diagnosis. 2015:1.
7. Tothill IE. Biosensors for cancer markers diagnosis. Seminars in Cell & Developmental Biology. 2009;20(1):55-62.
8. Ranjan R, Esimbekova EN, Kratasyuk VA. Rapid biosensing tools for cancer biomarkers. Biosensors and Bioelectronics. 2017;87:918-30.
9. Jayanthi VSPKSankara A, Das AB, Saxena U. Recent advances in biosensor development for the detection of cancer biomarkers. Biosensors and Bioelectronics. 2017;91:15-23.
10. Rebelo TSCR, Ribeiro JA, Sales MGF, Pereira CM. Electrochemical immunosensor for detection of CA 15-3 biomarker in point-of-care. Sensing and Bio-Sensing Research. 2021;33:100445.
11. Hosu O, Ravalli A, Lo Piccolo GM, Cristea C, Sandulescu R, Marrazza G. Smartphone-based immunosensor for CA125 detection. Talanta. 2017;166:234-40.
12. Cheraghi S, Taher MA, Karimi-Maleh H, Karimi F, Shabani-Nooshabadi M, Alizadeh M, et al. Novel enzymatic graphene oxide based biosensor for the detection of glutathione in biological body fluids. Chemosphere. 2022;287:132187.
13. Pothipor C, Aroonyadet N, Bamrungsap S, Jakmunee J, Ounnunkad K. A highly sensitive electrochemical microRNA-21 biosensor based on intercalating methylene blue signal amplification and a highly dispersed gold nanoparticles/graphene/polypyrrole composite. Analyst. 2021;146(8):2679-88.
14. Bodulev OL, Galkin II, Zhao S, Pletyushkina OY, Sakharov IY. Quantitation of MicroRNA-155 in Human Cells by Heterogeneous Enzyme-Linked Oligonucleotide Assay Coupled with Mismatched Catalytic Hairpin Assembly Reaction. Biosensors [Internet]. 2022; 12(8).
15. Wu Y, Chen X, Wang X, Yang M, Xu F, Hou C, et al. A fluorescent biosensor based on prismatic hollow Metal-polydopamine frameworks and 6-carboxyfluorescein (FAM)-labeled protein aptamer for CA15-3 detection. Sensors and Actuators B: Chemical. 2021;329:129249.
16. Yu Q, Zhao Q, Wang S, Zhao S, Zhang S, Yin Y, et al. Development of a lateral flow aptamer assay strip for facile identification of theranostic exosomes isolated from human lung carcinoma cells. Analytical Biochemistry. 2020;594:113591.
17. Yin Y, Cao Y, Xu Y, Li G. Colorimetric immunoassay for detection of tumor markers. International journal of molecular sciences. 2010;11(12):5077-94.
18. Liu W, Yang H, Ding Y, Ge S, Yu J, Yan M, et al. Paper-based colorimetric immunosensor for visual detection of carcinoembryonic antigen based on the high peroxidase-like catalytic performance of ZnFe2O4–multiwalled carbon nanotubes. Analyst. 2014;139(1):251-8.
19. Chen Y, Chu W, Liu W, Guo X. Distance-based carcinoembryonic antigen assay on microfluidic paper immunodevice. Sensors and Actuators B: Chemical. 2018;260:452-9.
20. Mohammadi S, Salimi A, Hamd-Ghadareh S, Fathi F, Soleimani F. A FRET immunosensor for sensitive

detection of CA 15-3 tumor marker in human serum sample and breast cancer cells using antibody functionalized luminescent carbon-dots and AuNPs-dendrimer aptamer as donor-acceptor pair. Analytical Biochemistry. 2018;557:18-26.
21. Li H, He J, Li S, Turner APF. Electrochemical immunosensor with N-doped graphene-modified electrode for label-free detection of the breast cancer biomarker CA 15-3. Biosensors and Bioelectronics. 2013;43:25-9.
22. Pereira AC, Sales MGF, Rodrigues LR. Chapter 3 - Biosensors for Rapid Detection of Breast Cancer Biomarkers. In: Inamuddin, Khan R, Mohammad A, Asiri AM, editors. Advanced Biosensors for Health Care Applications: Elsevier; 2019. p. 71-103.
23. Santos ART, Moreira FTC, Helguero LA, Sales MGF. Antibody Biomimetic Material Made of Pyrrole for CA 15-3 and Its Application as Sensing Material in Ion-Selective Electrodes for Potentiometric Detection. Biosensors. 2018;8(1):1-16.
24. Kasetsirikul S, Shiddiky MJA, Nguyen N-T. Challenges and perspectives in the development of paper-based lateral flow assays. Microfluidics and Nanofluidics. 2020;24(2):1-18.
25. Frasco MF, Truta LAANA, Sales MGF, Moreira FTC. Imprinting Technology in Electrochemical Biomimetic Sensors. Sensors (Basel, Switzerland). 2017;17(3):523.
26. Ranjan P, Parihar A, Jain S, Kumar N, Dhand C, Murali S, et al. Biosensor-based diagnostic approaches for various cellular biomarkers of breast cancer: A comprehensive review. Analytical Biochemistry. 2020;610:113996.
27. Wang K, Yang J, Xu H, Cao B, Qin Q, Liao X, et al. Smartphone-imaged multilayered paper-based analytical device for colorimetric analysis of carcinoembryonic antigen. Analytical and Bioanalytical Chemistry. 2020;412(11):2517-28.
28. Ozer T, McMahon C, Henry CS. Advances in Paper-Based Analytical Devices. Annual Review of Analytical Chemistry. 2020;13(1):85-109.
29. Murray LP, Mace CR. Usability as a guiding principle for the design of paper-based, point-of-care devices – A review. Analytica Chimica Acta. 2020;1140:236-49.
30. Tekade RK, Sun X. The Warburg effect and glucose-derived cancer theranostics. Drug Discovery Today. 2017;22(11):1637-53.
31. Organization WH. Cancer [Available from: https://www.who.int/news-room/fact-sheets/detail/cancer.
32. CP W, E W, BW S. World Cancer Report: Cancer Research for Cancer Prevention. 2020.
33. Cancer types: National Cancer Institute; [Available from: www.cancer.gov/types.
34. Azab MY, Hameed MFO, Obayya SSA. Overview of Optical Biosensors for Early Cancer Detection: Fundamentals, Applications and Future Perspectives. Biology [Internet]. 2023; 12(2).
35. Cancer tomorrow: International Agency for Research on Cancer; 2020 [Available from: https://gco.iarc.fr/tomorrow/en.
36. Ferlay J, Ervik M, Lam F, Colombet M, Mery L, Piñeros M, et al. Global Cancer Observatory - Cancer Today: International Agency for Research on Cancer; 2020 [Available from: https://gco.iarc.fr/today/home.
37. Hirata B, Massayo Maeda Oda J, Guembarovski R, Ariza C, Oliveira C, Watanabe M. Molecular Markers for Breast Cancer: Prediction on Tumor Behavior. Disease markers. 2014;2014:1-12.
38. Łukasiewicz SA-O, Czeczelewski M, Forma AA-O, Baj JA-O, Sitarz R, Stanisławek A. Breast Cancer - Epidemiology, Risk Factors, Classification, Prognostic Markers, and Current Treatment Strategies-An Updated Review. Cancers. 2021;13(2072-6694 (Print)).
39. About cancer: National Cancer Institute; [Available from: https://www.cancer.gov/.
40. Song C, Yang Y, Yang B, Min L, Wang L. Combination assay of lung cancer associated serum markers using surface-enhanced Raman spectroscopy. Journal of Materials Chemistry B. 2016;4(10):1811-7.
41. Suntornsuk W, Suntornsuk L. Recent applications of paper-based point-of-care devices for biomarker detection. ELECTROPHORESIS. 2020;41(5-6):287-305.
42. Mazzu-Nascimento T, Morbioli GG, Milan LA, Donofrio FC, Mestriner CA, Carrilho E. Development and statistical assessment of a paper-based immunoassay for detection of tumor markers. Analytica Chimica

Acta. 2017;950:156-61.
43. Ratajczak K, Stobiecka M. High-performance modified cellulose paper-based biosensors for medical diagnostics and early cancer screening: A concise review. Carbohydrate Polymers. 2020;229:115463.
44. Suh KS, Park SW, Castro A, Patel H, Blake P, Liang M, et al. Ovarian cancer biomarkers for molecular biosensors and translational medicine. Expert Review of Molecular Diagnostics. 2010;10(8):1069-83.
45. Weber JA, Baxter DH, Zhang S, Huang DY, Huang KH, Lee MJ, et al. The microRNA spectrum in 12 body fluids. Clinical chemistry. 2010;56(11):1733-41.
46. Wong DTW. Salivary extracellular noncoding RNA: emerging biomarkers for molecular diagnostics. Clinical therapeutics. 2015;37(3):540-51.
47. Fracchiolla NS, Artuso S, Cortelezzi A. Biosensors in clinical practice: focus on oncohematology. Sensors (Basel, Switzerland). 2013;13(5):6423-47.
48. Kabel AM. Tumor markers of breast cancer: New prospectives. Journal of Oncological Sciences. 2017;3(1):5-11.
49. DePolo J. 2023 [Available from: www.breastcancer.org.
50. Lee JS, Park S, Park JM, Cho JH, Kim SI, Park BW. Elevated levels of preoperative CA 15-3 and CEA serum levels have independently poor prognostic significance in breast cancer. Annals of Oncology. 2013;24(5):1225-31.
51. Duffy MJ, Shering S Fau - Sherry F, Sherry F Fau - McDermott E, McDermott E Fau - O'Higgins N, O'Higgins N. CA 15-3: a prognostic marker in breast cancer. The International journal of biological markers. 2000;15(4):330-33.
52. Park B, Oh J, Kim J, SH P, Kim K, Kim J, et al. Preoperative CA 15-3 and CEA serum levels as predictor for breast cancer outcomes. Annals of oncology. 2008;18(4):675-81.
53. Wang L. Early Diagnosis of Breast Cancer. Sensors. 2017;17(7).
54. Meirinho SG, Dias LG, Peres AM, Rodrigues LR. Voltammetric aptasensors for protein disease biomarkers detection: A review. Biotechnology Advances. 2016;34(5):941-53.
55. Kufe DW. Mucins in cancer: function, prognosis and therapy. Nature Reviews Cancer. 2009;9(1474-1768 (Electronic)):874-85.
56. Kufe DW. MUC1-C oncoprotein as a target in breast cancer: activation of signaling pathways and therapeutic approaches. Oncogene. 2013;32(9):1073-81.
57. Duffy MJ. CA 15-3 and related mucins as circulating markers in breast cancer. Annals of clinical biochemistry. 1999(0004-5632 (Print)):579-86.
58. Chen W, Zhang Z, Zhang S, Zhu P, Ko JK, Yung KK. MUC1: Structure, Function, and Clinic Application in Epithelial Cancers. International Journal of Molecular Sciences. 2021;22(12).
59. Duffy MJ, Evoy D, McDermott EW. CA 15-3: Uses and limitation as a biomarker for breast cancer. Clinica Chimica Acta. 2010;411(23):1869-74.
60. Ribeiro JA, Pereira CM, Silva AF, Sales MGF. Disposable electrochemical detection of breast cancer tumour marker CA 15-3 using poly(Toluidine Blue) as imprinted polymer receptor. Biosensors and Bioelectronics. 2018;109:246-54.
61. Hong R, Sun H, Li D, Yang W, Fan K, Liu C, et al. A Review of Biosensors for Detecting Tumor Markers in Breast Cancer. Life [Internet]. 2022; 12(3).
62. Chourin S Fau - Georgescu D, Georgescu D Fau - Gray C, Gray C Fau - Guillemet C, Guillemet C Fau - Loeb A, Loeb A Fau - Veyret C, Veyret C Fau - Basuyau JP, et al. Value of CA 15-3 determination in the initial management of breast cancer patients. Annals of Oncology. 2009;20(5).
63. Shering SG, Sherry F Fau - McDermott EW, McDermott Ew Fau - O'Higgins NJ, O'Higgins Nj Fau - Duffy MJ, Duffy MJ. Preoperative CA 15-3 concentrations predict outcome of patients with breast carcinoma. American Cancer Society. 1998(0008-543X (Print)).
64. Duffy M, Duggan C, Keane R, Arnold K, McDermott E, Crown J, et al. High Preoperative CA 15-3 Concentrations Predict Adverse Outcome in Node-Negative and Node-Positive Breast Cancer: Study of 600 Patients with Histologically Confirmed Breast Cancer. Clinical chemistry. 2004;50(3):559-63.
65. Metkar SK, Girigoswami K. Diagnostic biosensors in medicine – A review. Biocatalysis and Agricultural

Biotechnology. 2019;17:271-83.
66. Kamel S, Khattab T. Recent Advances in Cellulose-Based Biosensors for Medical Diagnosis. Biosensors. 2020;10:1-26.
67. Bhalla N, Jolly P, Formisano N, Estrela P. Introduction to biosensors. Essays in Biochemistry. 2016(1744-1358 (Electronic)).
68. IUPAC Gold Book: International Union of Pure and Applied Chamistry; [Available from: https://goldbook.iupac.org/terms/search.
69. Samuel VR, Rao KJ. A review on label free biosensors. Biosensors and Bioelectronics: X. 2022;11:100216.
70. Sadani K, Nag P, Thian XY, Mukherji S. Enzymatic optical biosensors for healthcare applications. Biosensors and Bioelectronics: X. 2022;12:100278.
71. Syahir A, Usui K, Tomizaki K-y, Kajikawa K, Mihara H. Label and Label-Free Detection Techniques for Protein Microarrays. Microarrays [Internet]. 2015; 4(2):[228-44 pp.].
72. Dukle AA-O, Nathanael AA-O, Panchapakesan BA-O, Oh TH. Role of Paper-Based Sensors in Fight against Cancer for the Developing World. Biosensors. 2022;12(9).
73. Nadar SA-O, Patil PA-O, Tiwari MA-O, Ahirrao DJ. Enzyme embedded microfluidic paper-based analytic device (μPAD): a comprehensive review. Critical Reviews in Biotechnology. 2021;41(1549-7801).
74. Liu L, Hao Y, Deng D, Xia N. Nanomaterials-Based Colorimetric Immunoassays. Nanomaterials (Basel, Switzerland). 2019;9(3):316.
75. Mahato K, Srivastava A, Chandra P. Paper based diagnostics for personalized health care: Emerging technologies and commercial aspects. Biosensors & bioelectronics. 2017(1873-4235):246-59.
76. Gopinath SCB, Tang T-H, Citartan M, Chen Y, Lakshmipriya T. Current aspects in immunosensors. Biosensors and Bioelectronics. 2014;57:292-302.
77. Sharma S, Byrne H, O'Kennedy RJ. Antibodies and antibody-derived analytical biosensors. Essays in biochemistry. 2016;60(1):9-18.
78. Cerda-Kipper A, Montiel B, Hosseini S. Radioimmunoassay and Enzyme-Linked Immunosorbent Assay. 2018.
79. Lindenmann J. Origin of the terms 'antibody' and 'antigen'. 1984(0300-9475 (Print)).
80. Yalow Rs Fau - Berson SA, Berson SA. Assay of plasma insulin in human subjects by immunological methods. 1959(0028-0836 (Print)).
81. Zhu G, Yin X, Jin D, Zhang B, Gu Y, An Y. Paper-based immunosensors: Current trends in the types and applied detection techniques. TrAC Trends in Analytical Chemistry. 2019;111:100-17.
82. Singh A, Chaudhary S, Agarwal A, Verma AS. Chapter 15 - Antibodies: Monoclonal and Polyclonal. In: Verma AS, Singh A, editors. Animal Biotechnology. San Diego: Academic Press; 2014. p. 265-87.
83. Trilling AK, Beekwilder J, Zuilhof H. Antibody orientation on biosensor surfaces: a minireview. Analyst. 2013;138(6):1619-27.
84. Zhu X, Xiong S, Zhang J, Zhang X, Tong X, Kong S. Improving paper-based ELISA performance through covalent immobilization of antibodies. Sensors and Actuators B: Chemical. 2018;255:598-604.
85. Peng Y, Gelder VV, Amaladoss A, Patel KH. Covalent Binding of Antibodies to Cellulose Paper Discs and Their Applications in Naked-eye Colorimetric Immunoassays. 2016(1940-087X (Electronic)).
86. Fu H, Liu X. Experimental comparison of surface chemistries for biomolecule immobilization on paper-based microfluidic devices. Journal of Micromechanics and Microengineering. 2019;29(12):124003.
87. Ahmed S, Bui M-PN, Abbas A. Paper-based chemical and biological sensors: Engineering aspects. Biosensors and Bioelectronics. 2016;77:249-63.
88. Hong W, Jeong S-G, Shim G, Kim DY, Pack SP, Lee C-S. Improvement in the Reproducibility of a Paper-based Analytical Device (PAD) Using Stable Covalent Binding between Proteins and Cellulose Paper. Biotechnology and bioprocess engineering : BBE. 2018;23(6):686-92.
89. Soler M, Lechuga LM. Biochemistry strategies for label-free optical sensor biofunctionalization: advances towards real applicability. Analytical and Bioanalytical Chemistry. 2022;414(18):5071-85.
90. Gao S, Guisán JM, Rocha-Martin J. Oriented immobilization of antibodies onto sensing platforms - A

critical review. Analytica Chimica Acta. 2022;1189:338907.
91. Engvall E, Perlmann P. Enzyme-linked immunosorbent assay (ELISA) quantitative assay of immunoglobulin G. Immunochemistry. 1971;8(9):871-4.
92. Jeong S, Park MJ, Song W, Kim HS. Current immunoassay methods and their applications to clinically used biomarkers of breast cancer. Clinical biochemistry. 2020;78(1873-2933):43-57.
93. Gonzalez A, Gaines M, Gallegos LY, Guevara R, Gomez FA. Thread- paper, and fabric enzyme-linked immunosorbent assays (ELISA). Methods. 2018;146:58-65.
94. Chi J, Gao B, Sun M, Zhang F, Su E, Liu H, et al. Patterned Photonic Nitrocellulose for Pseudopaper ELISA. Analytical Chemistry. 2017;89(14):7727-33.
95. Schirhagl R. Bioapplications for Molecularly Imprinted Polymers. Analytical Chemistry. 2014;86(1):250-61.
96. Dickey FH. Specific Adsorption. The Journal of Physical Chemistry. 1955;59(8):695-707.
97. Wulff G, Sarhan A, Zabrocki K. Wulff, G., Sarhan, A. & Zabrocki, K. Enzyme-analog built polymers and their use for the resolution of racemates. Tetrahedron Lett. 44, 4329-43321973. 4329–32 p.
98. Takagishi T, Klotz IM. Macromolecule-small molecule interactions; introduction of additional binding sites in polyethyleneimine by disulfide cross–linkages. Biopolymers. 1972;11(2):483-91.
99. Vlatakis G, Andersson LI, Müller R, Mosbach K. Drug assay using antibody mimics made by molecular imprinting. Nature. 1993;361:645.
100. Cieplak M, Kutner W. Artificial Biosensors: How Can Molecular Imprinting Mimic Biorecognition? Trends in Biotechnology. 2016;34(11):922-41.
101. Ertürk G, Mattiasson B. Molecular Imprinting Techniques Used for the Preparation of Biosensors. Sensors (Basel, Switzerland). 2017;17(2):288.
102. Vasapollo G, Sole RD, Mergola L, Lazzoi MR, Scardino A, Scorrano S, et al. Molecularly Imprinted Polymers: Present and Future Prospective. International Journal of Molecular Sciences. 2011;12(9).
103. Xu J, Miao H, Wang J, Pan G. Molecularly Imprinted Synthetic Antibodies: From Chemical Design to Biomedical Applications. Small. 2020;16(27):1906644.
104. Zhang C, Cui H, Han Y, Yu F, Shi X. Development of a biomimetic enzyme-linked immunosorbent assay based on molecularly imprinted polymers on paper for the detection of carbaryl. Food Chemistry. 2018;240:893-7.
105. Li W, Zhang X, Li T, Ji Y, Li R. Molecularly imprinted polymer-enhanced biomimetic paper-based analytical devices: A review. Analytica Chimica Acta. 2021;1148:238196.
106. Saylan Y, Denizli A. Molecularly Imprinted Polymer-Based Microfluidic Systems for Point-of-Care Applications. Micromachines. 2019;10(11):766.
107. Ansari S, Masoum S. Molecularly imprinted polymers for capturing and sensing proteins: Current progress and future implications. TrAC Trends in Analytical Chemistry. 2019;114:29-47.
108. Saylan Y, Yilmaz F, Özgür E, Derazshamshir A, Yavuz H, Denizli A. Molecular Imprinting of Macromolecules for Sensor Applications. Sensors (Basel, Switzerland). 2017;17(4):898.
109. Chen L, Xu S, Li J. Recent advances in molecular imprinting technology: current status, challenges and highlighted applications. Chemical Society Reviews. 2011;40(5):2922-42.
110. Chen L, Wang X, Lu W, Wu X, Li J. Molecular imprinting: perspectives and applications. Chemical Society Reviews. 2016;45(8):2137-211.
111. Uzun L, Turner APF. Molecularly-imprinted polymer sensors: realising their potential. Biosensors and Bioelectronics. 2016;76:131-44.
112. Hasanah AN, Safitri N, Zulfa A, Neli N, Rahayu D. Factors Affecting Preparation of Molecularly Imprinted Polymer and Methods on Finding Template-Monomer Interaction as the Key of Selective Properties of the Materials. Molecules [Internet]. 2021; 26(18).
113. Uysal A, Demirel G, Turan E, Çaykara T. Hemoglobin recognition of molecularly imprinted hydrogels prepared at different pHs. Analytica Chimica Acta. 2008;625(1):110-5.
114. Tavares APM, Ferreira NS, Truta L, Sales MGF. Conductive Paper with Antibody-Like Film for Electrical Readings of Biomolecules. Scientific Reports. 2016;6.

115. Bossi A, Piletsky SA, Piletska EV, Righetti PG, Turner APF. Surface-Grafted Molecularly Imprinted Polymers for Protein Recognition. Analytical Chemistry. 2001;73(21):5281-6.
116. Liu K, Wei Wz Fau - Zeng J-X, Zeng Jx Fau - Liu X-Y, Liu Xy Fau - Gao Y-P, Gao YP. Application of a novel electrosynthesized polydopamine-imprinted film to the capacitive sensing of nicotine. Analytical and Bioanalytical Chemistry. 2006;385(1618-2642).
117. Carneiro MCCG, Sousa-Castillo A, Correa-Duarte MA, Sales MGF. Dual biorecognition by combining molecularly-imprinted polymer and antibody in SERS detection. Application to carcinoembryonic antigen. Biosensors and Bioelectronics. 2019;146:111761.
118. Liu Z, He H. Synthesis and Applications of Boronate Affinity Materials: From Class Selectivity to Biomimetic Specificity. Accounts of Chemical Research. 2017;50(9):2185-93.
119. Erdőssy J, Horváth V, Yarman A, Scheller FW, Gyurcsányi RE. Electrosynthesized molecularly imprinted polymers for protein recognition. TrAC Trends in Analytical Chemistry. 2016;79(Supplement C):179-90.
120. Quazi S. Application of biosensors in cancers, an overview. Frontiers in Bioengeneering and biotechnology. 2023(2296-4185 (Print)).
121. Ribeiro JA, Sales MGF, Pereira CM. Electrochemistry-Assisted Surface Plasmon Resonance Biosensor for Detection of CA 15–3. Analytical Chemistry. 2021;93(22):7815-24.
122. Pacheco JG, Silva MSV, Freitas M, Nouws HPA, Delerue-Matos C. Molecularly imprinted electrochemical sensor for the point-of-care detection of a breast cancer biomarker (CA 15-3). Sensors and Actuators B: Chemical. 2018;256:905-12.
123. Huang J, Zhang T, Zheng Y, Liu J. Dual-Mode Sensing Platform for Cancer Antigen 15-3 Determination Based on a Silica Nanochannel Array Using Electrochemiluminescence and Electrochemistry2023; 13(3).
124. Kuswandi B, Ensafi AA. Perspective—Paper-Based Biosensors: Trending Topic in Clinical Diagnostics Developments and Commercialization. Journal of The Electrochemical Society. 2019;167(3):037509.
125. Singh AT, Lantigua D, Meka A, Taing S, Pandher M, Camci-Unal G. Paper-Based Sensors: Emerging Themes and Applications. Sensors. 2018;18(9):2838.
126. Zhang Z, Wang H, Chen Z, Wang X, Choo J, Chen L. Plasmonic colorimetric sensors based on etching and growth of noble metal nanoparticles: Strategies and applications. Biosensors and Bioelectronics. 2018;114:52-65.
127. Khosroshahi MA-O, Patel Y, Chabok R. Non-invasive optical characterization and detection of CA 15-3 breast cancer biomarker in blood serum using monoclonal antibody-conjugated gold nanourchin and surface-enhanced Raman scattering. Lasers in Medical Science. 2022;38(1).
128. Ranganathan V, Srinivasan S, Singh A, DeRosa MC. An aptamer-based colorimetric lateral flow assay for the detection of human epidermal growth factor receptor 2 (HER2). Analytical Biochemistry. 2020;588:113471.
129. Alizadeh N, Salimi A, Hallaj R. Mimicking peroxidase activity of Co2(OH)2CO3-CeO2 nanocomposite for smartphone based detection of tumor marker using paper-based microfluidic immunodevice. Talanta. 2018;189:100-10.
130. Sousa DA, Carneiro M, Ferreira D, Moreira FTC, Sales MGF, Rodrigues LR. Recent Advances in the Selection of Cancer-Specific Aptamers for the Development of Biosensors. Curr Med Chem 2022;29(1875-533X (Electronic)):5850-80.
131. Abou-Omar MN, Attia MS, Afify HG, Amin MA, Boukherroub R, Mohamed EH. Novel Optical Biosensor Based on a Nano-Gold Coated by Schiff Base Doped in Sol/Gel Matrix for Sensitive Screening of Oncomarker CA-125. ACS Omega. 2021;6(32):20812-21.
132. Chen W, Zhang Y, Di K, Liu C, Xia Y, Ding S, et al. A Washing-Free and Easy-to-Operate Fluorescent Biosensor for Highly Efficient Detection of Breast Cancer-Derived Exosomes. Frontiers in Bioengineering and Biotechnology. 2022(2296-4185 (Print)).
133. Loyez M, Lobry M, Hassan EM, DeRosa MC, Caucheteur C, Wattiez R. HER2 breast cancer biomarker detection using a sandwich optical fiber assay. Talanta. 2021;221:121452.
134. Szymańska B, Lukaszewski Z, Hermanowicz-Szamatowicz K, Gorodkiewicz E. A biosensor for

determination of the circulating biomarker CA125/MUC16 by Surface Plasmon Resonance Imaging. Talanta. 2020;206:120187.
135. Xue T, Liang W, Li Y, Sun Y, Xiang Y, Zhang Y, et al. Ultrasensitive detection of miRNA with an antimonene-based surface plasmon resonance sensor. Nature Communications. 2019;10(1):28.
136. Castaño-Guerrero Y, Romaguera-Barcelay Y, Moreira FT, Brito WR, Fortunato E, Sales MG. Poly(Thionine)-Modified Screen-Printed Electrodes for CA 19-9 Detection and Its Properties in Raman Spectroscopy. Chemosensors [Internet]. 2022; 10(3).
137. Turan E, Zengin A, Suludere Z, Kalkan NÖ, Tamer U. Construction of a sensitive and selective plasmonic biosensor for prostate specific antigen by combining magnetic molecularly-imprinted polymer and surface-enhanced Raman spectroscopy. Talanta. 2022;237:122926.
138. Aydindogan E, Ceylan AE, Timur S. Paper-based colorimetric spot test utilizing smartphone sensing for detection of biomarkers. Talanta. 2020;208:120446.
139. Fernandes GM, Silva WR, Barreto DN, Lamarca RS, Lima Gomes PCF, Flávio da SPJ, et al. Novel approaches for colorimetric measurements in analytical chemistry - A review. 2020(1873-4324 (Electronic)).
140. Abarghoei S, Fakhri N, Borghei YS, Hosseini M, Ganjali MR. A colorimetric paper sensor for citrate as biomarker for early stage detection of prostate cancer based on peroxidase-like activity of cysteine-capped gold nanoclusters. Spectrochimica Acta Part A: Molecular and Biomolecular Spectroscopy. 2019;210:251-9.
141. ImmunoChemistry Technologies L. HRP Redox Reaction Driven TMB Color Development. 2020.
142. Busa LSA, Maeki M, Ishida A, Tani H, Tokeshi M. Simple and sensitive colorimetric assay system for horseradish peroxidase using microfluidic paper-based devices. Sensors and Actuators B: Chemical. 2016;236:433-41.
143. Vazquez-Alvarado M, Vanasupa S, Valdez EH, Pama AM, Crowder MJ, Vanasupa L, et al. Evaluation of chromogenic substrates for horseradish peroxidase on paper-based microfluidic devices. Sensors and Actuators B: Chemical. 2023;377:133028.
144. Harpaz D, Eltzov E, Ng TSE, Marks RS, Tok AIY. Enhanced Colorimetric Signal for Accurate Signal Detection in Paper-Based Biosensors. Diagnostics. 2020(2075-4418 (Print)).
145. Ren W, Mohammed SI, Wereley S, Irudayaraj J. Magnetic Focus Lateral Flow Sensor for Detection of Cervical Cancer Biomarkers. Analytical Chemistry. 2019;91(4):2876-84.
146. Koczula KM, Gallotta A. Lateral flow assays. Essays in biochemistry. 2016;60(1):111-20.
147. Aldewachi H, Chalati T, Woodroofe MN, Bricklebank N, Sharrack B, Gardiner P. Gold nanoparticle-based colorimetric biosensors. Nanoscale. 2018;10(1):18-33.
148. Yuan Z, Hu C-C, Chang H-T, Lu C. Gold nanoparticles as sensitive optical probes. Analyst. 2016;141(5):1611-26.
149. Zhang Y, McKelvie ID, Cattrall RW, Kolev SD. Colorimetric detection based on localised surface plasmon resonance of gold nanoparticles: Merits, inherent shortcomings and future prospects. Talanta. 2016;152:410-22.
150. Jazayeri MH, Aghaie T, Avan A, Vatankhah A, Ghaffari MRS. Colorimetric detection based on gold nano particles (GNPs): An easy, fast, inexpensive, low-cost and short time method in detection of analytes (protein, DNA, and ion). Sensing and Bio-Sensing Research. 2018;20:1-8.
151. Ma Z, Sui S-F. Naked-Eye Sensitive Detection of Immunoglubulin G by Enlargement of Au Nanoparticles In Vitro. Angewandte Chemie International Edition. 2002;41(12):2176-9.
152. Liu H, Rong P, Jia H, Yang J, Dong B, Dong Q, et al. A Wash-Free Homogeneous Colorimetric Immunoassay Method. Theranostics. 2016;6(1):54-64.
153. Liana DD, Raguse B, Gooding JJ, Chow E. Recent advances in paper-based sensors. Sensors. 2012;12(9):11505-26.
154. Watt J, Banks J. On a new method of preparing a test liquor to shew the presence of acids and alkalies in chemical mixtures. Philosophical Transactions of the Royal Society of London. 1784;74:419-22.
155. Agarwal C, Csóka L. Recent Advances in Paper-Based Analytical Devices: A Pivotal Step Forward in Building Next-Generation Sensor Technology. Sustainable Polymer Composites and Nanocomposites: Springer International Publishing; 2019. p. 479-517.

156. Pelton R. Bioactive paper provides a low-cost platform for diagnostics. TrAC Trends in Analytical Chemistry. 2009;28(8):925-42.
157. Yamada K, Shibata H, Suzuki K, Citterio D. Toward practical application of paper-based microfluidics for medical diagnostics: state-of-the-art and challenges. Lab on a Chip. 2017;17(7):1206-49.
158. Klemm D, Heublein B, Fink H-P, Bohn A. Cellulose: Fascinating Biopolymer and Sustainable Raw Material. Angewandte Chemie International Edition. 2005;44(22):3358-93.
159. Nery EW, Kubota LT. Sensing approaches on paper-based devices: a review. Analytical and Bioanalytical Chemistry. 2013;405(24):7573-95.
160. Ye J, Hutchison JA, Uji-i H, Hofkens J, Lagae L, Maes G, et al. Excitation wavelength dependent surface enhanced Raman scattering of 4-aminothiophenol on gold nanorings. Nanoscale. 2012;4(5):1606-11.
161. Lim WY, Goh BT, Khor SM. Microfluidic paper-based analytical devices for potential use in quantitative and direct detection of disease biomarkers in clinical analysis. Journal of Chromatography B. 2017;1060:424-42.
162. Shende P, Prabhakar B, Patil A. Color changing sensors: A multimodal system for integrated screening. TrAC Trends in Analytical Chemistry. 2019;121:115687.
163. Nie J, Zhang Y, Lin L, Zhou C, Li S, Zhang L, et al. Low-Cost Fabrication of Paper-Based Microfluidic Devices by One-Step Plotting. Analytical Chemistry. 2012;84(15):6331-5.
164. Kim TH, Hahn YA-O, Kim MA-O. Recent Advances of Fluid Manipulation Technologies in Microfluidic Paper-Based Analytical Devices (μPADs) toward Multi-Step Assays. Micromachines. 2020(2072-666X).
165. West PW. Selective Spot Test for Copper. Industrial & Engineering Chemistry Analytical Edition. 1945;17(11):740-1.
166. Free AH, Adams EC, Kercher ML, Free HM, Cook MH. Simple Specific Test for Urine Glucose. Clinical Chemistry. 1957;3(3):163-8.
167. Liu L, Yang D, Liu G. Signal amplification strategies for paper-based analytical devices. Biosensors and Bioelectronics. 2019;136:60-75.
168. Hu J, Wang SQ, Wang L, Li F, Pingguan-Murphy B, Lu TJ, et al. Advances in paper-based point-of-care diagnostics. Biosensors & Bioelectronics. 2014;54:585-97.
169. Ma F, He L, Lindner E, Wu D-Y. Highly porous poly(l-lactic) acid nanofibers as a dual-signal paper-based bioassay platform for in vitro diagnostics. Applied Surface Science. 2021;542:148732.
170. Gao X, Xu H, Baloda M, Gurung AS, Xu L-P, Wang T, et al. Visual detection of microRNA with lateral flow nucleic acid biosensor. Biosensors and Bioelectronics. 2014;54:578-84.
171. Fakhri N, Abarghoei S, Dadmehr M, Hosseini M, Sabahi H, Ganjali MR. Paper based colorimetric detection of miRNA-21 using Ag/Pt nanoclusters. Spectrochimica Acta Part A: Molecular and Biomolecular Spectroscopy. 2020;227:117529.
172. Singer JM, Plotz CM. The latex fixation test: I. Application to the serologic diagnosis of rheumatoid arthritis. The American Journal of Medicine. 1956;21(6):888-92.
173. Martinez AW, Phillips ST, Butte MJ, Whitesides GM. Patterned paper as a platform for inexpensive, low-volume, portable bioassays. Angewandte Chemie (International ed in English). 2007;46(8):1318-20.
174. Ge L, Wang S, Yu J, Li N, Ge S, Yan M. Molecularly Imprinted Polymer Grafted Porous Au-Paper Electrode for an Microfluidic Electro-Analytical Origami Device. Advanced Functional Materials. 2013;23(24):3115-23.
175. Xu S, Xu Z, Liu Z. Paper-Based Molecular-Imprinting Technology and Its Application. Biosensors [Internet]. 2022; 12(8).
176. Cheng H, Wang Y, Wang Y, Ge L, Liu X, Li F. A visualized sensor based on layered double hydroxides with peroxidase-like activity for sensitive acetylcholinesterase assay. Analytical Methods. 2023;15(30):3700-8.
177. Brazaca LC, Moreto JR, Martín A, Tehrani F, Wang J, Zucolotto V. Colorimetric Paper-Based Immunosensor for Simultaneous Determination of Fetuin B and Clusterin toward Early Alzheimer's Diagnosis. ACS Nano. 2019;13(11):13325-32.

178. Correia BP, Sousa MP, Sousa CEA, Mateus D, Sebastião AI, Cruz MT, et al. Development of colorimetric cellulose-based test-strip for the rapid detection of antibodies against SARS-CoV2 virus. Cellulose. 2022
(0969-0239 (Print)).
179. Tsai T-T, Huang C-Y, Chen C-A, Shen S-W, Wang M-C, Cheng C-M, et al. Diagnosis of Tuberculosis Using Colorimetric Gold Nanoparticles on a Paper-Based Analytical Device. ACS Sensors. 2017;2(9):1345-54.
180. Kitchawengkul N, Prakobkij A, Anutrasakda W, Yodsin N, Jungsuttiwong S, Chunta S, et al. Mimicking Peroxidase-Like Activity of Nitrogen-Doped Carbon Dots (N-CDs) Coupled with a Laminated Three-Dimensional Microfluidic Paper-Based Analytical Device (Laminated 3D-μPAD) for Smart Sensing of Total Cholesterol from Whole Blood. Analytical Chemistry. 2021;93(18):6989-99.
181. Tong L, Wu L, Zai Y, Zhang Y, Su E, Gu N. Paper-based colorimetric glucose sensor using Prussian blue nanoparticles as mimic peroxidase. Biosensors and Bioelectronics. 2023;219:114787.
182. Wang S, Xu S, Zhou Q, Liu Z, Xu Z. State-of-the-art molecular imprinted colorimetric sensors and their on-site inspecting applications. Journal of Separation Science. 2023;n/a(n/a):2201059.
183. Carneiro M, Rodrigues L, Moreira F, Sales MG. Colorimetric Paper-Based Sensors against Cancer Biomarkers. Sensors. 2022;22(3221).
184. Cheng C-M, Martinez AW, Gong J, Mace CR, Phillips ST, Carrilho E, et al. Paper-Based ELISA. Angewandte Chemie International Edition. 2010;49(28):4771-4.
185. Vashist SK, Luong JHT. Chapter 5 - Enzyme-Linked Immunoassays. In: Vashist SK, Luong JHT, editors. Handbook of Immunoassay Technologies: Academic Press; 2018. p. 97-127.
186. Bai P, Luo Y, Li Y, Yu X-D, Chen H-Y. Study on Enzyme Linked Immunosorbent Assay Using Paper-based Micro-zone Plates. Chinese Journal of Analytical Chemistry. 2013;41(1):20-4.
187. Jarujamrus P, Tian J, Li X, Siripinyanond A, Shiowatana J, Shen W. Mechanisms of red blood cells agglutination in antibody-treated paper. Analyst. 2012;137(9):2205-10.
188. Nikolic T, Kostic M, Praskalo J, Pejic B, Petronijevic Z, Skundric P. Sodium periodate oxidized cotton yarn as carrier for immobilization of trypsin. Carbohydrate Polymers. 2010;82(3):976-81.
189. Gibbs J, Vessels M, Rothenberg M. Effective Blocking Procedures in ELISA Assays.
190. Drijvers JM, Awan IM, Perugino CA, Rosenberg IM, Pillai S. Chapter 7 - The Enzyme-Linked Immunosorbent Assay: The Application of ELISA in Clinical Research. In: Jalali M, Saldanha FYL, Jalali M, editors. Basic Science Methods for Clinical Researchers. Boston: Academic Press; 2017. p. 119-33.
191. Catt K, Niall HD, Tregear GW. Solid Phase Radioimmunoassay. Nature. 1967;213(5078):825-7.
192. C.C.G. Carneiro M, Rodrigues LR, Moreira FTC, Goreti F. Sales M. Paper-based ELISA for fast CA 15–3 detection in point-of-care. Microchemical Journal. 2022;181:107756.
193. Gomes RS, Moreira FTC, Fernandes R, Sales MGF. Sensing CA 15-3 in point-of-care by electropolymerizing O-phenylenediamine (oPDA) on Au-screen printed electrodes. PLOS ONE. 2018;13(5):e0196656.
194. Golmohammadi H, Morales-Narvaez E, Naghdi T, Merkoci A. Nanocellulose in Sensing and Biosensing. Chemistry of Materials. 2017;29(13):5426-46.
195. Samir M, Alloin F, Dufresne A. Review of recent research into cellulosic whiskers, their properties and their application in nanocomposite field. Biomacromolecules. 2005;6(2):612-26.
196. Lima MMD, Borsali R. Rodlike cellulose microcrystals: Structure, properties, and applications. Macromolecular Rapid Communications. 2004;25(7):771-87.
197. George J, Sabapathi SN. Cellulose nanocrystals: synthesis, functional properties, and applications. Nanotechnology Science and Applications. 2015;8:45-54.
198. Sugiyama J, Vuong R, Chanzy H. ELECTRON-DIFFRACTION STUDY ON THE 2 CRYSTALLINE PHASES OCCURRING IN NATIVE CELLULOSE FROM AN ALGAL CELL-WALL. Macromolecules. 1991;24(14):4168-75.
199. Helbert W, Nishiyama Y, Okano T, Sugiyama J. Molecular imaging of Halocynthia papillosa cellulose. Journal of Structural Biology. 1998;124(1):42-50.
200. Mahmud MM, Perveen A, Jahan RA, Matin MA, Wong SY, Li X, et al. Preparation of different polymorphs of cellulose from different acid hydrolysis medium. International Journal of Biological

Macromolecules. 2019;130:969-76.
201. Shahabi-Ghahafarrokhi I, Khodaiyan F, Mousavi M, Yousefi H. Preparation and Characterization of Nanocellulose from Beer Industrial Residues Using Acid Hydrolysis/Ultrasound. Fibers and Polymers. 2015;16(3):529-36.
202. Xie HX, Du HS, Yang XG, Si CL. Recent Strategies in Preparation of Cellulose Nanocrystals and Cellulose Nanofibrils Derived from Raw Cellulose Materials. International Journal of Polymer Science. 2018.
203. Hastuti N, Kanomata K, Kitaoka T. Hydrochloric Acid Hydrolysis of Pulps from Oil Palm Empty Fruit Bunches to Produce Cellulose Nanocrystals. Journal of Polymers and the Environment. 2018;26(9):3698-709.
204. Araki J, Wada M, Kuga S. Steric stabilization of a cellulose microcrystal suspension by poly(ethylene glycol) grafting. Langmuir. 2001;17(1):21-7.
205. Habibi Y, Chanzy H, Vignon MR. TEMPO-mediated surface oxidation of cellulose whiskers. Cellulose. 2006;13(6):679-87.
206. Li L, Zhao S, Zhang J, Zhang ZX, Hu HQ, Xin ZX, et al. TEMPO-mediated oxidation of microcrystalline cellulose: Influence of temperature and oxidation procedure on yields of water-soluble products and crystal structures of water-insoluble residues. Fibers and Polymers. 2013;14(3):352-7.
207. Perez DD, Montanari S, Vignon MR. TEMPO-mediated oxidation of cellulose III. Biomacromolecules. 2003;4(5):1417-25.
208. Denooy AEJ, Besemer AC, Vanbekkum H. HIGHLY SELECTIVE TEMPO MEDIATED OXIDATION OF PRIMARY ALCOHOL GROUPS IN POLYSACCHARIDES. Recueil Des Travaux Chimiques Des Pays-Bas-Journal of the Royal Netherlands Chemical Society. 1994;113(3):165-6.
209. Isogai A, Kato Y. Preparation of polyglucuronic acid from cellulose by TEMPO-mediated oxidation. Cellulose. 1998;5(3):153-64.
210. Tahiri C, Vignon MR. TEMPO-oxidation of cellulose: Synthesis and characterisation of polyglucuronans. Cellulose. 2000;7(2):177-88.
211. Saito T, Isogai A. TEMPO-mediated oxidation of native cellulose. The effect of oxidation conditions on chemical and crystal structures of the water-insoluble fractions. Biomacromolecules. 2004;5(5):1983-9.
212. Saito T, Shibata I, Isogai A, Suguri N, Sumikawa N. Distribution of carboxylate groups introduced into cotton linters by the TEMPO-mediated oxidation. Carbohydrate Polymers. 2005;61(4):414-9.
213. Montanari S, Rountani M, Heux L, Vignon MR. Topochemistry of carboxylated cellulose nanocrystals resulting from TEMPO-mediated oxidation. Macromolecules. 2005;38(5):1665-71.
214. Zhuang C, Tao FR, Cui YZ. Eco-friendly biorefractory films of gelatin and TEMPO-oxidized cellulose ester for food packaging application. Journal of the Science of Food and Agriculture. 2017;97(10):3384-95.
215. Haniffa M, Ching YC, Chuah CH, Ching KY, Nazri N, Abdullah LC, et al. Effect of TEMPO-oxidization and rapid cooling on thermo-structural properties of nanocellulose. Carbohydrate Polymers. 2017;173:91-9.
216. Guo X, Liu L, Hu YC, Wu YQ. Water vapor sorption properties of TEMPO oxidized and sulfuric acid treated cellulose nanocrystal films. Carbohydrate Polymers. 2018;197:524-30.
217. Portaccio M, Durante D, Viggiano A, Di Martino S, De Luca P, Di Tuoro D, et al. Amperometric glucose determination by means of glucose oxidase immobilized on a cellulose acetate film: Dependence on the immobilization procedures. Electroanalysis. 2007;19(17):1787-93.
218. Incani V, Danumah C, Boluk Y. Nanocomposites of nanocrystalline cellulose for enzyme immobilization. Cellulose. 2013;20(1):191-200.
219. Morales-Narvaez E, Golmohammadi H, Naghdi T, Yousefi H, Kostiv U, Horak D, et al. Nanopaper as an Optical Sensing Platform. Acs Nano. 2015;9(7):7296-305.
220. Tavakolian M, Lerner J, Tovar FM, Frances J, van de Ven TGM, Kakkar A. Dendrimer directed assembly of dicarboxylated hairy nanocellulose. Journal of Colloid and Interface Science. 2019;541:444-53.
221. Uddin KMA, Jokinen V, Ahangiri F, Franssila S, Rojas OJ, Tuukkanen S. Disposable Microfluidic Sensor Based on Nanocellulose for Glucose Detection. Global Challenges. 2019;3(2).
222. Yuan HB, Chen L, Hong FF, Zhu MF. Evaluation of nanocellulose carriers produced by four different bacterial strains for laccase immobilization. Carbohydrate Polymers. 2018;196:457-64.

223. Potzinger Y, Rahnfeld L, Kralisch D, Fischer D. Immobilization of plasmids in bacterial nanocellulose as gene activated matrix. Carbohydrate Polymers. 2019;209:62-73.
224. Xiao YM, Rong LD, Wang BJ, Mao ZP, Xu H, Zhong Y, et al. A light-weight and high-efficacy antibacterial nanocellulose-based sponge via covalent immobilization of gentamicin. Carbohydrate Polymers. 2018;200:595-601.
225. Wulandari WT, Rochliadi A, Arcana IM, Iop, editors. Nanocellulose prepared by acid hydrolysis of isolated cellulose from sugarcane bagasse. 10th Joint Conference on Chemistry; 2015 Sep 08-09; Solo, INDONESIA2016.
226. Abdi MM, Razalli RL, Tahir PM, Chaibakhsh N, Hassani M, Mir M. Optimized fabrication of newly cholesterol biosensor based on nanocellulose. International Journal of Biological Macromolecules. 2019;126:1213-22.
227. Hoenders D, Guo JQ, Goldmann AS, Barner-Kowollik C, Walther A. Photochemical ligation meets nanocellulose: a versatile platform for self-reporting functional materials. Materials Horizons. 2018;5(3):560-8.
228. Siqueira G, Bras J, Dufresne A. Cellulosic Bionanocomposites: A Review of Preparation, Properties and Applications. Polymers. 2010;2(4):728-65.
229. Sher M, Zhuang R, Demirci U, Asghar W. Paper-based analytical devices for clinical diagnosis: recent advances in the fabrication techniques and sensing mechanisms. Expert Review of Molecular Diagnostics. 2017;17(4):351-66.
230. Gomes HIAS, Sales MGF. Development of paper-based color test-strip for drug detection in aquatic environment: Application to oxytetracycline. Biosensors and Bioelectronics. 2015;65:54-61.
231. Liberti MV, Locasale JW. The Warburg Effect: How Does it Benefit Cancer Cells? Trends in Biochemical Sciences. 2016;41(3):211-8.
232. Muti P, Quattrin T Fau - Grant BJB, Grant Bj Fau - Krogh V, Krogh V Fau - Micheli A, Micheli A Fau - Schünemann HJ, Schünemann Hj Fau - Ram M, et al. Fasting glucose is a risk factor for breast cancer: a prospective study. Cancer Epidemiology, Biomarkers & Prevention. 2002(1055-9965 (Print)):1361-8.
233. Melvin JC, Garmo H, Holmberg L, Hammar N, Walldius G, Jungner I, et al. Glucose and lipoprotein biomarkers and breast cancer severity using data from the Swedish AMORIS cohort. BMC Cancer. 2017;17(1):246.
234. Monzavi-Karbassi B, Gentry R, Kaur V, Siegel ER, Jousheghany F, Medarametla S, et al. Pre-diagnosis blood glucose and prognosis in women with breast cancer. Cancer & Metabolism. 2016;4(1):7.
235. Piątkiewicz P, Czech A. Glucose metabolism disorders and the risk of cancer. 2011(1661-4917 (Electronic)).
236. Barone BB, Yeh Hc Fau - Snyder CF, Snyder Cf Fau - Peairs KS, Peairs Ks Fau - Stein KB, Stein Kb Fau - Derr RL, Derr Rl Fau - Wolff AC, et al. Long-term all-cause mortality in cancer patients with preexisting diabetes mellitus: a systematic review and meta-analysis. (1538-3598 (Electronic)).
237. Lebelo MT, Joubert AM, Visagie MA-O. Warburg effect and its role in tumourigenesis. (0253-6269 (Print)).
238. Mei Y, Zhao L, Jiang M, Yang F, Zhang X, Jia Y, et al. Characterization of glucose metabolism in breast cancer to guide clinical therapy. Frontiers in Surgery. 2022;9.
239. Warburg O, Wind F, Negelein E. The metabolism of tumors in the body. The Journal of general physiology. 1927;8(6):519-30.
240. Marín-Hernández A, Gallardo-Pérez JC, Rodríguez-Enríquez S, Encalada R, Moreno-Sánchez R, Saavedra E. Modeling cancer glycolysis. Biochimica et Biophysica Acta (BBA) - Bioenergetics. 2011;1807(6):755-67.
241. Posthuma-Trumpie GA, Korf J, van Amerongen A. Lateral flow (immuno) assay: its strengths, weaknesses, opportunities and threats. A literature survey. Analytical and Bioanalytical Chemistry. 2009;393(2):569-82.
242. Dyerberg J, Pedersen L, Aagaard O. EVALUATION OF A DIPSTICK TEST FOR GLUCOSE IN URINE. Clinical Chemistry. 1976;22(2):205-10.

243. Hamilton R, Young S. Identifying CSF using urine glucose dipstick testing. International Journal of Obstetric Anesthesia. 2007;16(3):294-5.
244. Bushman ET, Jauk VC, Szychowski JM, Mazzoni S, Tita AT, Harper LM. Utility of routine dipstick urinalysis for glucose screening as a predictor for gestational diabetes. American Journal of Obstetrics and Gynecology. 2020;222(1):S161-S2.
245. Kim JH, Mun S, Ko HU, Yun GY, Kim J. Disposable chemical sensors and biosensors made on cellulose paper. Nanotechnology. 2014;25(9).
246. Fischer C, Fraiwan A, Choi S. A 3D paper-based enzymatic fuel cell for self-powered, low-cost glucose monitoring. Biosensors & Bioelectronics. 2016;79:193-7.
247. Newman JD, Setford SJ. Enzymatic biosensors. Molecular Biotechnology. 2006;32(3):249-68.
248. Sassolas A, Blum LJ, Leca-Bouvier BD. Immobilization strategies to develop enzymatic biosensors. Biotechnology Advances. 2012;30(3):489-511.
249. Moreira FTC, Sale MGF, Di Lorenzo M. Towards timely Alzheimer diagnosis: A self-powered amperometric biosensor for the neurotransmitter acetylcholine. Biosensors & Bioelectronics. 2017;87:607-14.
250. Nguyen HH, Lee SH, Lee UJ, Fermin CD, Kim M. Immobilized Enzymes in Biosensor Applications. Materials. 2019;12(1).
251. Dai GY, Hu JL, Zhao XY, Wang P. A colorimetric paper sensor for lactate assay using a cellulose-Binding recombinant enzyme. Sensors and Actuators B-Chemical. 2017;238:138-44.
252. Derikvand F, Yin DT, Barrett R, Brumer H. Cellulose-Based Biosensors for Esterase Detection. Analytical Chemistry. 2016;88(6):2989-93.
253. Palanisamy S, Ramaraj SK, Chen SM, Yang TCK, Yi-Fan P, Chen TW, et al. A novel Laccase Biosensor based on Laccase immobilized Graphene-Cellulose Microfiber Composite modified Screen-Printed Carbon Electrode for Sensitive Determination of Catechol. Scientific Reports. 2017;7.
254. Arciuli M, Palazzo G, Gallone A, Mallardi A. Bioactive paper platform for colorimetric phenols detection. Sensors and Actuators B-Chemical. 2013;186:557-62.
255. Liu Y, Chen JY. Enzyme immobilization on cellulose matrixes. Journal of Bioactive and Compatible Polymers. 2016;31(6):553-67.
256. Lawrence CSK, Tan SN, Floresca CZ. A "green" cellulose paper based glucose amperometric biosensor. Sensors and Actuators B-Chemical. 2014;193:536-41.
257. Bohm A, Trosien S, Avrutina O, Kolmar H, Biesalski M. Covalent Attachment of Enzymes to Paper Fibers for Paper-Based Analytical Devices. Frontiers in Chemistry. 2018;6.
258. Firooz NS, Panahi R, Mokhtarani B, Yazdani F. Direct introduction of amine groups into cellulosic paper for covalent immobilization of tyrosinase: support characterization and enzyme properties. Cellulose. 2017;24(3):1407-16.
259. Zhou M, Yang MH, Zhou FM. Paper based colorimetric biosensing platform utilizing cross-linked siloxane as probe. Biosensors & Bioelectronics. 2014;55:39-43.
260. Guerrero MP, Bertrand F, Rochefort D. Activity, stability and inhibition of a bioactive paper prepared by large-scale coating of laccase microcapsules. Chemical Engineering Science. 2011;66(21):5313-20.
261. Wang JJ, Myung NV, Yun MH, Monbouquette HG. Glucose oxidase entrapped in polypyrrole on high-surface-area Pt electrodes: a model platform for sensitive electroenzymatic biosensors. Journal of Electroanalytical Chemistry. 2005;575(1):139-46.
262. Rosa MF, Medeiros ES, Malmonge JA, Gregorski KS, Wood DF, Mattoso LHC, et al. Cellulose nanowhiskers from coconut husk fibers: Effect of preparation conditions on their thermal and morphological behavior. Carbohydrate Polymers. 2010;81(1):83-92.
263. Wang QQ, Zhu JY, Reiner RS, Verrill SP, Baxa U, McNeil SE. Approaching zero cellulose loss in cellulose nanocrystal (CNC) production: recovery and characterization of cellulosic solid residues (CSR) and CNC. Cellulose. 2012;19(6):2033-47.
264. Nie K, Song Y, Liu SY, Han GT, Ben HX, Ragauskas AJ, et al. Preparation and Characterization of Microcellulose and Nanocellulose Fibers from Artemisia Vulgaris Bast. Polymers. 2019;11(5).

265. Li X, Xu Y, Zhang L. Chapter Fifteen - Serum CA153 as biomarker for cancer and noncancer diseases. In: Zhang L, editor. Progress in Molecular Biology and Translational Science. 162: Academic Press; 2019. p. 265-76.
266. Sharifi M, Hasan A, Attar F, Taghizadeh A, Falahati M. Development of point-of-care nanobiosensors for breast cancers diagnosis. Talanta. 2020;217:121091.
267. Yonet-Tanyeri N, Ahlmark BZ, Little SR. Advances in Multiplexed Paper-Based Analytical Devices for Cancer Diagnosis: A Review of Technological Developments. Advanced Materials Technologies. 2021;6(8):1-31.
268. Li Z, You M, Bai Y, Gong Y, Xu F. Equipment-Free Quantitative Readout in Paper-Based Point-of-Care Testing. Small Methods. 2020;4(4):1900459.
269. Liu W, Guo Y, Zhao M, Li H, Zhang Z. Ring-Oven Washing Technique Integrated Paper-based Immunodevice for Sensitive Detection of Cancer Biomarker. Analytical Chemistry. 2015;87(15):7951-7.
270. Liang L, Ge S, Li L, Liu F, Yu J. Microfluidic paper-based multiplex colorimetric immunodevice based on the catalytic effect of Pd/Fe3O4@C peroxidase mimetics on multiple chromogenic reactions. Analytica Chimica Acta. 2015;862:70-6.
271. Yokchom R, Laiwejpithaya S, Maneeprakorn W, Tapaneeyakorn S, Rabablert J, Dharakul T. Paper-based immunosensor with signal amplification by enzyme-labeled anti-p16INK4a multifunctionalized gold nanoparticles for cervical cancer screening. Nanomedicine: Nanotechnology, Biology and Medicine. 2018;14(3):1051-8.
272. Mwai LM, Mutinda CK, Ngugi CW, Walong E. Development of HPV 16/18 E6 oncoprotein paper-based nanokit for enhanced detection of HPV 16/18 E6 oncoprotein in cervical cancer screening. Journal of Nanotechnology and Nanomaterials. 2020;1(2):31-45.
273. Mesgari F, Beigi SM, Fakhri N, Hosseini M, Aghazadeh M, Ganjali MR. Paper-based chemiluminescence and colorimetric detection of cytochrome c by cobalt hydroxide decorated mesoporous carbon. Microchemical Journal. 2020;157:104991.
274. Duchemin BJC. Mercerisation of cellulose in aqueous NaOH at low concentrations. Green Chemistry. 2015;17(7):3941-7.
275. John MJ, Anandjiwala RD. Recent developments in chemical modification and characterization of natural fiber-reinforced composites. Polymer Composites. 2008;29(2):187-207.
276. Singha AS, Thakur VK. Synthesis and Characterizations of Silane Treated Grewia optiva Fibers. International Journal of Polymer Analysis and Characterization. 2009;14(4):301-21.
277. Siller M, Amer H, Bacher M, Roggenstein W, Rosenau T, Potthast A. Effects of periodate oxidation on cellulose polymorphs. Cellulose. 2015;22(4):2245-61.
278. Xu Y, Huang C. Effect of Sodium Periodate Selective Oxidation on Crystallinity of Cotton Cellulose. Advanced Materials Research. 2011;197-198:1201-4.
279. Hospodarova V, Singovszka E, Stevulova N. Characterization of Cellulosic Fibers by FTIR Spectroscopy for Their Further Implementation to Building Materials. American Journal of Analytical Chemistry. 2018;09:303-10.
280. Bradford MM. A rapid and sensitive method for the quantitation of microgram quantities of protein utilizing the principle of protein-dye binding. Analytical Biochemistry. 1976;72(1):248-54.
281. Tal M, Silberstein A, Nusser E. Why does Coomassie Brilliant Blue R interact differently with different proteins? A partial answer. 1985;260(18):9976-80.
282. Xiao Y, Isaacs SN. Enzyme-linked immunosorbent assay (ELISA) and blocking with bovine serum albumin (BSA)—not all BSAs are alike. Journal of Immunological Methods. 2012;384(1):148-51.
283. Konishi E, Kitai Y, Nishimura K, Harada S. Antibodies to bovine serum albumin in human sera: problems and solutions with casein-based ELISA in the detection of natural Japanese encephalitis virus infections. Japanese Journal of Infectious Diseases. 2010;63(1884-2836):296-8.
284. Neubauerova K, Carneiro MCCG, Rodrigues LR, Moreira FTC, Sales MGF. Nanocellulose- based biosensor for colorimetric detection of glucose. Sensing and Bio-Sensing Research. 2020;29:100368.
285. Surugiu I, Ye L, Yilmaz E, Dzgoev A, Danielsson B, Mosbach K, et al. An enzyme-linked molecularly

imprinted sorbent assay. Analyst. 2000;125(1):13-6.
286. Bi X, Liu Z. Facile Preparation of Glycoprotein-Imprinted 96-Well Microplates for Enzyme-Linked Immunosorbent Assay by Boronate Affinity-Based Oriented Surface Imprinting. Analytical Chemistry. 2014;86(1):959-66.
287. Kong Q, Wang Y, Zhang L, Ge S, Yu J. A novel microfluidic paper-based colorimetric sensor based on molecularly imprinted polymer membranes for highly selective and sensitive detection of bisphenol A. Sensors and Actuators B: Chemical. 2017;243:130-6.
288. Zeng L, Cui H, Chao J, Huang K, Wang X, Zhou Y, et al. Colorimetric determination of tetrabromobisphenol A based on enzyme-mimicking activity and molecular recognition of metal-organic framework-based molecularly imprinted polymers. Microchimica Acta. 2020;187(2):142.
289. Huang K, Chen Y, Zhou F, Zhao X, Liu J, Mei S, et al. Integrated ion imprinted polymers-paper composites for selective and sensitive detection of Cd(II) ions. Journal of Hazardous Materials. 2017;333:137-43.
290. Xiao L, Zhang Z, Wu C, Han L, Zhang H. Molecularly imprinted polymer grafted paper-based method for the detection of 17β-estradiol. Food Chemistry. 2017;221:82-6.
291. Wang S, Ge L, Li L, Yan M, Ge S, Yu J. Molecularly imprinted polymer grafted paper-based multi-disk micro-disk plate for chemiluminescence detection of pesticide. Biosensors and Bioelectronics. 2013;50:262-8.
292. Ou SH, Wu MC, Chou TC, Liu CC. Polyacrylamide gels with electrostatic functional groups for the molecular imprinting of lysozyme. Analytica Chimica Acta. 2004;504:163-6.
293. Hermanson GT. Chapter 22 - Enzyme Modification and Conjugation. In: Hermanson GT, editor. Bioconjugate Techniques (Third Edition). Boston: Academic Press; 2013. p. 951-7.
294. Ibraheem N, Hasan M, Khan RZ, Mishra P. Understanding Color Models: A Review. ARPN Journal of Science and Technology. 2012;2.
295. Zhang Y-Z, Zhang J-W, Wang C-Z, Zhou L-D, Zhang Q-H, Yuan C-S. Polydopamine-Coated Magnetic Molecularly Imprinted Polymers with Fragment Template for Identification of Pulsatilla Saponin Metabolites in Rat Feces with UPLC-Q-TOF-MS. Journal of Agricultural and Food Chemistry. 2018;66(3):653-60.
296. Palladino P, Bettazzi F, Scarano S. Polydopamine: surface coating, molecular imprinting, and electrochemistry-successful applications and future perspectives in (bio)analysis. Analytical and Bioanalytical Chemistry. 2019;411(1618-2650):4327-38.
297. Fu G, Zhao J, Yu H, Liu L, He B. Bovine serum albumin-imprinted polymer gels prepared by graft copolymerization of acrylamide on chitosan. Reactive and Functional Polymers. 2007;67(5):442-50.
298. Lamaoui A, Karrat A, Amine A. Molecularly imprinted polymer integrated into paper-based analytical device for smartphone-based detection: Application for sulfamethoxazole. Sensors and Actuators B: Chemical. 2022;368:132122.
299. Zhang X, Wang Z, Huang X, Huang Q, Wen Y, Li B, et al. Uniform stain pattern of robust MOF-mediated probe for flexible paper-based colorimetric sensing toward environmental pesticide exposure. Chemical Engineering Journal. 2023;451:138928.
300. Song J, He K, Xing B, Pei Y, Wang D, Wang Y, et al. Rapid Measurement of Residual Kanamycin Using Highly Specific Biomimetic Recognition Paper-Based Chip. Analytical Chemistry. 2022;94(50):17567-76.
301. Amatatongchai M, Thimoonnee S, Somnet K, Chairam S, Jarujamrus P, Nacapricha D, et al. Origami 3D-microfluidic paper-based analytical device for detecting carbaryl using mesoporous silica-platinum nanoparticles with a molecularly imprinted polymer shell. Talanta. 2023(1873-3573 (Electronic)).
302. Attaallah R, Amine A. Highly selective and sensitive detection of cadmium ions by horseradish peroxidase enzyme inhibition using a colorimetric microplate reader and smartphone paper-based analytical device. Microchemical Journal. 2022;172:106940.